DOUBLE DEGREE PROJECT
FOR MASTER OF SCIENCE WITH SPECIALIZATION IN ROBOTICS AND AUTOMATION
DEPARTMENT OF ENGINEERING SCIENCE
AT UNIVERSITY WEST
AND
FOR MASTER OF SCIENCE WITH SPECIALIZATION IN MECHANICAL ENGINEERING
DEPARTMENT OF ENGINEERING SCIENCE
HOCHSCHULE KAISERSLAUTERN

Human-Robot Collaboration for a Vision-Based Quality Inspection: A Safety-Oriented Design Framework

- From Concept to Prototype in an Industrial Lab Environment

Marco Seibert

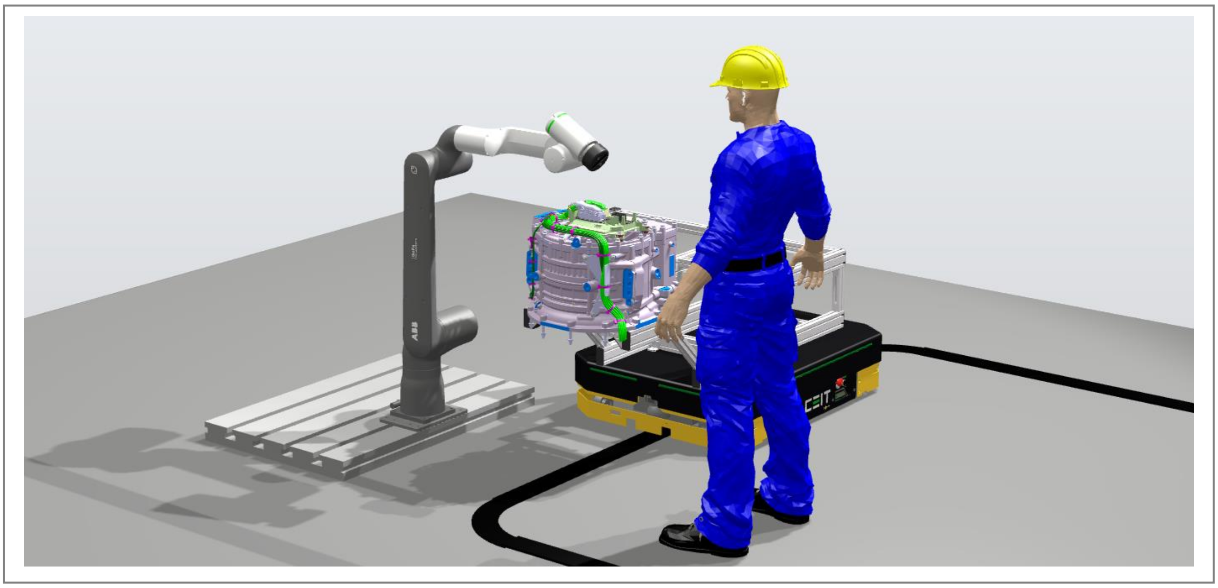

UNIVERSITY WEST

Hochschule Kaiserslautern
University of Applied Sciences

SCANIA

A THESIS SUBMITTED TO THE DEPARTMENT OF ENGINEERING SCIENCE

IN PARTIAL FULFILMENT OF THE REQUIREMENTS FOR THE DOUBLE DEGREE OF

MASTER OF SCIENCE WITH SPECIALIZATION IN ROBOTICS AND AUTOMATION

AT UNIVERSITY WEST IN SWEDEN

AND

MASTER OF SCIENCE WITH SPECIALIZATION IN MECHANICAL ENGINEERING

AT HOCHSCHULE KAISERSLAUTERN IN GERMANY

2025

Date:	June 16, 2025
Author:	Marco Seibert
Examiner:	Yongcui Mi from University West in Sweden and Gerd Bitsch from Hochschule Kaiserslautern in Germany
Supervisor:	Svante Augustsson from University West
Advisor:	Fredrik Ore from Scania CV AB
Programme:	Master of Science with specialization in Robotics and Automation
Credits:	120 Higher Education credits
Keywords:	Collaborative Robotics, Power and Force Limiting, Safety, Quality Control
Template:	University West, IV-Master 2.10
Publisher:	University West, Department of Engineering Science S-461 86 Trollhättan, SWEDEN Phone: + 46 520 22 30 00 Fax: + 46 520 22 32 99 Web: www.hv.se

Summary

This thesis explores the design and validation of a human-robot collaboration workstation for a vision-based quality inspection in an industrial-like setting. The goal is to develop a safe, flexible, and efficient system suitable for deployment in environments such as the Smart Factory Lab at Scania CV AB and showing therefore the possibility for an implementation in the real manufacturing. An industrial robot used in a collaborative application equipped with a vision system is integrated into a modular workstation capable of identifying missing components in assembled products.

The technical design and vision system of this workstation achieve reliable detection of missing components under industrial conditions and demonstrates adaptability through AI-assisted training and modular software design. Key ergonomic and usability aspects such as station layout, reduced cognitive load, and simplified reprogramming are considered to support flexible task allocation between human and robot. Overall, this workstation is ready to operate in the industrial-like environment and can be implemented in the overall connectivity.

Safety is the primary focus of this thesis. The system is designed according to ISO 12100:2010 [1], ISO 10218:2025 [2, 3] and the Machinery Regulation [4] and uses power and force limiting strategies as the only safety feature. Therefore, this thesis guides through the risk assessment methods to minimize hazards. Biomechanical risk validations are performed through both calculation and physical measurement. The results confirmed that under normal operating conditions, all relevant contact forces and pressures remained within the safety thresholds. Proving that only the power and force limiting strategies can be implemented in a human-robot collaboration workstation for a safe vision-based quality inspection.

The prototype demonstrates that collaborative vision-based inspection is feasible and safe when operating below head height. The findings support the real-world applicability of the system and provide a strong basis for future work involving full CE compliance, broader defect detection, and further ergonomic studies.

Acknowledgments

At this point, I would like to express my sincere gratitude to everyone who supported and accompanied me during the writing and development of this thesis, which is completed as part of the Double Degree Program in collaboration between University West in Sweden and Hochschule Kaiserslautern in Germany. This thesis fulfils the requirements for the Master of Science with specialization in Robotics and Automation at the Department of Engineering Science at University West, as well as the Master of Science with specialization in Mechanical Engineering at the Department of Engineering Science at Hochschule Kaiserslautern.

I would like to thank my examiners, Yongcui Mi from University West and Gerd Bitsch from Hochschule Kaiserslautern, for their professional guidance throughout the writing process. I also wish to express my appreciation to my supervisor, Svante Augustsson from University West, for his valuable support.

My special thanks go to Fredrik Ore from Scania CV AB, who supported me throughout this thesis with both expertise and personal dedication.

I am also very grateful to Scania CV AB, and especially to the Smart Factory Lab, for providing the opportunity to carry out this thesis within their organization. My sincere appreciation goes to all colleagues in the Smart Factory Lab, who were always helpful and supportive whenever I faced questions or challenges. I would also like to thank the engineers at Scania who played a key role in shaping the final state of the risk assessment in this thesis, making this thesis even more comprehensive and applicable.

I am especially thankful to my family and my girlfriend, who have always believed in me, supported me, and given me the strength to follow my path. Without them, I would not have come this far.

Finally, I would like to thank everyone who contributed to this thesis in any way, even if not mentioned here by name.

Preface

This master's thesis was carried out as part of a Double Degree Program between the Hochschule Kaiserslautern in Germany and the University West in Sweden. This thesis was submitted to the department of Engineering Science in partial fulfilment of the requirements for the Double Degree for the Master of Science with specialization in Robotics and Automation and the Master of Science with specialization in Mechanical Engineering.

The work was conducted in collaboration with Scania CV AB during a 5-month period in the spring of 2025. The project was developed at the Smart Factory Lab at Scania CV AB in Södertälje in Sweden, with support from both academic supervisors and industrial experts.

Their contributions and feedback have been valuable throughout the process. I would like to thank everyone involved for their support and cooperation during the completion of this thesis.

Marco Seibert
Södertälje, May 08, 2025

Affirmation

This master degree report, *Human-Robot Collaboration for a Vision-Based Quality Inspection: A Safety-Oriented Design Framework*, was written as part of the Master Double Degree Program needed to obtain a Master of Science with specialization in Robotics and Automation degree at University West in Sweden and a Master of Science with specialization in Mechanical Engineering degree at Hochschule Kaiserslautern in Germany. All material in this report, which is not my own, is clearly identified and used in an appropriate and correct way. The main part of the work included in this degree project has not previously been published or used for obtaining another degree.

04.06.2025

Signature by the author — Date

Marco Seibert

Contents

Preface

Main Chapters

Appendices

Symbols and glossary

AGV	*Automated Guided Vehicle*, a mobile robot used in industrial settings to transport materials without human intervention, typically guided by markers, wires, or sensors.
AI	*Artificial Intelligence*, the simulation of human intelligence in machines that are programmed to think, learn, and perform tasks typically requiring human intelligence, such as learning, problem-solving, perception, and decision-making.
CE	*Conformité Européene*, a marking indicating that a product complies with EU safety, health, and environmental requirements.
EC	*European Community*, a regional organization that was a parent to the European Union.
EU	*European Union*, a political and economic union of European countries.
HG	*Hand-Guiding*, a mode of robot operation where a human guides the robot's movements by hand.
HMI	*Human-Machine Interface*, the user interface or dashboard that connects a human operator to a machine, system, or device, allowing control, monitoring, and interaction.
HRC	*Human-Robot Collaboration*, the interaction between humans and robots working together in a shared space in industrial automation.
HRI	*Human-Robot Interaction*, the broader study of communication and cooperation between humans and robots.
ISO	*International Organization for Standardization*, a global body that develops and publishes standards to ensure quality, safety, and efficiency across various industries.
MQTT	*Message Queuing Telemetry Transport*, a lightweight messaging protocol for small sensors and mobile devices optimized for high-latency or unreliable networks, commonly used in Internet of Things and automation systems.
PFL	*Power and Force Limiting*, a safety mechanism that ensures a robot operates within a certain power and force thresholds to prevent injuries.
PFMD	*Pressure and Force Measurement Device*, a sensor-based instrument used to detect and quantify physical pressure and force, often for safety validation and compliance in robotic systems.
SRMS	*Safety-Rated Monitored Stop*, a control function that stops a robot motion when a human enters the workspace.
SSM	*Speed and Separation Monitoring*, a method of ensuring safe distances between robots and humans by adjusting speed dynamically.
TCP/IP	*Transmission Control Protocol / Internet Protocol*, the foundational communication protocols for the internet and most modern networks.
YOLO	*You Only Look Once*, a fast computer vision method that helps robots quickly detect and recognize objects in images from Ultralytics Limited.

1 Introduction

Industry 4.0 has boosted the use of robots in manufacturing processes. Traditional industrial robotic systems rely on extensive fence guarding and safety equipment, which limit the flexibility to move the robot elsewhere while increasing costs and space requirements [5]. While industrial robots in a collaborative application reduce the need for such barriers at low speeds, these systems also require larger safety zones when operating at high speed to comply with risk assessments. Therefore, highlighting the need for a robot which can sense the human presence and dynamically adjust the behaviour to maintain safety without compromising efficiency. At the same time, Industry 4.0 is driving the need for a high-quality and zero-defect manufacturing [6]. This is leading to a growing reliance in automated quality control solutions involving both, industrial robots and humans in the manufacturing environment [7]. These developments are not only reducing costs, saving space, and increasing flexibility, but are also significantly improving production quality. To address this, industrial robotic systems have emerged as a research area in Human-Robot Collaboration (HRC) to allow industrial robots to operate safely alongside humans without fixed barriers. Once safety requirements are met, industrial robots in a collaborative application tend to be able to be easily reprogrammed by non-experts, further enhancing flexibility, efficiency, and quality in production [5]. Therefore, a market analysis report by the consulting firm Grand View Research Inc. estimates that the market for HRC systems will experience a compound annual growth rate of 31.6% from 2025 to 2030, driving the global market size for industrial robots designed for collaborative applications from yearly 2.14 billion United States Dollars in 2024 to 11.04 billion United States Dollars by 2030 [8].

Given the increasing research and implementation of HRC systems in manufacturing, companies like Scania CV AB are exploring ways to integrate such technologies to improve the production quality. Scania CV AB is moving further towards becoming a sustainable transport solution provider, always focusing on delivering the highest quality to the customers. In the current production state, quality control is often done manually, with humans inspecting the parts and writing down the results. This process can happen several times during the production process and is repetitive, time-consuming, and cognitively intensive. Therefore, introducing HRC combined with a vision system can improve these intermediate quality control tasks. By using an industrial robot in a collaborative application with an attached vision system to handle the inspections, the goal is to make the process less repetitive and cognitively intensive for the human, while keeping the system flexible enough to adapt to the needs of the production line. This approach creates new possibilities for improving quality control in modern factories.

To explore how such collaborative systems can be practically implemented, previous work is investigating real-world applications of vision-equipped HRC workstations. The bachelor thesis from A. Gisginis [9] explores different layouts of an industrial robot is used in a collaborative application with an separated vision system. By focusing on implementation in a real industrial setting at Scania CV AB, this study offers particularly relevant insights, offering both time-efficiency analysis and operator perspectives. This study supports the idea that a vision-equipped HRC workstation could positively impact the quality control process and reduce the stress on the human. The work is based on real-world observations, interviews, and time studies which makes the information practical relevant. Although the study is a bachelor thesis conducted at Scania CV AB and not a peer-reviewed paper, the study is well-structured and includes important aspects about workflow improvements. Since A. Gisginis [9] is focusing on one specific factory and one case the results might not be generalizable. Building on these findings, this thesis further investigates the feasibility of such an approach in a quality control setting. Extending previous work, this thesis includes the development of a prototype and the evaluation in a real-world scenario. Inspired by this previous thesis, the present work develops an integrated robot-vision system to further enhance coordination, reduce task complexity, and explore greater flexibility in collaborative quality control setups. Moreover, combining vision and industrial robotics into a collaborative system, rather than treating them as separate components, further enhancing the flexibility explored in this work of this thesis.

Finally, in this thesis the term collaborative robot or collaborative operation are not used due to the misleading nature. Based on Directive 2006/42/EC of the European Parliament and of the Council of 17th of May 2006 [10] which is becoming the Regulation (EU) 2023/1230 of the European Parliament and of the Council of 14th of June 2023 [4] a robot is not considered a fully completed machinery and requires additional equipment, programming, and safety validation to operate safely in a collaborative application. The updated standard ISO 10218-1:2025, Robotics - Safety requirements - Part 1: Industrial robots [2] and ISO 10218-2:2025, Robotics - Safety requirements - Part 2: Industrial robot applications and robot cells [3] refers to industrial robots or industrial robot applications highlighting only the application, not the robot entity, can be developed, verified, and validated as collaborative. Therefore, in this thesis, only an industrial robot used in collaborative application is referred to. For clarity and conciseness, Directive 2006/42/EC is referred as the Machinery Directive, Regulation (EU) 2023/1230 as the Machinery Regulation throughout this thesis [4, 10].

1.1 Aims

The overall aim of this thesis is to theoretically investigate and design a framework for HRC in a quality control process of an industrial like environment. More specifically a prototype assembly line in the Smart Factory Lab at Scania CV AB. The focus is mainly on design principles, safety considerations, and a system capable of detecting missing components in assembled products. The goal is to contribute to a deeper understanding of a safe HRC workstation in an industrial like setting, and to demonstrate, guide, and document the process of how such a system can be effectively implemented. The specific sub-aims are the following:

- Designing an HRC workstation: Identifying key principles for structuring a conceptual collaborative quality control application with an industrial robot.
- Ensuring safety in HRC: Evaluating risk assessment methodologies and power-and-force-limiting strategies.
- Integrating vision-based quality inspection: Investigating how a conceptual industrial robotic vision system can identify missing components in assembled products.

The next chapter presents the investigation questions, explains their importance, and describes the approach used in the study.

1.2 Investigation questions

The investigation questions are mainly focused on designing a safe HRC workstation for the quality control process. Therefore, the main questions are the following:

- What theoretical frameworks and design principles can be applied to design a safe and efficient HRC workstation for a quality control task?
- How do risk assessment methodologies, power-and-force-limiting strategies, and international compliance standards influence the feasibility, implementation, and scalability of a human-robot collaborative workstation in a quality control process?

For the additional vision system part, the question is held to fulfil the quality inspection process by answering the following:

- How can a basic vision system be integrated into a HRC workstation to enhance quality control by detecting missing components?

While these investigation questions guide the development of a safe and efficient HRC workstation, certain constraints define the scope of this research.

1.3 Methodology

This thesis uses a design research methodology to explore the feasibility of a HRC workstation for intermediate quality control tasks. A prototype system that combines an industrial robot and a vision system is developed and tested in a lab environment at Scania CV AB. The methodology integrates theoretical design with practical implementation, focusing on safety, flexibility, and usability. The development process follows an iterative approach, including risk assessments based on ISO standards and feedback from safety engineers. This approach aims to bridge the gap between academic research and industrial practice by validating the system through functional testing and real-world observations. A detailed description of the methodology is provided in Chapter 3.

1.4 Contribution

This thesis contributes to the field of HRC by designing, implementing, and evaluating a prototype quality control workstation that integrates an industrial robot with a vision system. The main contributions are:

- A practical design of an HRC workstation tailored for intermediate quality control tasks in an industrial-like setting.
- The implementation of a vision-based inspection system mounted on an industrial robot, enabling automated detection of missing components.
- A risk assessment and validation process based on ISO 12100:2010 [1] and the updated ISO 10218:2025 [2, 3] standards, ensuring compliance and human safety.
- An evaluation of system flexibility, usability, and safety through real-world testing at Scania CV AB.

Together, these contributions provide actionable insights for deploying a safe, flexible, and efficient HRC system in the quality control application.

1.5 Limitations

While the thesis aim is to ensure compliance with international safety standards there is no design of a new safety protocol. Instead, existing frameworks for risk assessment and safety compliance are implemented and validated. This thesis involves not a complete "Conformité Européene" (CE) marking. The CE marking indicates that a product has been evaluated and complies with the high safety, health, and environmental protection standards of the Machinery Regulation required for sale within the European Economic Area [4]. However, the system is designed to align with safety and compliance requirements so that the system can be prepared for potential production implementation in the future. The scope is limited to industrial robots equipped with power-and-force-limiting strategies without the integration of external safety devices e.g., laser scanners or light curtains into the system.

The thesis is limited to an industrial robot used in a collaborative application programming to a predefined set of tasks related to quality control. Advanced machine learning algorithms adaptability and autonomous decision-making of the robot is not designed.

The thesis focuses on integrating an already existing machine vision framework, based on the artificial intelligence (AI) model YOLO which stands for You Only Look Once from the company Ultralytics Limited, for the quality control task. Specifically, to identify missing objects on the product. Tasks outside the inspection process, such as assembly or sorting, is not addressed. The machine vision system is done for detecting anomalies in specific product configurations. Particularly, identifying missing components. The thesis may not generalize to other product types, defects, or manufacturing lines without significant reconfiguration or retraining. Advanced machine learning algorithms for autonomous vision adaptability are not designed.

The thesis focuses on ensuring interaction between industrial robots in a collaborative application and humans during a quality control task. Broader aspects of human factors, such as long-term ergonomic studies or psychological impacts are not investigated. Testing and validation are conducted in a controlled lab environment, the Smart Factory Lab at Scania CV AB. Implementation on a production line is limited to proof-of-concept demonstrations and covers not the implementation in the real-world production.

Together with the aims and investigation questions, these limitations define the scope of this research, ensuring a focused approach to designing a safe HRC workstation for a quality control task while laying the groundwork for future advancements and real-world implementation.

1.6 Thesis Structure

This thesis is structured into eight chapters to guide the reader through the development, implementation, and evaluation of a HRC workstation for quality control. The Introduction outlines the background, goals, and methods. Related Work reviews literature on HRC, safety, and vision systems. Method describes the research design and evaluation approach. Design of the Workstation explains the hardware, software, and vision integration. Safety Analysis and Risk Assessment focuses on identifying and minimizing risks. System Validation verifies safety and functionality. Results and Discussion presents the findings. Conclusion and Future Work summarizes the work and suggests further steps.

2 Related Work

This chapter presents a literature review of research areas relevant to this thesis. In the following a literature search in IEEE Xplore, Science Direct and the Swedish Institute for Standards is conducted to ensure a comprehensive and structured literature review. The following keywords are used to identify significant contributions in the field: "Cobots", "Collaborative Robotics", "Human-Robot Collaboration", "Power and Force Limiting" and "Safety". These search terms assisted in identifying existing frameworks, safety methodologies, and recent advancements in industrial robots used in collaborative applications and risk mitigation strategies.

2.1 Future Industry and Human Robot Interaction

The further development of HRC is driven by Industry 4.0, Industry 5.0, safety standards and intelligent automation systems. With the increasing demand on flexible, efficient and safe workspaces, researchers have explored different methods to integrate industrial robots into a human-centric environment.

2.1.1 The Role of Human-Robot Interaction in the Industrial Automation

The current ongoing transition to Industry 4.0 is considered as introducing automation to the production lines. In the context of Industry 4.0, traditional industrial robotic systems have been widely implemented to fulfil the need for automation. These systems operate at high speeds and handle significant payloads and require therefore fences and physical separation from the human to guarantee safety. As a result, the production process often becomes either fully automated or remains entirely manual, leaving parts of the production line in isolated robotic cells while other sections rely entirely on humans.

This traditional setup tends to force a choice between fully manual or fully automated production, leaving little room for a flexible and adaptive manufacturing. Manufacturing lines still require both humans and robots. Humans are essential for tasks that involve complex judgment, fine motor skills, or adaptability to variation, where current automation technologies have limitations. At the same time, for humans involved in mass-produced production lines, the tasks are often repetitive, cognitively intensive, and can lack ergonomic support, leading to potential physical strain or injury. As a result, separating robots and humans into distinct workspaces not only reduces flexibility but also introduces inefficiencies in layout, workflow, and communication. HRI addresses these challenges by enabling safe, shared workspaces where robots and humans can work together and complement each other's capabilities.

HRI represents a major transition in this industrial automation setting of Industry 4.0 enabling industrial robots and humans to work in shared spaces without physical barriers [11]. This approach eliminates the traditional need for fencing and other types of inflexible safety equipment, such as fixed guards, hard enclosures, and physical interlocks. These types of equipment are designed to prevent human access to hazardous areas but can be rigid and difficult to reconfigure. As a result, these systems often limit the adaptability and responsiveness of the system to changes in the production layout. By removing the dependency on such static safety measures, the system gains greater operational flexibility while still ensuring a high level of safety. Additionally, HRI can enable the automation of complex manufacturing processes which can be difficult to fully automate [12].

The first concept of HRI is introduced in 1996 where J. Edward Colgate and Michael Peshkin created a first concept of an industrial robot which is used in a collaborative application with a passive interaction level, which could be operated by humans [13]. Years later, the company KUKA AG introduced the first industrial robot used in a collaborative application, the LBR 3 which is a German acronym for lightweight robot, in 2004, followed by the LBR 4 in 2008, leading to the first industrial implementation by a Danish plastics and rubber supplier and the Danish robotics company Universal Robots A/S [11]. Similarly in 2008 the company ABB Ltd. released SafeMove, a safety system that enabled HRI by allowing industrial robots to remain powered on while ensuring safe collaboration [14].

This highlights the advancements in HRI are not limited to industrial robots in a collaborative application but also included traditional industrial robots with integrated safety features. Since the first development and introduction of industrial robots in a collaborative application and traditional industrial robots with integrated safety features these systems have evolved significantly, becoming more advanced in terms of safety, efficiency, and adaptability.

The different demands on manufacturing capabilities within Industry 4.0 are illustrated in Figure 1. With the specifications of a high product volume and a low variance this field fits best the traditional industrial robotic system. A separated industrial robot area where the human cannot enter, and the industrial robot is working at maximum payload with the maximum required speed. On the other side a low product volume and a high product variance requires currently a full manual capacity to fulfil the manufacturing process.

These scenarios illustrated in Figure 1 create a significant gap in the manufacturing process, highlighting the need for a cellular manufacturing in producing high product volumes with high product variants. Within cellular manufacturing having the need for a higher product volume, this process can be achieved with smart automation technologies where the process will be highly automated. Having the need for a higher product variance the demand for HRI comes into the main scope having a human and

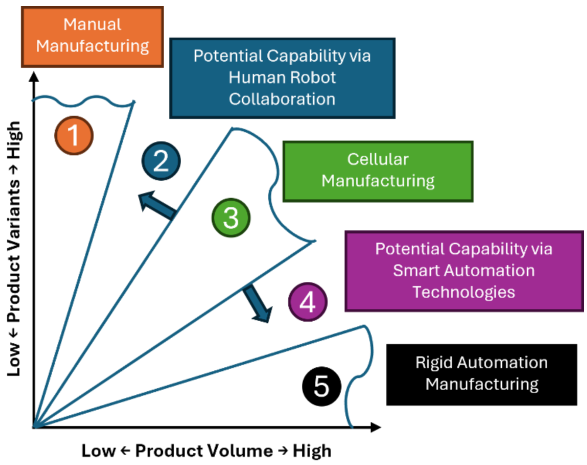

Figure 1 Demonstration of the transition from manual and rigid automation manufacturing towards cellular manufacturing, enabling higher product volume and greater variant flexibility. The illustration highlights the role of HRI and smart automation technologies in Industry 4.0, adapted with permission from Bi et al. [12].

an industrial robot working together to achieve the highest possible outcome in a human-centric environment.

This gap between high automation and manual processes not only underscores the need for flexible manufacturing but also sets the stage for the growing importance of HRI. The industry is currently shifting towards Industry 4.0, but with a forward-looking perspective to Industry 5.0, the role of HRI becomes even more significant by moving from a system centric to a human centric production environment [15]. Industry 5.0 represents the next stage of manufacturing evolution, building on Industry 4.0 by highlighting human collaboration, where industrial robots operate safely and efficiently alongside humans [15].

Based on the literature study from Dhanda et al. [15], which explores the opportunities and challenges of HRC in future Industry 5.0 manufacturing, the study highlights the potential opportunities of integrating human creativity, judgement and well-being into the production process by improving flexibility, sustainability and resilience.

Additionally, highlighting emerging technologies such as AI, digital twins, augmented reality, virtual reality as well as HRC play an important role in adaptive and intelligent manufacturing environments that align with the human-centric goal in the future production environment. As automation advances, HRI must address ethical issues, data security, and job displacement to keep Industry 5.0 focused on human needs while using technology to improve the productivity and safety aspects in the production environment [15]. Humans and industrial robots in a collaborative application should be seen as connected parts of a larger system, not as separate entities. This requires a thoughtful approach in designing a HRC environment which is explained in the following Subsection 2.1.2.

2.1.2 Enabling Human-Robot Interaction through Modes of Collaboration

To fulfil this need for HRI, several technologies have emerged to enhance collaboration, improve safety, and optimize efficiency in shared workspaces. Nowadays, industrial robots in a collaborative application are equipped with advanced sensors, algorithms or AI models to respond dynamically to human presence and actions. These technologies need to be aligned with safety standards to ensure compliance and reliability in shared workspaces. To comply with these requirements there are different approaches in the technology of an industrial robot is used in a collaborative application which leads to different terminologies.

According to the safety standard ISO 10218-1:2011 - Robots and robotic devices - Safety requirements for industrial robots - Part 1: Robots [16], ISO 10218-2:2011 - Robots and robotic devices - Safety requirements for industrial robots - Part 2: Robot systems and integration [17] and the technical guideline ISO/TS 15066:2016 - Robots and robotic devices - Collaborative robots [18] an industrial robot is used in a collaborative application is differentiated in different categories presented in Figure 2.

The safety-rated monitored stop (SRMS), speed and separation monitoring (SSM), hand-guiding (HG), and in power and force limiting (PFL) mechanisms. To better understand these technologies, exploring the key features of SRMS, SSM, HG, and PFL is crucial. These technologies play an important role in ensuring a safe and efficient HRC environment.

In SRMS, illustrated in Figure 2, the operation ensures the industrial robot stops the movement before the human enters the collaborative workspace. The human can enter the workspace if the stop is active and then start the work. After leaving the workspace the industrial robot resumes the operation automatically without intervention leading to coexistent workspaces. When there is no human present the industrial robot operates in a non-collaborative mode. Early implementations of this concept are seen in industrial robots using safety systems for example ABB SafeMove and KUKA SafeOperation, which enabled controlled HRI in collaborative settings, marking one of the first HRI and HRC cases [14, 19].

According to the updated ISO 10218-1:2025 [2] and ISO 10218-2:2025 [3] this operation is no longer considered as an HRI case potentially due to that SRMS, by design, requires the robot to stop when a human is present, meaning no interaction occurs during the motion of the robot.

In SSM, illustrated in Figure 2, the human and the industrial robot can work coexistent or sequential in the shared workspace, while maintaining safety through protective separation distance. The distance of the human and the industrial robot are constantly monitored to prevent the industrial robot from moving closer than a defined limit to the human. This distance includes calculations about the speed the industrial robot has and the needed distance to stop safely before the human could reach the position. The safety distance is adjusted based on the industrial robot speed, with slower speeds allowing closer proximity.

The HG mode, as demonstrated in Figure 2, requires a SRMS before the human can enter the workspace. The human controls an industrial robot equipped with a hand-operated device, allowing direct interaction and movement adjustments in response to the humans HG input [18]. The industrial robot remains stationary in the HG mode until the human exits the workspace and the industrial robot resumes the automation mode.

In a PFL operation method, as depicted in Figure 2, the human and the industrial robot are working in a coexistence, sequentially or within a responsive collaboration in the workspace. Physical contact between the industrial robotic system and the human can happen, either intentionally or unintentionally [18]. The industrial robot must be designed to limit the power and force and detect contact upon occurrence. These systems are either inherently safe or such systems need to be equipped with a control systems to measure small changes in the industrial robot movement [18].

Arents et al. [21] conducted a systematic review on HRC applications in the context of smart manufacturing in Industry 4.0 and Industry 5.0. The study is looking through 46 peer-reviewed research articles from 2017 until 2021 and analysed actual implementations, lab testing and simulations of HRC systems with safety mechanisms or standards. Based on the literature review the most used safety action are SSM with 19 studies, SRMS with 13 studies, and HG with 10 studies. Contrary, the least used

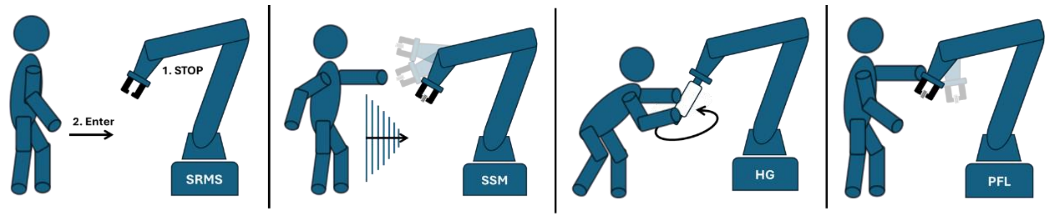

Figure 2 Progression of different approaches in the technology of an industrial robot is used in a collaborative application in HRC, differentiated in safety-rated monitored stop (SRMS), speed and separation monitoring (SSM), hand-guiding (HG), and in power and force limiting (PFL) mechanisms, adapted with permission from Emeric et al. [20].

action is PFL with 6 studies [21]. The study highlights that SSM, SRMS, and HG have been more extensively investigated in research compared to PFL. This may be attributed to the fact that SSM, SRMS, and HG modes are generally easier to implement using existing sensor technologies and require fewer changes to the mechanical design of the robot. In contrast, PFL relies on integrated force and torque sensing and strict compliance with biomechanical limits, making it more technically demanding and subject to rigorous safety validations, which could explain the lower frequency of its application in the reviewed literature.

Whereas these technologies describe different interaction scenarios, these systems do not inherently define the interaction levels within HRI. Instead, HRI is categorized into different sublevels based on the degree of collaboration between the human and the industrial robot which is presented in the following Subsection 2.1.3.

2.1.3 Levels of Human-Robot Interaction from separation to responsive Collaboration

These interaction levels, which are further illustrated in Figure 3, range from fully separated workspaces to highly integrated and responsive collaboration. This distinction can differ depending on the literature, but in general most literature describes similar interactions with slight differences in terminology and distinctions. The distinctions used in this thesis are one of the common used terminology and based on Madzharova-Atanasova and Shakev [11].

The first level, demonstrated in Figure 3, shows a traditional industrial robotic system with a separated workspace where the human and industrial robot do not interact directly. The industrial robot is fenced and protected from unwanted access to the cell. This ensures the human is completely isolated from the industrial robotic operation. Moreover, the industrial robot operates at high speed and high payload.

Following Figure 3 to the second level of HRI is showing the coexistence where the industrial robot and the human share the same workspace without being physically separated. In this level of collaboration, the human and the industrial robot work independently from each other in their own workspace and coexisting next to each other without a physical separation. Safety measures are required to prevent accidental interference of both workspaces.

This level of interaction changes in the third level where the industrial robot and the human work sequentially in the same workspace, which needs a certain level of coordination. Therefore, the workspace is shared by the human and the industrial robot in a working sequence presented in Figure 3 by the red arrows indicating the sequential movement of the robot and the human. This ensures a smooth transition between the tasks of the human and industrial robot on the same object.

Instead of working sequentially in the shared workspace the human and the industrial robot can work together simultaneously in a cooperation. Meaning that the human and the industrial robot are working on the same object in the same workspace but having different tasks, as depicted in Figure 3. This requires coordination and safety measures to ensure a safe workflow.

Increasing further the interaction and coordination as well as the safety considerations leading to the level of responsive collaboration in Figure 3. There, the industrial robot and the human work in a shared workspace on the same object and the same task at the same time in close proximity. This requires the highest level of coordination as well as the highest safety measures to prevent any harm of the human in the workspace. Responsive collaboration is the highest level of collaboration in HRI.

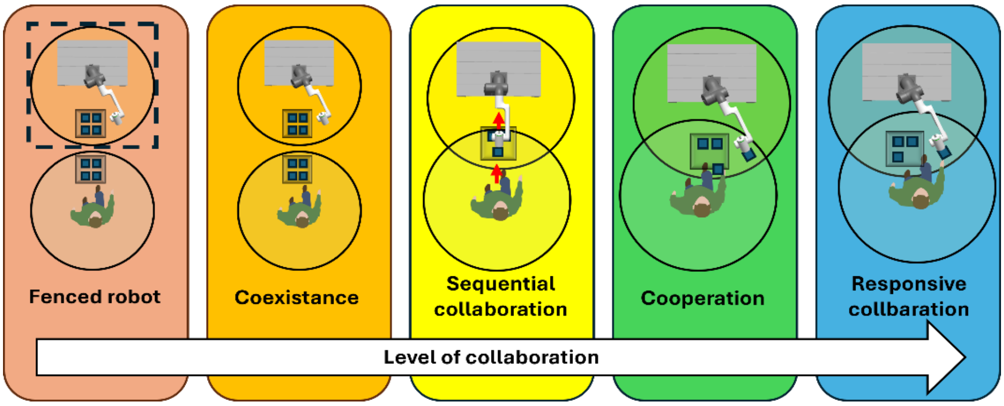

Figure 3 Progression of HRI levels, demonstrating increasing human engagement within a shared workspace. The transition moves from fenced industrial robots to responsive collaboration, highlighting the changes of interaction and cooperation, adapted with permission from Madzharova-Atanasova and Shakev [11].

Based on the already mentioned literature review study conducted by Arents et al. [21], looking through 46 peer-reviewed research articles from 2017 until 2021 and reviewing actual implementations, lab testing and simulations of HRC systems, the findings where that 22 out of 46 articles had cooperation, 16 articles had responsive collaboration, 14 articles studies had coexistence and 7 articles did not meet the criteria of the authors for HRC [21]. Since this study differentiated only between three HRI levels, highlighting most research focuses on cooperation, which is followed by responsive collaboration and coexistence.

This leads to the conclusion that all HRI levels have been heavily investigated, demonstrating a strong research interest in all HRI levels. However, sequential collaboration was not specifically addressed in some studies, as the differentiation between levels was limited or less granular. Supporting this Proia et al. [22] also highlight the importance of HRC in improving production efficiency and reducing human workload, especially in repetitive, time-consuming, and cognitively intensive tasks. This underscores the great potential for HRI and HRC in the future Industry 4.0 and 5.0.

At the same time Industry 4.0 is driving the demand for high-quality, zero-defect manufacturing, highlighting the importance of quality control to ensure that products meet required standards before leaving the production line [6]. Zero-defect manufacturing aims to prevent failures in the production environment by ensuring every component is made perfectly from the beginning [23].

In the context of quality control, industrial robots in a collaborative application can handle tasks such as repetitive inspections, freeing humans to focus on decision-making and complex problem-solving tasks [22] which is introduced in Section 2.4 on page 20. In a collaborative workspace the safety aspect must always be the highest priority, therefore applicable safety standards are discussed in the following Section 2.2.

2.2 Safety in Human Robot Collaboration

In a HRC case the industrial robot is used in a collaborative application and needs to meet certain safety requirements which are acting on the safety assurances of the HRC application which is demonstrated in Figure 4. Starting by local laws and regulations, such as the Machinery Directive [10] which is becoming the Machinery Regulation [4], have to be followed. Going further into standards from the International Organization for Standardization (ISO) which has Type-A, Type-B and Type-C standards.

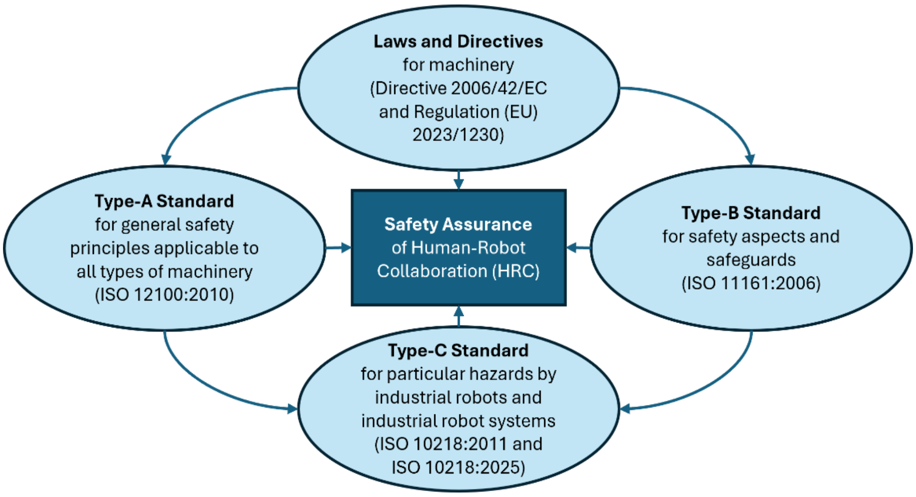

Figure 4 Overview of safety standards and regulations influencing the safety assurance of HRC. The framework integrates laws, directives, and ISO standards to ensure compliance and risk mitigation in HRC, adapted with permission from Bi et al. [12].

Type-A standards are for basic safety in an overall sense of a safe machine, whereas the Type-B standards are for specific safety aspects and safeguards inside a machine. Type-C standards are for machine safety and product level. If a Type-C standard conflicts with Type-A or Type-B standards, the Type-C standard takes priority for the designed machines and is built according to the laws and standards [16].

2.2.1 Laws and Directives

The industrial robot is used in a collaborative application and must meet the general safety requirements for machinery, complying with relevant laws and directives such as the Machinery Directive [10] or the Machinery Regulation [4]. The Machinery Directive [10] transits to the new Machinery Regulation, is valid and all countries in the European Economic Area are required by law to fulfil the new regulation by the 20th of January 2027 [4]. The Machinery Directive [10] and the new Machinery Regulation [4] builds the framework to ensure the safety of machinery within the European Economic Area. This guarantees that machinery products meet specific safety and performance requirements before being placed on the market inside the European Economic Area by additionally marking the machinery with a CE sign [4, 10].

The Machinery Directive and the Machinery Regulation are starting by explaining on what applies and which exceptions there are, by covering machinery, interchangeable equipment, safety components, lifting accessories, chains, ropes and webbing, removable mechanical transmission devices and partly completed machinery [4, 10]. An industrial robot is classified as a partially completed machinery, meaning the device lacks full operational capability and depends on additional components or integration to function as a complete system. The industrial robot needs an end-effector and a control system is to be considered a fully completed machinery [4, 10]. The application of a HRC workstation is considered a machinery in the final design and must fulfil the requirements of the Machinery Directive [10] and the new Machinery Regulation [4]. Therefore, the machinery must be designed to be safe for the intended use but also taking into consideration the reasonably foreseeable misuse [4, 10]. The foreseeable misuse can be the human doing tasks out of curiosity which are not related to the intended HRC case.

Therefore, an extensive risk assessment and risk reduction according to ISO 12100:2010 - Safety of machinery - General principles for design - Risk assessment and risk reduction [1] needs to be done in an iterative manner to ensure the workstation fulfils the safety standards of the Machinery Directive [10] and the new Machinery Regulation [4]. Once compliance is verified, the European Community Declaration of Conformity, as stated in Annex II of Machinery Directive becoming Annex V in the Machinery Regulation, can be completed [4, 10]. Only then can the CE marking be applied by following the guidelines in Annex III of the Machinery Directive or article 24 of the Machinery Regulation [4, 10]. Additionally, a technical file for machinery must demonstrate that the machinery complies with the requirements as well as a file for the intended use must be created [4, 10].

According to both the Machinery Directive and the Machinery Regulation, a potential source of injury or a damage to the humans health is considered an hazard, the combination of the probability and the degree of injury or damage to the health is considered a risk in an hazardous environment and the intended use is the use of machinery that is provided in the instructions [4, 10]. Readily predictable human behaviour is using the machinery in a way that is not intended, which needs to consider as a reasonably foreseeable misuse [4, 10].

The new Machinery Regulation [4] builds on the Machinery Directive [10] and puts more focus on cybersecurity and software safety, recognizing the growing role of digital technology and AI in machinery [4]. Manufacturers now must consider risks from software updates, remote access, and network connections. Including clearer guidelines for HRC and directly addresses safety in shared workspaces. Additionally, strengthens risk assessments by setting stricter rules on foreseeable misuse, ensuring safety measures protected against unintended human actions.

In terms of industrial robots in a collaborative application this Machinery Directive [10] and the new Machinery Regulation [4] is important since the application is bound to follow these laws and regulations. More precise implementation strategies which comply with the Machinery Directive [10] and Machinery Regulation [4] are considered in the following standards. The application in the risk assessment is explained in Subchapter 2.2.5 on page 15.

2.2.2 Type-A and Type-B Standard

The Type-A standards provide general safety principles applicable to all types of machinery. These standards establish broad guidelines for assessing and preventing risks and for how to design safe machinery in general [1]. One of the important Type-A standards in HRC is ISO 12100:2010 [1], which defines the general principles for a risk assessment and the following risk reduction. This risk assessment is elaborated and the specific task which needs to be carried out is defined in the Type-C standard. Therefore, this standard ensures that all types of machinery as well as an industrial robot in a collaborative application and their components comply with essential safety principles before further specialization through Type-B or Type-C standards.

Type-B standards are for safety aspects and safeguards. The specific application of an industrial robot is used in a collaborative application and must meet Type-B standards, for example, the manufacturing applications by ISO 11161:2007 - Safety of machinery - Integrated manufacturing systems - Basic requirements [24]. This standard provides guidance on how to ensure safety when multiple machines are combined into a single system. Outlining risk reduction strategies and how ensuring protective measures are applied across machinery.

2.2.3 Type- C Standard

The following Type-C standards represent particular hazards by industrial robots and industrial robot systems [16]. Therefore, Figure 5 illustrates the hierarchical structure from the Type-B standard covering the overall integrated manufacturing system to the Type-C standards covering robot cell and furthermore only the robot.

While this thesis builds upon the versions ISO 10218-1:2011 [16] and ISO 10218-2:2011 [17] references to the edition ISO 10218-1:2025 [2] and ISO 10218-2:2025 [3] are provided where applicable to reflect current standardization developments. The ISO 10218:2025 [2, 3] editions incorporate aspects previously covered in the technical guideline ISO/TS 15066:2016 [18]. Figure 5 demonstrates an industrial robotic work cells is considered by the second part of the standard which is ISO 10218-2:2011 [17] as well as ISO 10218-2:2025 [3]. Whereas robots is considered by the first part of the standard which is ISO 10218-1:2011 [16] as well as ISO 10218-1:2025 [2].

The ISO 10218-1:2011 [16] as well as ISO 10218-1:2025 [2] sets out the requirements and guidelines on how to ensure safety when designing and building industrial robots, by addressing and minimizing the associated hazards of the industrial robot and excluding the industrial robot from the environment. Therefore, for example noise emissions are excluded as hazards in this scope of this standard. An industrial robot should provide a visual indication while operating within a collaborative application [16] by e.g. floor marking or signs [17].

ISO 10218-2:2011 [17] as well as ISO 10218-2:2025 [3] provides guidelines to keep humans safe during the industrial robot integration, installation, testing, programming, operation, maintenance and repair. By following these guidelines, the workplace can be designed to be safe and to minimize potential hazards. An industrial robot which has PFL alone is not considered a fully equipped machinery and requires additional equipment to operate. Therefore, this alone is not enough to ensure a safe operation in a collaborative application. A risk assessment must be conducted during the design of the system to ensure safety, as outlined in ISO 10218-2:2011 [17] with further guidance provided in ISO/TS 15066:2016 [16]. The risk assessment should consider the entire collaborative task and workspace [17]. Notably, ISO 10218-2:2025 [3] has absorbed much of the guidance from ISO/TS 15066 [18], consolidating future collaborative application safety into the main standard. While ISO/TS 15066:2016 [18] and ISO 10218-2:2011 [17] remain valid, future-oriented designs should consider the integrated 2025 guidance. Additionally, ISO 10218-2:2025 [3] includes detailed validation procedures for collaborative applications based on PFL mechanisms, reflecting a shift

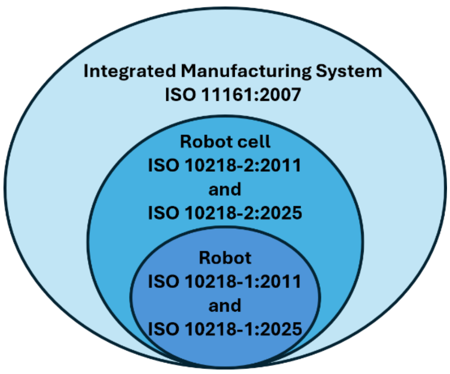

Figure 5 Relationship between Type-B and Type-C standards in industrial robotics, illustrating their hierarchical structure within the integrated manufacturing system, based on ISO 10218-2:2011:2011 [17].

from guiding through a technical specification to a standardized guidance. The application of ISO 10218-1:2011 [16] and ISO 10218-2:2011 [17] as well as ISO 10218-1:2025 [2] and ISO 10218-2:2025 [3] in the risk assessment is explained in Subchapter 2.2.5.

2.2.4 Applicable Guidelines

ISO/TS 15066:2016 - Robots and robotic devices - Collaborative robots [18] is a technical specification published by ISO that provides guidelines for the safe implementation of industrial robots in a collaborative application in shared workspaces. According to ISO/TS 15066:2016 [18], ISO 10218-1:2011 [16] and ISO 10218-2:2011 [17], a collaborative workspace is defined as an environment where a human and an industrial robot application can perform tasks on the same object within the same operating workspace [18].

This workspace is characterized by specific safety requirements to ensure seamless HRI. However, in the updated ISO 10218-1:2025 [2] and ISO 10218-2:2025 [3] standards, the term collaborative workspace has been removed. Instead, the standards define a collaborative application containing one or more collaborative tasks where the robot and the human work in a sequence within the same safeguarded space. This shift outlines that safety and collaboration are determined by the application design and validation, not by a predefined physical workspace.

In a collaborative application, the industrial robot system and the human are designed to work within a shared environment while ensuring safety [18]. Two types of contact scenarios are outlined within the technical guideline outlined in Figure 6. The quasi-static contact occurs when the human can be clamped between a moving part of the industrial robot system and a fixed environment, whereas transient contact refers to situations where the human can retract themselves from a moving part without being clamped in a fixed position [18]. These contact scenarios and their implications are specified in ISO/TS 15066:2016 [18], providing essential safety measures for industrial robot used in a collaborative application. The demonstrated contact events in Figure 6, originally introduced in ISO/TS 15066:2016 [18], have now been incorporated into ISO 10218-2:2025 [3], emphasizing their importance in designing and validating a collaborative application.

This thesis focuses on industrial robots used in a collaborative application with PFL strategies. Therefore, the following guideline from ISO/TS 15066:2016 [18] is explained specifically in the context of PFL operation in the following Subsection 2.2.5.

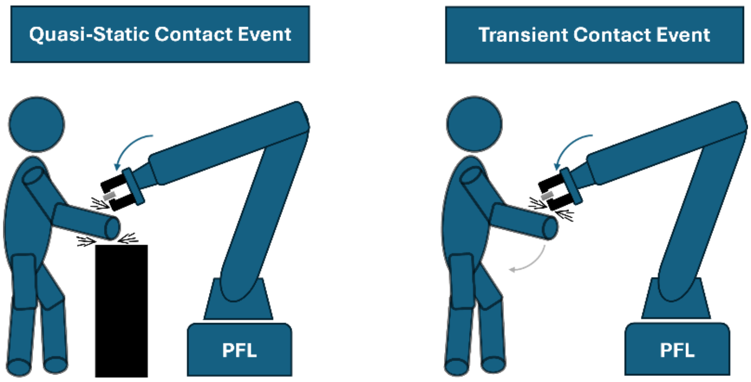

Figure 6 Demonstration of a quasi-static contact event where the human can be clamped and a transient contact event where the human can retract himself, based on ISO 10218-2:2025 [3].

2.2.5 Risk assessment methodologies for HRC

The standard risk assessment process must follow ISO 12100:2010 [1] and is presented in Figure 7. This process needs to be conducted iteratively to ensure a safe application. According to Machinery Directive and Machinery Regulation manufacturers or their authorized representatives must prioritize eliminating or minimizing risks through inherently safe machinery design and construction [4, 10]. For any remaining risks, there must be protective measures implemented to ensure the highest level of safety in a machinery use [10].

The Machinery Regulation [4] emphasizes the importance of safe interactions between humans and advanced machines. With the growing use of industrial robots in a collaborative application, companies must ensure these interactions are safe by designing machines which can work alongside humans while minimizing the risk of accidents. The Machinery Regulation also states that safety measures need to prevent contact related hazards and psychological stress caused by interaction with machinery, either in human-machine coexistence in a shared workspace without direct collaboration or a direct human-machine interaction [4].

In this thesis, the risk assessment is conducted for an HRC workstation using only an industrial robot with PFL. Therefore, the risk assessment process specific to such a workstation is described in detail. In the beginning of the risk assessment, the scope of the application must be clearly defined. Explicitly stating the parameters, conditions, and constraints to ensure a structured and transparent assessment process is crucial.

The process of a risk assessment consists of multiple stages, demonstrated in Figure 7, starting with a risk analysis that identifies potential hazards within the application. ISO 10218-2:2011 [17] highlights a comprehensive evaluation of the collaborative tasks and workspaces, considering factors such as industrial robot characteristics, end-effector hazards, system layout, human positioning, fixture design, environmental influences, and safety functions. This evaluation process is further detailed and updated in ISO 10218-2:2025 [3], particularly in Annex M, which outlines guidance on a contact analysis and biomechanical thresholds for collaborative applications.

Based on the guidelines from ISO/TS 15066:2016 [18] this identification process should also consider the following criteria for potential contact events which are the:

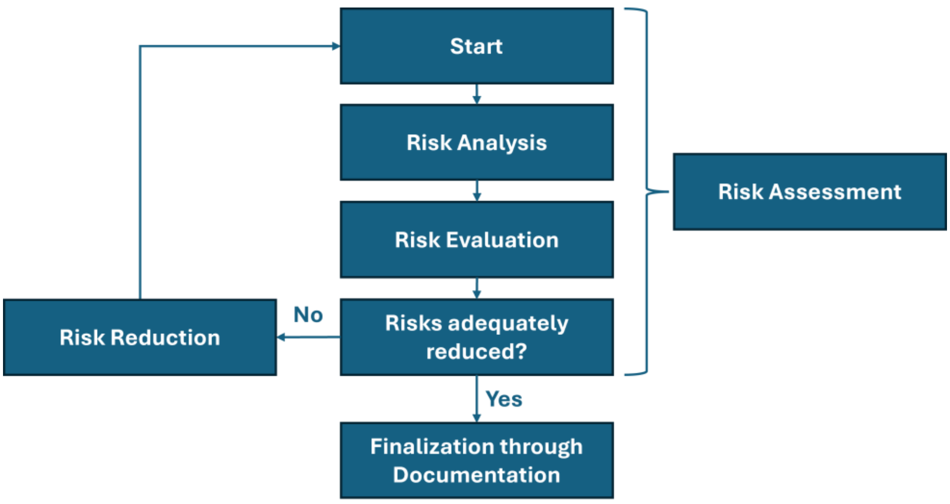

Figure 7 Risk assessment process flow, highlighting the steps from risk analysis to evaluation, followed by risk reduction if necessary to ensure a safe machine, based on ISO 12100:2010:2010 [1].

- exposed human body regions,
- origin of contact events, i.e., intentional action as part of intended use vs. unintentional contact or reasonably foreseeable misuse,
- probability or frequency of occurrence,
- type of contact event, quasi-static or transient,
- contact areas, speeds, forces, pressures, momentum, mechanical power, energy and other quantities characterizing the physical contact event [18].

Secondly the risk evaluation, based on ISO 12100:2010 [1], which identifies hazards by assessing the potential associated risks. The severity level can be divided into the severity of injuries or damage to health, for example, into slight, serious or death and the extent of harm to one human or several humans [1]. The frequency of exposure to hazard can be estimated by considering the following factors:

- The duration and regularity of the humans presence in the hazardous area [1].
- The probability of interaction between the human and the hazardous element [1].
- The speed and unpredictability of the hazardous event [1].
- The working environment, including visibility, noise levels, and potential distractions [1].
- The nature of the task, whether involving repetitive movements, in close proximity to moving parts, or manual interventions [1].

By analysing these factors, the risk evaluation determines whether the existing protective measures are adequate or if further risk reduction strategies are necessary to ensure compliance with ISO 12100:2010 [1] and enhance workplace safety. The verification and validation can be done by ISO 10218-1:2011 for example with practical tests (B), measurements (C), reviewing of application-specific schematics, circuit diagrams and design material (E) and reviewing the task-based risk assessment (F) [16]. Based on Annex F in ISO 10218-1:2011 [16] focussing on risk evaluation for the PFL case:

- The industrial robot limits dynamic power output, static force, and speed or energy in compliance with ISO 10218-1:2011 (B, C, E) [16].
- If any parameter limit is exceeded, a protective stop is issued (B, C, E) [16].
- The collaborative application is determined by the risk assessment performed during the application system design (B, E, F) [16].
- Information for use includes details for setting parameter limits to the industrial robot controller (G) [16].

ISO 10218-1:2025 [2] maintains these validation strategies and further formulates guidelines for PFL strategies. The risk assessments can require practical tests and measurements to validate that the risk is mitigated. Therefore, the risk reduction should consider situations in which the contact between the human and industrial robot would not result in harm of the human [18]. This can be done by identifying different conditions in which this form of contact would not occur, by evaluating the potential risk of this form of contacts, by designing an inherently safe industrial robot system and collaborative workspace to avoid such contacts or by keeping the contact situations below the threshold limit values [18] which are defined in the following Subsection 2.2.6.

2.2.6 Review of existing research on risk mitigation strategies in HRC

The biomechanical limits which different body parts of a human can withstand differ depending on the exposed body region depicted in Figure 8. The limits are established to ensure forces generated by industrial robot motion do not impose excessive biomechanical loads, minimizing the risk of minor injuries in the event of a contact between the human and the industrial robot [18].

Risk mitigation strategies based on ISO/TS 15066:2016 [18] can be categorized as passive or active for the quasi-static and transient contact. These strategies, along with the associated biomechanical thresholds, have now been incorporated into ISO 10218-2:2025 [3], Annex M, providing a reference for designing and validating safe collaborative applications.

Passive risk mitigation strategies in ISO/TS 15066:2016 [18] focus on the mechanical design of industrial robot systems to reduce injury risks. This can be achieved by increasing the contact surface area using rounded edges, smooth or soft surfaces. Additionally, impact forces can be minimized by incorporating energy-absorbing features such as padding, cushioning, deformable components, and compliant joints or links. Lastly, reducing the moving mass of the industrial robot further assists in lowering potential risks during contact. ISO 10218-1:2025 [2] and ISO 10218-2:2025 [3] continue to emphasize these design considerations under their sections on PFL and safety requirements.

Active risk mitigation strategies in ISO/TS 15066:2016 [18] focus on reducing risks by controlling the industrial robot movement and response. This includes limiting forces, torques, and velocities of moving parts, as well as restricting momentum, mechanical power, or energy based on mass and speed.

Safety-rated functions, such as soft axis and space limiting or monitored stop functions, supports to ensure a safer operation. Additionally, sensing technologies, like proximity or contact detection, can anticipate or detect contact to reduce quasi-static forces and enhance overall safety. These active strategies are explained in ISO 10218-2:2025 [3], Annex N, which provides detailed procedures for validating collaborative robot systems based on PFL mechanisms.

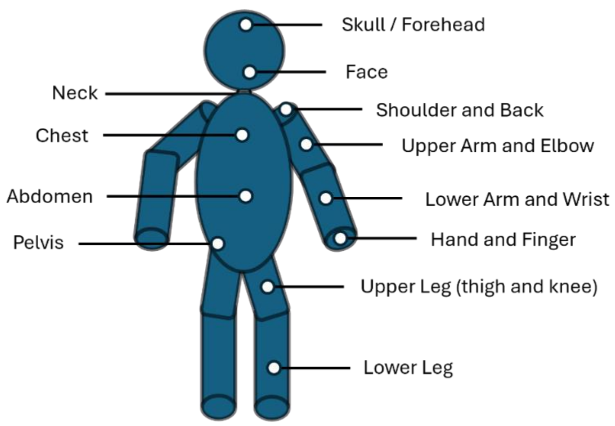

Figure 8 Illustration of different human body regions used to assess contact safety limits in human-robot collaboration, as defined in ISO/TS 15066:2016 [18] and ISO 10218-2:2025 [3].

2.3 Vision Based Quality Inspection in Manufacturing

This chapter outlines the hierarchical structure of quality management in manufacturing, emphasizing the roles of quality assurance, quality control, and inspection in ensuring product reliability and supporting zero-defect production. Followed by different machine vision system configurations, comparing their applications, limitations and relevance for quality control in modern manufacturing environments.

2.3.1 Quality Management and Control in Manufacturing

In a production setting, quality management focuses on how well the defined design specifications align with the manufacturing process [7]. This concept can be categorized into different subgroups, as displayed in Figure 9. The overall quality framework is called quality management, where quality assurance plays a strategic role in preventing defects and ensuring compliance with predefined quality standards [7].

Quality assurance focuses on the proactive identification of potential quality issues early in the manufacturing process, ensuring both customer satisfaction and product reliability [7]. As a subgroup of quality assurance, quality control takes a reactive approach, focusing on activities and procedures that ensure the product meets the highest quality standards [7]. These procedures, activities and proactive identifications are important to ensure the quality in the process and needs to be quantified by evaluation metricise to confirm the quality precautions are working and the quality of the product is met.

Therefore, quality inspection is an important task in the quality control process. This involves the systematic evaluation of a product either during or after the manufacturing process [7]. Deviations from the desired quality standard is quickly identified and corrected [7]. Typical steps in quality control involves evaluating the actual performance, comparing the system to the defined goals and taking corrective actions by addressing any discrepancies [7]. This ensures the product meets the quality standards defined by the design specifications. In the current production state quality control is often done manually, with humans inspecting the parts and writing down the results [25]. This process can happen several times during the production process and is repetitive, time-consuming, and cognitively intensive [25].

Quality control is considered as a non-value adding activity since this process ensures and not improves the quality of a product. However, the quality inspection process adds indirectly value by preventing faulty products from leaving the manufacturing, protecting customer satisfaction, and reducing waste [23]. This is essential for a zero-defect manufacturing.

Figure 9 Demonstrating the hierarchy of the quality sense in the production, highlighting quality control as a subset within the framework of quality management and assurance, based on Papavasileiou et al. [7].

2.3.2 Use case of Machine Vision in Quality Control

Machine vision plays a central role in modern automated quality control systems by capturing and analysing images to detect defects, inconsistencies, or deviations in products. By identifying issues early on, actions can be taken to ensure the product quality before leaving the production line. Machine vision is a general term to describe image-based methodologies and automatic inspection techniques which are used in manufacturing and engineering [7]. The key hardware components of a machine vision system typically include high-resolution cameras, appropriate lighting, and depth sensors. On the software side, image processing algorithms are applied to interpret visual data, identify quality deviations, and initiate appropriate actions. Additionally, a vision system is used to dynamically recognize the human presence and adjust the industrial robot behaviour.

Several studies have focused on integrating fixed machine vision systems into industrial quality control environments. One such example is presented by A. Gisginis [9] who developed and evaluated a fixed machine vision approach with an industrial robot system. The core objective is to fully automate the inspection process, reducing the reliance on manual quality checks. In this system, a dedicated stationary vision setup is used to inspect parts for surface and dimensional defects before a separate industrial robot is handling them. The study investigates through production lines which are currently operated almost entirely manually and are being considered for optimization using Industry 4.0 technologies such as industrial robots in a collaborative application and automated visual inspection systems. Concluding that implementing an automated vision inspection system is both possible and beneficial, improving accuracy, consistency, and efficiency in the quality control process [9]. The study highlights that an automated vision inspection system outperforms human inspectors in repetitive visual tasks and reduces human error in the quality assurance process. However, the study also acknowledged challenges in adapting the system to product variations, especially in terms of object size, inspection angle, and lighting conditions. These limitations suggest that while fixed systems are highly efficient in standardized environments, also highlighting the missing adaptability in dynamic production lines.

To increase flexibility without fully automating camera positioning, Bindel [26] introduced a semi-fixed vision system integrated into a metrology stand. Although the study offers useful insights, the study is not peer-reviewed and should be interpreted as a design concept rather than a validated industrial solution. The system is capable of inspecting more complex regions of automotive components by allowing the vision system to be repositioned manually for each inspection point. The core goal of the study is to achieve high accuracy using point cloud data captured by the vision system in comparison to the digital model.

The point clouds are analysed using mathematical algorithms to detect dimensional deviations and surface irregularities. Any discrepancies beyond a set tolerance are flagged as defects. While the results outline this approach could capture complex geometries with high precision, exposes several drawbacks which are the needed time, as well as needing an human to change the position[26]. Other concerns are the potential for mechanical fatigue in repetitive use, including accuracy inconsistencies, lack of reproducibility and complex setup requirements [26].

Modern machine vision systems are using pattern recognition, deep learning, and anomaly detection to improve the quality control process. The YOLO-based object detection model, which is investigated by Hsu et al. [27], can assist the robot to spot missing parts by comparing expected features with real-time images. In this research the focus is on a fixed vision system and a gripper mounted as an end-effector on the industrial robot in a collaborative application. Newer systems can combine the model with 3D point cloud data, so the robot also knows exactly where the object is in space. This makes the movement and interaction for the robot and the parts easier, even if the setup changes.

While A. Gisginis [9] already demonstrated the use of both a fixed vision system and an industrial robot in separate stages, combining these into a robot-mounted vision system presents an opportunity for a fully flexible inspection platform. This concept and the application to industrial robots in a collaborative application is explored further in following Section 2.4.

2.4 Overview of HRC Workstations using Vision Systems

Recent explorative studies investigate the combination of HRC and a machine vision system in the context of the manufacturing and quality control process. A. Gisginis [9] investigates the feasibility of integrating industrial robots in a collaborative application with a vision systems for the quality inspection process. The study explores how different setups can address production bottlenecks and improve consistency in inspection outcomes. Highlighting the possibility that the combination of HRC and a machine vision system can reduce production bottlenecks and enhance product reliability. Similarly, Papavasileiou et al. [7] review advancements in industrial robots used in a collaborative application for a quality control process. Their review focuses on setups that aim to make the process more flexible and efficient. While these studies show that such systems could work in theory, more research is needed to test them in real production settings and to solve integration and setup challenges. Matheson et al. [5] explore the challenges of integrating HRC in real-world manufacturing, highlighting safety and adaptability as the key parameters for possible widespread implementation. However, research on real-world quality control applications remains limited, making this difficult to assess their full industrial potential.

Instead of exploring complete real-world applications in a production environment, recent explorative studies investigate laboratory and simulation applications. One of this studies is the research in zero-defect manufacturing by Villalonga et al. [23] which supports the importance of a HRC vision based quality inspection system to improve productivity and sustainability. The prototype line in this study uses two industrial robots and a computer vision with AI models for the quality inspection, resulting in an accurate and efficient process. This study introduces a flexible and adaptable quality inspection system for various manufacturing processes. The system consists of an industrial robotic manipulator, a high-resolution camera, visual inspection with classification based on AI, and an Automated Guided Vehicle (AGV) for transporting the inspected piece based on the classification results. This approach enhances automation, accuracy, and efficiency in quality control [23]. A key feature of this prototype is the integration of the YOLO version 10 object detection model. By leveraging deep learning the system can efficiently classify different products while reducing human involvement to improve the safety aspect [23]. The study demonstrates that AI based vision inspection significantly improves quality control, reduces waste, and enhances operational efficiency, aligning with Industry 5.0 principles.

In a related study, Jafari-Tabrizi et al. [25] present and assess a methodology for automated scanning of 3D surfaces in a quality inspection, relying only on visual feedback. The study demonstrates that industrial robot learning trajectory optimization can work with AI-driven decision-making. Also demonstrating that the automatic trajectory can be generated only with an industrial robot and a camera as the end-effector as the only sensor which saves costs and reduces complexity [25]. This suggests that an industrial robots used in a collaborative application equipped with a vision system as the end-effector can autonomously determine trajectories for specific tasks.

Similarly Bindel [26] develops an automatic quality measuring device designed for an ease of use by combining an industrial robot used in a collaborative application based on PFL strategies and a vision system as an end-effector. The system offers effective handling, precise positioning, glowing ring feedback, and mobility on wheels [26]. The built-in operator station further simplifies operation, making the system both efficient and user-friendly. One of the main features of this study is the customised GUI which simplifies the industrial robot operation by enabling an intuitive playback programming method. With the "zero gravity mode" humans can easily guide the industrial robot arm to record precise motions, which are then stored for future use. Another significant advantage of the HRC workstation in general is the ability to add and hold positions for measurement to ensure the accurate data collection while maintaining an efficient and user-friendly process [26].

Based on the previously mentioned literature review study conducted by Arents et al. [21], looking through 46 peer-reviewed research articles from 2017 until 2021 and reviewing actual implementations, lab testing and simulations of HRC systems. The findings are that 3D cameras are the most used devices, followed by force/tactile sensors and wearables. Laser scanners appeared in some studies, while virtual reality and augmented reality, 2D cameras, and microphones/speakers are the least used. This highlights a strong preference for 3D vision and tactile sensing technologies in HRC applications.

Both studies by Jafari-Tabrizi et al. [25] and Bindel [26] are presenting potential advantages and feasibility of having an industrial robot is used in a collaborative application with PFL strategies and a machine vision as an end-effector. Showing also the possibility of planning an automatic trajectory by one sensor in the system, the machine vision system. Having the possibility of a HG operation in a PFL mode highlights an ease of use by dynamically positioning the new measurement points.

Additionally, Villalonga et al. [23] support the feasibility and advantages of using an industrial robot in a collaborative application with PFL strategies and a machine vision system as an end-effector. Furthermore, demonstrating how deep learning-based models like the YOLO-based object detection to improve an HRC quality inspection workstation and can be trained on a custom dataset to classify manufacturing defects with high precision. The experimental results demonstrate a high true positive rate for defect detection, significantly improving inspection accuracy compared to traditional visual checks. The YOLO-based system enables automated decision-making, where the autonomous mobile robots dynamically routes inspected pieces based on the output of the classification algorithm. This integration reduces manual intervention but also accelerates defect identification, supporting the goal of zero-defect manufacturing.

However, safety remains a major challenge in these implementations the study by Jafari-Tabrizi et al. [25] and Villalonga et al. [23] considers no safety aspects and shows therefore only the possibility of such a system whereas the study by Bindel [26] outlines implemented safety measures to ensure a secure and efficient HRC workstation by complying with ISO 10218-1:2011 [16] and ISO/TS 15066:2016 [26]. The system ensures safety through collision risk assessments, physical safeguards with a protection cage and secure docking, human features such as a three-way enabling switch and glowing status rings, and automated error detection with controlled movement to prevent unintended operations [26]. Mentioning that these measures create a reliable and safe working setup for the quality measurement tasks [26]. The HRC prototype by Bindel [26] also proposes that a comprehensive risk assessment and risk reduction needs to be done to ensure that the prototype is mature enough for implementation in the manufacturing process [26].

The design of the end-effector is not part of the industrial robots system used in a collaborative application which is designed to be safe and therefore meets not necessarily the requirements of the safety assurance [12]. The study neglects mentioning if the collision by the tool is within the thresholds of ISO/TS 15066. Villalonga et al. [23] research further supports that machine vision, AI, and industrial robots used in a collaborative application can drive zero defect manufacturing strategies, enabling real-time defect detection, automated decision-making, and improved human-robot safety. Therefore, this study is implementing some safety aspects but is not guaranteeing a comprehensive risk assessment and evaluation. Based on the previously mentioned literature review study conducted by Arents et al. [21], the findings where that 12 studies does not use any safety actions and 29 studies did not use any standard to assure safety in a workspace [21]. This presents that proper risk assessment and safety improvements are often missing in research and even more in real-world applications, especially since HRI studies are labelled as real-world but are not fully implemented in actual industrial environments.

2.5 Summary

This section summarizes the related work and key findings, focusing on the design of a safe and efficient HRC workstation. Examining theoretical frameworks, design principles, and safety standards while exploring the impact of risk assessments, PFL strategies, and regulations on feasibility, implementation, and scalability. Finally, the integration of a vision system is discussed to enhance quality control.

2.5.1 Theoretical Frameworks and Design Principles for a HRC Workstation

A safe and efficient HRC workstation for the quality control process relies on several theoretical frameworks and design principles. Theoretical frameworks, such as task allocation frameworks assist in dividing the work effectively between the industrial robot and the human. Where the industrial robot can focus on the repetitive and mentally demanding tasks whereas the human focusses on complex decision making. Additionally, HRI models define the different levels of collaboration showing the task allocation in the form of workspaces. These levels range from coexistence, where humans and industrial robots work independently in the same space, to responsive collaboration, where industrial robots dynamically adapt to human actions. Furthermore, HRI safety frameworks such as PFL strategies can support the application of an industrial robot to operate safely in close proximity to humans, minimizing risks and enhancing collaborative efficiency. Finally, an easily reprogrammable inspection pipeline should be included, ensuring adaptability to different product variations and a smooth quality control integration.

Incorporating key design principles is essential for creating a safe and efficient HRC workstation. A modular and flexible layout allows for easy reconfiguration in a fenceless HRI setup ensuring adaptability to different tasks. Together with passive and active risk mitigation strategies, outlined in ISO/TS 15066:2016 [18], these modular and flexible layouts enhance both safety and efficiency in collaborative environments. Passive strategies focus on mechanical design, using rounded edges, soft materials, and energy-absorbing features to reduce impact severity. Active strategies control industrial robot behaviour dynamically, limiting forces, torques, and velocities, while safety-rated functions like soft axis limiting and monitored stops prevent hazardous movements. Additionally, integrating a user-friendly programming interface and HG features enhances the accessibility by non-experts. Prioritizing human protection from the beginning in the design process ensures a safe workstation. This can be achieved by integrating safety measures such as PFL strategies to minimize risks during the collaboration task. The industrial robot needs to be designed to limit the power and force and to detect an occurring contact situation.

By applying these theoretical frameworks and design principles, HRC workstations can achieve optimal safety and efficiency, enabling smooth HRC while minimizing risks and maximizing productivity.

2.5.2 The Feasibility, Implementation, and Scalability of a HRC Workstation

The success of a HRC workstation depends on feasibility, implementation, and scalability. All of them are influenced by risk assessment methods, safety strategies and compliance standards.

Feasibility requires compliance with ISO 12100:2010 [1], which is mandatory for CE marking under the Machinery Regulation [4], replacing Machinery Directive [10]. Requiring a comprehensive risk assessment process with following risk mitigations. The risk assessment process is based on ISO 12100:2010 [1] and needs to be done iteratively based on Machinery Directive [10] and Machinery Regulation [4]. Based on ISO 10218-2:2011 [17] and ISO 10218-2:2025 [3] the risk assessment needs to evaluate the industrial robot characteristics, workplace layout, human interactions, and safety functions, leading to an increasing design complexity. This process must also consider foreseeable misuse, requiring diverse input to identify all potential hazards. Only using an industrial robot with a PFL strategy would simplify the risk assessment by limiting the industrial robot force and power, reducing the need for additional safety measures. ISO/TS 15066:2016 [18] and ISO 10218-2:2025 [3] set biomechanical limits for the HRI, but since these do not apply to the head, feasibility becomes more difficult.

Influence on the implementation, following international compliance standards ensures regulatory approval and reduces legal risks and operational inconsistencies. The risk assessment process, based on ISO 12100:2010 [1], involves three key steps. Firstly, the identification of risks which can be done with ISO/TS 15066:2016 [18] and ISO 10218:2011 [16, 17] and ISO 10218:2025 [2, 3]. Secondly, the evaluation of hazard severity and likelihood, and risk reduction through a safe design and protective measures like speed limits and emergency stops which can be done with ISO/TS 15066:2016 [18] and ISO 10218:2011 [16, 17] and ISO 10218:2025 [2, 3]. Finally, the verification and validation mentioned in 10218:2011 [16, 17] and ISO 10218:2025 [2, 3] can require practical testing, compliance evaluations, and protective stop mechanisms to ensure industrial robots remain within safe operating limits. However, multiple compliance checks increase implementation time and cost.

For scalability, a repeatable risk assessment framework allows easy expansion to multiple workstations. Compliance with ISO 12100:2010 [1], 10218:2011 [16, 17] and ISO 10218:2025 [2, 3] and standardizes safety procedures ensure consistency across different sites. Additional risk assessments must be conducted when modifying or expanding the system in a new environment, ensuring continued safety. Lastly, compliance with ISO/TS 15066:2016 [18] and ISO 10218:2025 [2, 3] ensure that force and pressure limits stay within safe thresholds, potentially enabling a reliable and scalable HRC workstation.

2.5.3 Vision System Integration into a HRC Quality Control Workstation

Integrating a vision system into a HRC workstation is important for automating the quality control tasks. A well-designed vision system improves the ability of an industrial robot to inspect dynamically and to provide feedback of the quality of the object. Different vision system approaches offer varying levels of flexibility, each with advantages and limitations.

Fixed vision systems are designed for inspecting static objects at predefined positions and can provide high accuracy under consistent conditions. These systems are typically configured for specific tasks and may require adjustments if the object design or inspection requirements change. Semi-fixed vision systems offer adjustable viewing angles, which can support a wider range of inspection tasks. Although these semi-flexible systems provide more flexibility than fixed systems, these systems generally involve manual repositioning to select different measurement points.

The most flexible approach in automation is a vision system mounted on an industrial robot. This allows the industrial robot to dynamically adjust the inspection trajectory. These systems integrate machine vision-based defect detection, reducing human workload and enabling autonomous quality control. A key implementation method for missing component detection is a YOLO-based object detection. This technology allows the industrial robot to recognize missing parts by comparing expected product features with captured images, improving accuracy and efficiency in the quality control task.

Successful integration requires real-time feedback, allowing industrial robots in a collaborative application to adjust their inspection process dynamically. Additionally, consistent lighting and precise camera calibration are crucial for maintaining accuracy.

2.6 Research Gap

Research on HRC and machine vision advanced significantly by improving automation and safety in the manufacturing environment. While previous studies highlight the advantages and possibilities of integrating an HRC system with a vision system, these studies do not extensively explore the real-world application of a fully integrated vision system in an industrial robot which is used in a collaborative application for automated quality control in a flexible, fenceless industrial setting. Despite the extensive research on HRC and machine vision, several critical gaps are remaining.

Most existing research focuses on theoretical frameworks or isolated subsystems rather than real-world applications in flexible, fenceless industrial settings. Despite the wide research area and the availability, there are few implemented HRC cases in the real-world manufacturing process [12]. A key challenge is the practical design and implementation of industrial robots used in a collaborative application, where safety must be embedded in the structures, motion controls, mechanical systems, and shared workspaces of the industrial robot is used in a collaborative application [12]. Matheson et al. [5] come to the conclusion that the key parameter for widespread implementation of HRC in manufacturing is the safety and adaptability aspect.

Based on the explorative study conducted by Arents et al. [21] , looking through 46 peer-reviewed research articles from 2017 until 2021 and reviewing actual implementations, lab testing and simulations of HRC applications, the conclusion is PFL in an HRC case shows the most promising results. Analysing these studies found that a real-world HRC prototype is not applied in the manufacturing or that any reviewed research has done a proper risk analysis [21]. Additionally, demonstrating in half of the conducted studies with PFL and HRC relevant safety standards have been referenced, leading to the other half with no referencing of any relevant safety standard [21]. This highlights the need for a comprehensive risk assessment and safety integration in both research and real-world applications.

This thesis aims to bridge these gaps by designing, implementing, and evaluating a prototype of a real-world HRC workstation with an embedded vision system that ensures both efficiency and compliance with safety standards in a practical use case. The thesis contributes knowledge to the fields of industrial robots in a collaborative application and industrial automation by advancing research on a safe HRC and vision-based defect detection system. Furthermore, the thesis provides insights into the feasibility of integrating a safe machine vision and industrial robot is used in a collaborative application design to reduce human workload in repetitive, time-consuming, and cognitively intensive tasks.

This thesis builds on these findings by designing a prototype HRC workstation with an integrated vision system. This advances the state-of-the-art in automated quality control. The thesis aims to address gaps related to real-world implementation, safety compliance, and dynamic HRI in industrial environments based on the quality control process.

The field HRC holds great potential in both Industry 4.0, where the efficiency, safety, and productivity can be enhanced, and Industry 5.0, which emphasizes human creativity and collaboration with machines which is the core principles of HRI and HRC [15].

3 Method

The following sub-sections outline the applied methodology in this thesis. Beginning with a justification of the methodology by highlighting the reasons for the selection and resulting benefits. This is followed by an explanation, including the method, resources, and evaluation methods which are applied in this thesis.

3.1 Introduction

The method of this thesis is the Design Research Methodology, selected from K. Säfsten and M. Gustavsson, Research methodology 2.0 : For engineers and other problem-solvers [28]. This provides a structured approach for researching and integrating various methods to support the product and process development [28]. The reason for selecting this method in this thesis is due to the structured, iterative nature which allows for theoretical exploration as well as practical implementation, as presented in Figure 10.

Other methods also offer useful perspectives. Action Research focuses on working with people in real situations, aiming to improve collaboration and organizational practices rather than creating a product [28]. Case Study Research helps to understand existing systems in depth but does not support developing and refining a new prototype [28].

The Design Research Methodology approach ensures a balance between understanding existing challenges, designing an effective solution, and evaluating the real-world applicability. Each step in Figure 10 from the methodology until the product and process development provides knowledge and leads to further improvement for the following step. This methodology is particularly advantageous for the context of HRC, by progressing through research and safety compliances by ending up at the final design of a functional prototype. Therefore, this approach supports the problem-solving systematics by validating the proposed solution.

3.2 Design Research Methodology

This thesis follows the Design Research Methodology based on K. Säfsten and M. Gustavsson [28]. This method in Figure 10 investigates and designs a framework for a

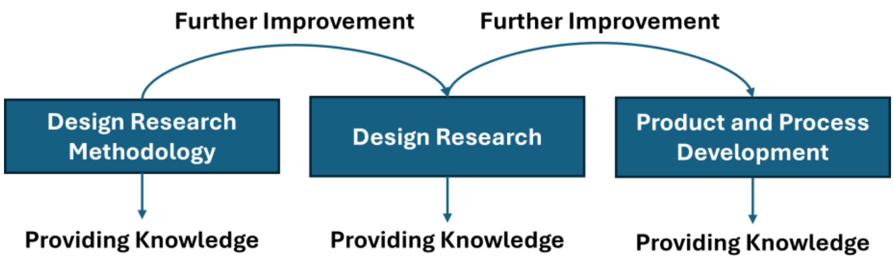

Figure 10 Demonstrating the Design Research Methodology, highlighting the improvement until the development of the product and process, by providing knowledge at each step, based on K. Säfsten and M. Gustavsson [28].

safe HRC case in a quality control process. The method progresses through four structured phases: The Research Clarification, Descriptive Study I, Prescriptive Study, and Descriptive Study II to ensure a methodical approach [28].

The approach of each step and the deliverables as well as the results are demonstrated in Figure 11. Starting with the first step the Research Clarification. This establishes the foundation for the thesis. This phase involves a brief overview of key areas relevant to the thesis. Including HRC, machine vision in quality control, and safety considerations for industrial robots in a collaborative application. The objective is to identify existing solutions, challenges, and research gaps. Additionally, an initial assessment of the current quality control process for a specific part at the Smart Factory Lab of Scania CV AB is conducted. The desired future state of an HRC workstation is outlined, envisioning a system where the human and industrial robot collaborate in a quality control application. Finally, the overall research plan, objectives, and goals are structured to guide the thesis.

The second step, presented in Figure 11, is the Descriptive Study I. By understanding the present state, the baseline for the further design needs to be formed. This phase involves a detailed literature review to understand the current state of HRC, the machine vision applications, and the required safety features and standards. The thesis examines how the inspection task can be performed, how humans and industrial robots in a collaborative application interact and how machine vision can support in detecting missing objects. Key success criteria, such as task efficiency and safety compliance are established for system evaluation. The outcome is a comprehensive understanding of the present state. This forms a baseline for the further design.

The third step, demonstrated in Figure 11, is the Prescriptive Study. Therefore, designing and implementing the solution is based on the previous phase and building the foundation for the last phase. Using insights from Descriptive Study I, the HRC workstation prototype is designed and implemented conceptual in a prototype line at the Smart Factory Lab of Scania CV AB. The industrial robot is used in a collaborative application is programmed to perform a quality inspection by adjusting the movement to capture images from multiple angles. The vision system is configured to detect missing components and safety measures get tested to ensure compliance with industry standards. This phase ensures the system is functional and aligns with the defined success criteria.

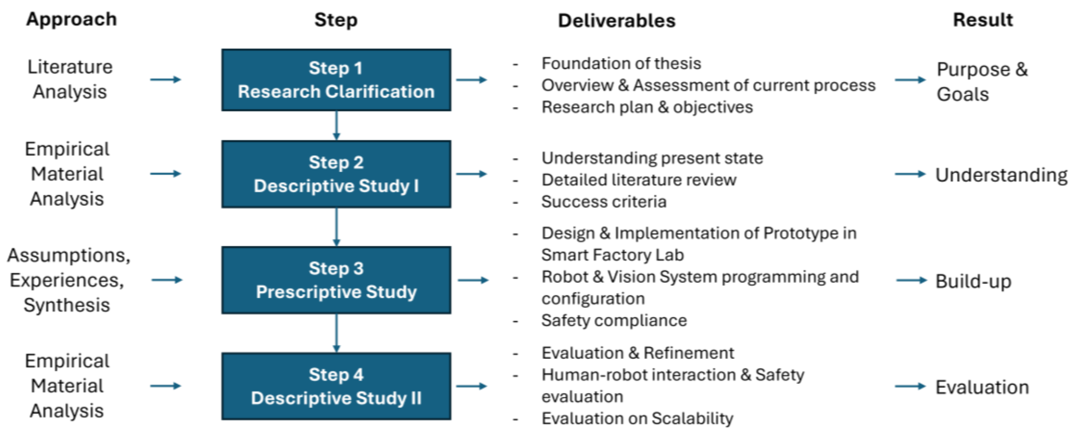

Figure 11 Illustration of the Design Research Methodology, showing the step-by-step improvement leading to product and process development by providing knowledge at each step, based on K. Säfsten and M. Gustavsson [28].

The last step, outlined in Figure 11, is the Descriptive Study II and is evaluating and refining the system. The final phase evaluates the HRC workstation performance in identifying missing parts, HRI, and safety compliance. The data of the vision system accuracy, the movement of the industrial robot is used in a collaborative application and engineer feedback from Scania CV AB assesses how well the system supports automated quality control while ensuring safety. The safety evaluation verifies the additionally needed risk management. Based on the findings, refinements are made to optimize the safety integration. This phase concludes with an assessment of the system success and recommendations for future industrial implementation.

3.3 Resources

The used resources in this thesis are divided into used hardware, software, and other resources. Starting with the hardware to make this thesis possible in a real-world scenario there is a need for an industrial robot used in a collaborative application. Therefore, the ABB GoFa CRB 15000-10/1.52, a PFL industrial robot used in a collaborative application is applied for conducting the quality control tasks in the HRC environment. Additionally, there is a need for an industrial camera and an efficient lighting setup to make the inspection process possible and to ensure consistent image quality. The integration of the vision system to the industrial robot is used in a collaborative application needs to be done by printing additional mounting equipment in a 3D-Printer. The real-world test scenario is a component from the manufacturing line within Scania CV AB and is already on site.

Going further to the software needs for this thesis. For once there is the industrial robot is used in a collaborative application programming tool which is called Wizard Easy Programming from ABB and can be done within RobotStudio 2024.2.1 to configure and simulate the industrial robot is used in a collaborative application task. Additionally, to create basic image processing the framework for implementing a vision system needs to be available. These are tools such as OpenCV and the YOLO-based object detection model. Since the main scope in this thesis is on the HRC and safety part the existing YOLO-based object detection framework is serving as a foundation for vision system integration in the HRC workstation. This model can be trained on object detection and is designed to detect missing components using a machine vision camera.

Other resources which are not hardware or software based is for example the required lab space. Therefore, access to the Smart Factory Lab of Scania CV AB for deploying and testing the prototype in a controlled environment and getting additional support from engineers of Scania CV AB for system testing and safety feedback.

3.4 Evaluation Methods

The success of this thesis is determined based on key performance criteria related to safety validation, risk reduction, and industrial feasibility. Compliance with international safety standards is verified through force and pressure calculations as well as physical measurements. The response of the robot is tested in a controlled worst-case collision scenario to assess the behaviour of the system under realistic operating conditions.

Risk assessments are conducted using international safety frameworks, including ISO 12100:2010 [1] and ISO 10218-2:2025 [3], to ensure a safe HRI. Calculated and measured values are compared against biomechanical safety thresholds from ISO 10218-2:2025 to validate safe operation during transient contact.

The potential industrial deployment of the system is assessed through a proof-of-concept demonstration in a laboratory environment, supported by Automation and Safety Engineers at Scania CV AB. The input regarding the layout, safety concept, and operational flexibility is gathered and analysed to evaluate practical readiness.

Quantitative data, such as calculated and measured contact forces and pressures, are presented in tables and compared to normative limits from ISO 10218-2:2025 [3]. Qualitative data, including professional evaluations from Engineers, are summarized to assess the relevance of the system for future use in real production environments. These findings are compared to the research aims to determine whether the workstation meets the requirements for safe HRC workstation.

4 Design of the Workstation

This chapter describes the design and setup of the HRC workstation which is developed for the vision-based quality inspection task in this thesis. The goal is to create a safe, flexible, and modular system which integrates an industrial robot with a mounted vision system to inspect components. The design process focuses on a practical application in an industrial-like environment. Key elements include the hardware layout, software architecture, vision system integration, and collaboration design based on PFL which is following safety standards.

4.1 Application Scope and Context

This thesis focuses on the design of a collaborative robot application for the quality inspection in a flexible production environment at the Smart Factory Lab from Scania CV AB. In the context of Industry 4.0 and 5.0, ensuring high product quality while enabling a flexible human centred automation is a key challenge. This thesis addresses this by integrating machine vision, robot control, and safety mechanisms into an HRC workstation. The system is designed to detect missing components early in the process, allowing for corrections before the final assembly. The following sections outline the process context, the ideal concept, and the detailed inspection steps.

4.1.1 Process Context and Operational Environment

In the industrial manufacturing environment of Industry 4.0 and Industry 5.0, ensuring the high-quality standards are met is important in fulfilling the customer expectations as well as in reducing the production losses. One of the defined challenges from the literature study in this thesis are the intermediate quality control tasks between different production sections, as highlighted in Figure 12.

In the manufacturing and in this thesis, the component is assembled in earlier steps of the line and transferred on an AGV to the quality inspection station. The quality of the part is assessed and results in a final decision about the approved or not approved quality of the component. These results are sent to an overall Manufacturing Execution

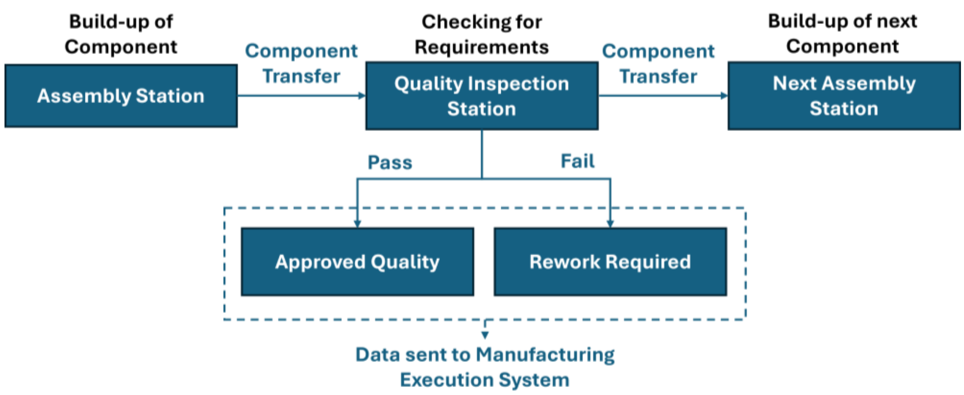

Figure 12 Manufacturing process in a general production line, with a focus on quality assurance by verifying that components meet defined quality requirements and transmitting the status to the Manufacturing Execution System.

System. The following step is dependent on the design of the complete process and the severity of the failure. When the quality failure is fixable the system can trigger a rework which is required on this part. If the failure is deemed too severe, the part is no longer repairable and is classified as a complete production loss

The specific task addressed in this thesis involves detecting missing components in a prototype of a Flexible Assembly Line in the Smart Factory Lab from Scania CV AB. These failures can result in missing components and are therefore fixable in future steps of the line or can be solved by routing the AGV through the same station again. To achieve zero-defect manufacturing, quality checks are required to ensure the standards and requirements are met [6]. Therefore, the following section is formulating the ideal HRC workstation to achieve an automated and collaborative solution.

4.1.2 Design Criteria for the HRC Workstation

The concept of an ideal HRC workstation is shown in Figure 13 in the centre of the three key topics concerning and always influencing this thesis work in the following sections. These are the areas of machine vision, robot integration, and safety compliance. For a collaborative application to be effective in a real industrial context, these topics must work seamlessly together.

A robust vision-based robot requires both accurate object recognition and the ability to adapt to dynamic conditions. However, this is only effective when paired with a safe integration approach by ensuring the robot motion and human interaction are both predictable and controlled. Also, the vision-based safety layer ensures that the machine vision does not only inspect quality but also contributes actively to a safe collaboration.

By combining the three elements, the ideal HRC quality control workstation can be demonstrated in the centre of Figure 13, where a vision system is not only functional and precise, but also safely embedded within the robotic structure. This configuration ensures compliance with safety standards, supports intuitive human interaction through technologies like HG, and bridges the gap between a prototype lab setup and a deployable industrial solution.

By selecting an industrial relevant use case and applying safety and system design methods, this thesis bridges the gap between academic research and industrial

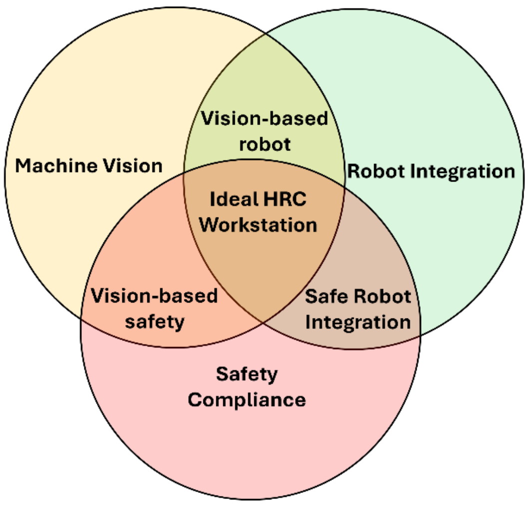

Figure 13 Demonstrating the overlap between machine vision, robot integration, and safety compliance. The central intersection represents the ideal HRC workstation, by integrating an industrial robot with machine vision and safety.

application. The solution is not only theoretically grounded but also practically oriented, responding directly to the needs of Scania CV AB.

4.1.3 Overview and the Task Sequence in the Quality Inspection Process

The inspection process begins, as visualized in Figure 14, when the AGV arrives and stops the movement at the HRC workstation. The robot is ready and in a predefined home position waiting for the AGV to stop and send a signal. Once the signal arrives, both the robot and the AGV are ready to begin the operation.

The first step in the inspection sequence involves the examination of the top bracket with the fixture screws. This step makes sure that all components are correctly positioned according to the assembly specifications. Once this is verified, the system proceeds to inspect the alignment of the cables and the red tape indicator, which serves as a visual reference or quality indicator for proper component orientation. Following this inspection a general check of all relevant screws is performed, ensuring none are missing. The final inspection task involves the evaluation of the side bracket and the screws. This step confirms that the bracket, cables and screws are placed and meets the quality requirements.

After all inspection tasks are completed, the robot returns to the predefined home position and the AGV resumes the movement. The AGV then exits the station, marking the end of the inspection cycle, as visualized in Figure 14. This process allows for a fully automated, sequential quality control routine which minimises the human intervention.

Due to time constraints, the quality inspection process in this thesis focuses on checking whether components are present or missing. The objective is not to evaluate the accuracy of the YOLO-based object detection model in detail, but to demonstrate that the approach provides a fast and reliable solution that supports the main objective of the thesis. The developing of a safe and effective HRC workstation with appropriate safety considerations.

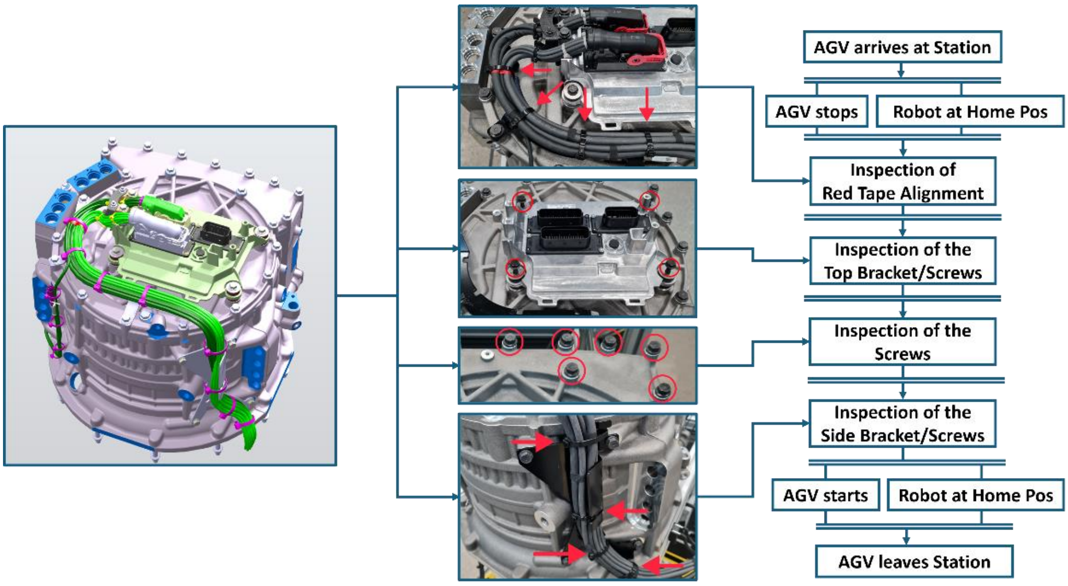

Figure 14 Process flow of the automated inspection sequence at the station. The AGV arrives and stops at the station, triggering the robot to perform a series of inspections on various components. After the inspection is completed, the AGV resumes movement and leaves the station.

4.2 Workstation Structure

The workstation structure lays out the foundation of the HRC workstation. Only by combining the robotic hardware, an integrated vision system, and the communication between the components as well as to the overall system the HRC workstation is a completely functional station inside the prototype line. The system is designed for flexibility, fast decision-making, and seamless interaction between the human and the robot as well as to the overall system. The following sections outline the key hardware components, software setup, and communication structures that support this HRC workstation.

4.2.1 Hardware Components and Layout

The initial layout of the workstation is designed to conduct a collaborative quality inspection as presented in Figure 15. There the key hardware components and the spatial arrangement are displayed within the layout. One of the main elements is the articulated industrial robot arm with PFL strategies, which is mounted on a fixed stage. Industrial robots in a collaborative application like the ABB GoFa CRB 15000-10/1.52 can sense the changes in the torque of the joint and apply thresholds to these changes. Therefore, once the contact occurs these discrepancies between the theoretical movement and the actual movement is measured and can be inferred to an impact event [29].

Additionally, the zero gravity mode from Bindel [26] is considered as an industrial robot which is used in a collaborative application with HG which is for example in an ABB GoFa CRB 15000-10/1.52 a build in function. The human can press one of the programmed arm-side interface buttons and teach the industrial robot with HG a certain position of the tool. Using such an industrial robot from the beginning reduces the time in building such a system and keeps the advantage that the humans can easily guide the industrial robot arm. These arm-side interface buttons are two buttons located on the robot itself, implemented directly on the robot arm to allow the human to interact with the system during HG or setup tasks.

To enable mobility and integration with the existing logistics processes, the workstation also includes an AGV as displayed in Figure 15. The AGV autonomously

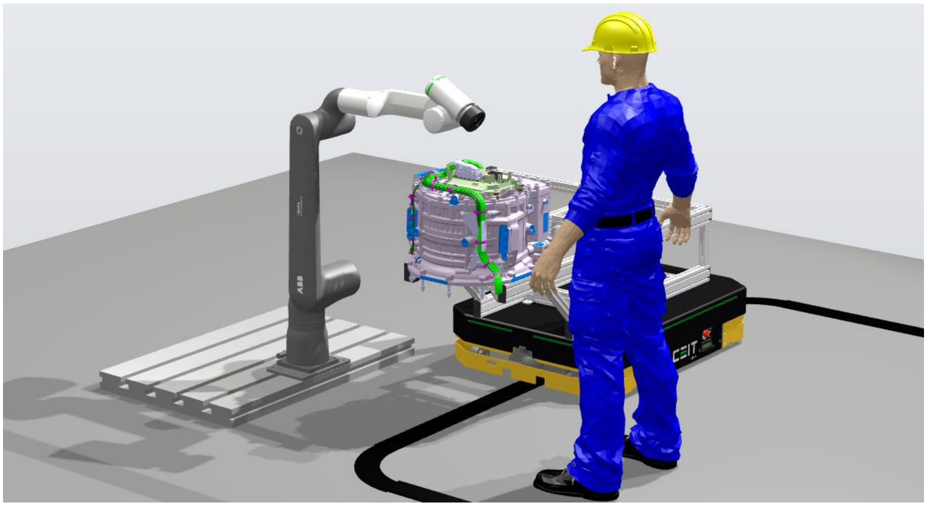

Figure 15 Illustration of the collaborative workstation setup featuring the ABB GoFa CRB 15000-10/1.52 robotic arm equipped with an Intel RealSense Depth Camera D435, an AGV transporting a part to the HRC workstation and a human.

transports parts and components between designated stations. In this specific setup, the part to be inspected is a component sourced from Scania CV AB. The AGV delivers the part directly to the robot workstation, where the collaborative inspection process starts.

The industrial robot is equipped with an integrated vision system which is shown in Figure 16 and is mounted as the end-effector, to perform the inspection task. For this application, the Intel RealSense Depth Camera D435 is selected as the optimal vision system based on a thorough evaluation of key performance criteria including field of view, image resolution, focus capabilities, and system integration.

The Intel RealSense D435 offers stereo vision and utilizes a global shutter, making this well-suited for motion-heavy or low-light environments, where minimizing motion blur is crucial. Featuring a field of view of 87° × 58°, the widest among all Intel RealSense cameras, which is ideal for applications requiring large area coverage with minimal repositioning [30]. This fits the case of the different angles in this inspection task of the robot.

In terms of resolution and responsiveness, the Intel RealSense D435 provides 2 megapixels in red, green and blue pixels at 1920 × 1080 which are 30 frames per second and a depth output up to 1280 × 720 which are 90 frames per second [30]. The auto focus range from 0.3 meters to 3 meters ensures that image sharpness is maintained across different inspection distances [30]. This highlights an advantage for a robotic arm that adjusts height and orientation during operation. This flexibility outperforms fixed-focus systems like the InspectorP65x from the SICK AG, especially in dynamic multi-depth inspections.

Another significant advantage is the compatibility with open-source platforms, including full integration with Python and the Intel RealSense Software Development Kit 2.0 [30]. This allows direct connection to the YOLO-based object detection model used in this thesis. Alternative systems such as the Balluff GmbH or SICK AG cameras impose complexity or licensing constraints. The Universal Serial Bus Type-C connection also simplifies connectivity, eliminating the need for industrial power over ethernet switches or converters required by other stereo cameras like the OAK-D Pro PoE from the Luxonis Corporation.

Beyond the technical possibilities, the Intel RealSense D435 stands out as a robust and flexible all-rounder. The compact design and broad operating range up to 3 meters, and low-light sensitivity highlights a good solution for robotic navigation, object recognition, and collaborative inspection tasks. Enabling quick deployment, seamless integration, and consistent performance which highlights an appropriate choice for this collaborative workstation setup. The camera together with a specifically designed tool made from a micro carbon fibre filled nylon material to fit the hardware as illustrated in Figure 16 can be mounted as the end-effector on the robot.

Figure 16 Custom end-effector design for the Intel RealSense D435 depth camera, designed for a seamless and safe integration into the robotic inspection system.

4.2.2 Software Components and internal System Communication

In order to meet the layout and hardware requirements, several software components and internal communication protocols must be configured. Reliable communication between the machine vision system and the robot is important to ensure an accurate quality evaluation. Only once this underlying system is in place the collaborative workstation tasks can be built upon, setting the foundation for HRC.

Figure 17 illustrates the structure of the Server/Client-Communication used for this robotic quality inspection system. The server side in Figure 17 is represented by the robot and initiates the inspection sequence by moving to the predefined quality inspection position. The server sends information about which inspection model to use and waits for the evaluation results from the vision system.

If the initial quality assessment fails, the robot can slightly adjust the position and recheck the part to mitigate potential false negatives. If the second assessment also fails, this status is communicated to the higher-level system, which can then trigger the necessary rework in subsequent steps. Regardless, the robot continues with the next quality inspection. If the part passes the inspection, this status is also reported to the upper system, and the robot proceeds directly to the next inspection point.

The client side shown in Figure 17, implemented as a Python script running on a computer, receives the instruction regarding which trained model to use for the vision inspection. This accesses the camera, captures an image, and processes the data using a YOLO-based object detection model. The detection result, along with a confidence score, is evaluated against a predefined threshold to minimize the likelihood of error.

More detailed information on this process is provided in Section 4.3 on page 37. The final quality status is then sent back to the robot, which executes the next corresponding sequence and starts the process again. This setup ensures a modular, flexible, and closed-loop system for an automated visual quality control using AI-based object detection.

The socket-based communication structure between the server running on the robot and the client, both implemented in Python, is illustrated in Figure 18 as a continuation of the setup shown in Figure 17. The underlining structure is the Transmission Control Protocol / Internet Protocol (TCP/IP). On the server side, the process begins with a creation of a socket, followed by binding the socket to an IP and port, and then listening for incoming connections.

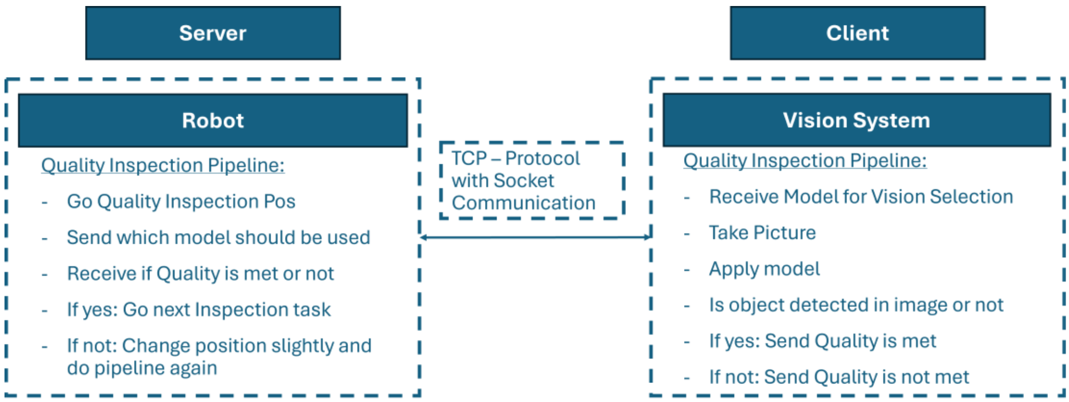

Figure 17 Illustration of an integrated quality inspection system, where a robotic unit performs operational tasks, and an AI-powered vision system conducts defect detection. Data exchange is achieved via Transmission Control Protocol (TCP/IP) socket communication, enabling synchronized decision-making.

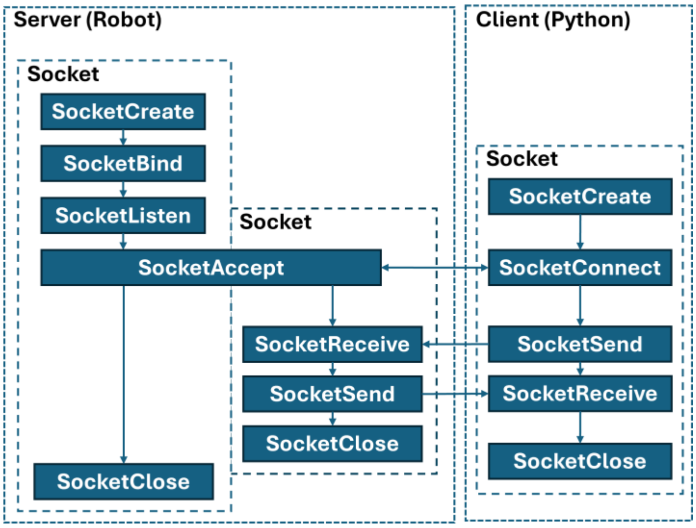

Figure 18 Illustration of the socket communication between the server, represented by the robot, and the client, a Python script running on a computer, based on ABB Ltd. [31]

When the client in Figure 18 attempts to connect, the server accepts the connection and creates a new communication socket dedicated to this client. Data is then exchanged in both directions by receiving and sending a socket. When the communication ends the socket is closed.

On the client side in Figure 18, a socket is similarly created and connects to the server. The client can similarly send and receive data through the corresponding socket until the communication is complete. This structure forms the underlying communication between the robot and the external vision system, ensuring synchronized operations in the collaborative quality inspection process.

4.2.3 System Overview Diagram

The HRC workstation needs to determine whether the inspected product meets the quality requirements. As previously described in Subsection 4.1.1 on page 30, this quality status needs to be communicated to the overall Manufacturing Execution System or to the Product-Lifecycle-Management System. In the industrial-like setting of the Smart Factory Lab at Scania CV AB, communication is intended to take place via the Message Queuing Telemetry Transport (MQTT) protocol in the future. As the complete line is not fully built, the proposed connection to the overall system is described but not fully implemented in the scope of this thesis. Figure 19 presents the suggestion for the communication to the overall system. To bridge the gap between the workstation and the system, a Broker/Client-Communication structure needs to be employed.

This structure needs to ensure a seamless, safe and reliable data exchange between the HRC workstation which operates on a TCP/IP based communication protocol, and the central server system, which communicates via the MQTT protocol a publish and subscribe messaging model used in industrial internet of things environments.

The TCP/IP communication allows for stable, real-time interaction at the production level, where the robot workstation performs the quality inspections. In contrast, MQTT supports asynchronous, scalable communication to the overall system, enabling status updates, alerts, and data logs to be efficiently routed without interrupting the ongoing processes.

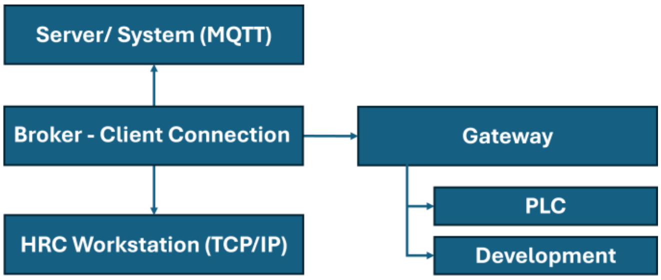

Figure 19 Overview of the communication structure integrating MQTT and TCP protocols for connecting the HRC workstation to the centralized system. The Gateway links the production-level devices and the server system by either a special development or a Programmable Logic Controller (PLC).

At the centre of this system there is a need for a gateway, acting as a translation layer between the TCP/IP based workstation communication and the MQTT server to ensure a compatibility between both systems. This can be done either by a Programmable Logic Controller or a special gateway in the Smart Factory Lab. The industrial standard with safety features would be a Programmable Logic Controller.

This system structure supports a modular and scalable solution for integrating the robotic quality inspection process with the higher-level production systems. This solution ensures a safe, robust and real-time data flow across layers of the industrial automation while remaining adaptable to future protocol extensions.

4.3 Vision System Integration

To enable the autonomous quality inspection within the HRC workstation, a vision system is integrated. The vision system allows the robot to make decisions based on a visual input by detecting specific features of the product. This section outlines the technical setup of the camera, the configuration of the YOLO-based object detection model, and the full inspection workflow, including model training, dataset preparation, and the feedback loop to the robot which is used during the operation. Together, these components form a flexible and robust structure while being able to adapt to evolving production requirements and maintaining accuracy and efficiency.

4.3.1 Inspection Workflow and Feedback Loop

To approach an efficient integration of the vision system within the HRC workstation, the Python environment is designed in a modular structure. The requirements for the environment are that the modern production line can have products, inspection criteria, or detection models which may change over time. By separating core functionalities into dedicated modules, the system can be updated or extended.

The structure of the Main Environment is shown in Figure 20 and acts as a central controller with three following key modules. The YOLO-Model-Communication module handles the interaction with the trained object detection model, processing the captured image and returning detection results. Therefore, deciding the quality is approved or not. The Server/Client-Communication module manages the data exchange between the robot, which is acting as a server, and the vision system, which is acting as the client, enabling real-time feedback to trigger robot actions based on inspection outcomes. The Camera-Communication module accesses directly the camera hardware, capturing images when triggered and preparing for processing.

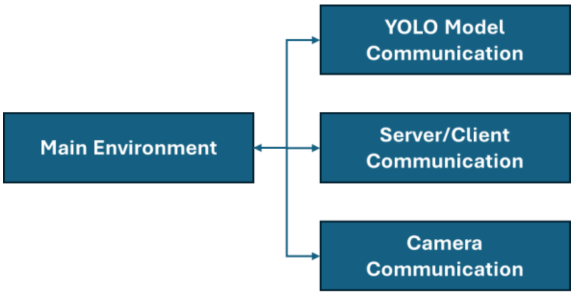

Figure 20 Modular structure of the Python-based inspection environment, illustrating the interaction between the Main Environment and the key components which are the YOLO-Model-Communication, Server/Client-Communication, and the Camera-Communication.

This modular setup in Figure 20 enables flexible substitution or upgrading of individual components, by switching to a different camera model or retraining the new YOLO-based object detection model. The feedback loop is closed by sending the inspection result from the YOLO-based object detection model back through the Server/Client-Communication module to inform the robot which is responding by sending the next action. This streamlined structure ensures a reliable and responsive inspection workflow within the collaborative environment.

4.3.2 Vision Pipeline Development and Model Training

The integration of the vision system requires a robust pipeline to process the images captured by the camera and evaluating by using an object detection algorithm. In this case, a YOLO-based object detection model is used for the detection. The model must first be properly trained with relevant data before deployment.

By configuring the pipeline, the future adaptability and ease of use for a production line is considered. Therefore, the process needs to be modular, scalable, and easily maintainable, allowing for quick adjustments to new product variants, changes in inspection criteria, or integration of improved models without requiring major reengineering.

Figure 21 illustrates the training workflow used to train the YOLO-based object detection model for the HRC quality inspection task. The process begins in Figure 21 by image acquisition, where a comprehensive dataset of the component images is captured. Creating a high-quality dataset is important for the process. The dataset includes variations in angle, lighting conditions and background to ensure the model learns to generalize across different scenarios. The data is labelled and is classified.

Following the image collection in Figure 21, the next step is the manual labelling, where bounding boxes are drawn around key features or defect areas of interest. In this thesis the software Roboflow from Roboflow Inc. is used to organize and label the data which introduces no license constrains for this process. Each labelled object is assigned a class, helping the model to understand the important features in the image. However, other software tools can also be used for data labelling, as long as they support annotation formats compatible with the chosen model and offer sufficient flexibility for organizing and managing the dataset.

Preprocessing the dataset and training the model would introduce license constrains. Therefore, the dataset then feeds into the local training phase, where the YOLO-based object detection model is trained on the annotated dataset using computational resources either on a local workstation or a remote device.

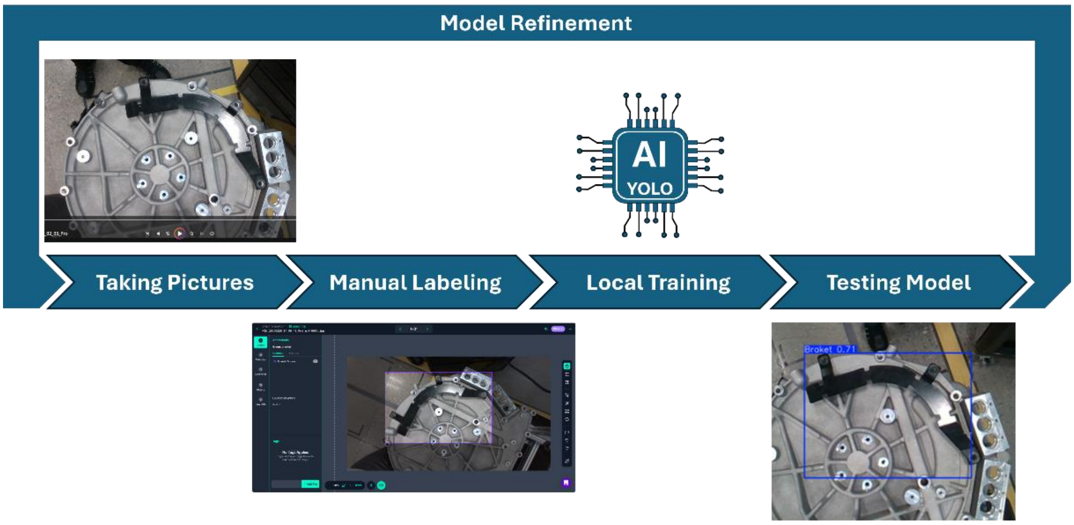

Figure 21 Workflow of the YOLO-based object detection model refinement process, illustrating the steps of capturing images, manually labelling key features, performing local training, and testing the model to ensure accurate detection for automated quality inspection in the HRC workstation.

After the training of the model in Figure 21 the testing begins to validate the solution, is predicting the missing objects on the models. The model should only determine whether the part is fully present and correctly assembled. Additionally, the system can feedback which feature is or is not meeting the requirement.

4.3.3 Training steps and parameters

In this thesis, YOLO11 is used as the foundation for training. YOLO11 enables several improvements for better and faster computer vision tasks. An upgraded design helps in detecting objects more accurately and handling complex situations [32]. The model runs quickly and efficiently, maintaining a strong balance between speed and accuracy [32]. Deployment works across various environments, including edge devices, cloud systems, and NVIDIA GPU platforms and a wide range of tasks are supported, such as object detection, image classification, pose estimation [32]. These enhancements make YOLO11 a reasonable choice for deployment in collaborative robot inspection tasks, where both speed and accuracy are important.

To fully leverage the capabilities of YOLO11, careful attention must be given to the structure and balance of the training data, as the quality and distribution of the input directly impact the performance of the model in detecting both the present and missing components.

The labelled images are categorized as true positives and true negatives. To ensure the model performs well across both classes, the importance is to manage the class distribution carefully. Ideally, the dataset should be balanced, meaning the number of true positives and true negatives are approximately equal. This helps to prevent the model from becoming biased toward predicting one class over the other. This is particularly important in cases in which the two classes are equally important as this is the case in this thesis by detecting both the presence and absence of an object. If the dataset is highly imbalanced, with many more true negatives than true positives, techniques such as class weighting or resampling can be used to correct this imbalance.

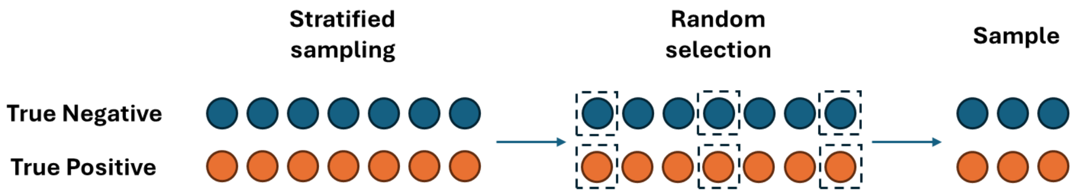

Figure 22 Stratified random sampling process is used to ensure balanced representation of classes. True Negative and True Positive samples are first grouped by class, followed by random selection within each group to create a representative and balanced final sample set.

As illustrated in Figure 22 the dataset is split using stratified random sampling, which ensures that both classes are represented proportionally in the training, validation, and test set, preventing bias and supporting the ability of the model to generalize to unseen data. The training set, which is 70 % of the images, the validation set which is 20% of the images, and the test set which is 10 % of the images.

After splitting the dataset using stratified random sampling, several preprocessing and data augmentation steps are applied to the training set before training the model. First, auto-orient is applied to the images to ensure the images are correctly aligned, followed by auto contrast adjustment to enhance the visibility and clarity of the whole dataset.

To further expand the training dataset and make the model more robust, data augmentation is performed. This involves adjusting the brightness of the images within a range of -15% to +15% to simulate different lighting conditions and rotating the images between -15 to +15 degrees to account for variations in orientation. These augmentations create diverse variations of the original images, helping the model generalize better. The validation and test sets remain unaltered, maintaining their role as unbiased evaluations of model performance. The augmentation process generates 6 variants per image, significantly expanding the size of the training dataset. This increase helps the model learn more robust features by exposing to a wide range of transformations.

By using the training set, the model learns how to recognize and differentiate the target features based on the labelled data. The validation set helps to fine-tune the model during the training by evaluating the performance after each epoch and preventing overfitting. The test set remains unseen during training and is used after the model is fully trained to provide an unbiased evaluation of the real-world detection performance.

The YOLO-based object detection model is a machine learning model [33]. This is trained by adjusting the internal parameters to minimize the error. The model is fed a large training dataset with labelled images and makes predictions. These are compared to the actual labels to calculate the error which shows how far the model is away from the true values. The model iteratively makes predictions and updates the parameters to minimize the error which is called Backpropagation [33]. With increasing epochs, the model learns the features and improves the accuracy and reduces the error. This happens until a certain point where the training error still decreases but the validation error goes up again. There the model is overfitting, and the model becomes too complex and does not generalize well. Therefore, the model needs early stopping to prevent this from happening. The selected hyperparameters for training are summarized in Table 1. These include the number of training epochs and the early stopping patience value, which helps to balance learning efficiency and model generalization.

Table 1. Selected hyperparameters used during model training, including the maximum number of training epochs and the early stopping patience threshold.

Hyperparameter	Values
Epochs	500
Patience	50

The test set will be used to assess the accuracy, precision, recall, and overall confidence scores of the model, ensuring the model generalizes well to new images and is suitable for deployment in the production like prototype environment. This structured approach in training and evaluation helps to guarantee the reliability of the vision system in the real-world HRC tasks.

Once training is complete, the model is tested on new, unseen images in the real process to evaluate the detection accuracy. This test phase verifies whether the model can correctly identify the required features under different environmental conditions. If the results are unsatisfactory, additional refinement through more training data or hyperparameter tuning may be necessary.

Ultimately, once the trained model reaches a reliable level of accuracy, the model can be deployed within the vision system pipeline. During operation, the camera captures live images, which are then processed through the trained YOLO-based object detection model to detect specific quality indicators. The resulting evaluation is used to decide whether the product passes inspection, contributing directly to the collaborative decision-making process in the HRC workstation.

4.3.4 Limitations of Training the Vision System

Despite the overall robustness of the implemented vision pipeline, several limitations exist which influence the performance and adaptability of the models in this thesis. Due to the time constraints of this thesis building a comprehensive dataset with representative variations across different setups and changes in lighting, angles, position and hyperparameter to generalize and better train the model is not possible.

To overcome these challenges and prepare the system for an industrial-scale deployment, the pipeline is intentionally developed to be modular, scalable, and easy to maintain. This allows for rapid integration of new product variants, updates in inspection criteria, and the application of enhanced detection models without requiring a complete change of the system.

Creating models through the vision pipeline development process, as described in Subchapter 4.3.2 on page 38, can be automated and contributes significantly to time efficiency by reducing the need for manual intervention during model development. In this context, Intel Geti is evaluated as a complementary tool. Intel Geti supports automated labelling, training, and deployment, and in practice, shows how to reduce the development time compared to the traditional manual workflow involving data acquisition and hyperparameter tuning.

Although the initial model in this thesis is trained using a custom YOLO-based pipeline, the same training sequence is replicated in Intel Geti to increase the speed of deployable YOLO-based object detection models.

4.4 Human-Robot Collaboration Design

The following section details the design behind the HRC workstation developed in this thesis. The proposed setup directly aligns with the overall aim of this thesis in designing a safe and effective HRC workstation by combining PFL technology with a vision-based inspection system in an industrial-like environment at the Smart Factory Lab from Scania CV AB. The design integrates established safety standards and theories about HRI, translating academic principles into practical, safety-driven engineering decisions. Furthermore, addresses the core investigative questions by implementing real-world safety mechanisms and HRI strategies.

4.4.1 Inspection Workflow and Feedback Loop

To approach an efficient integration of the robot system within the HRC workstation, the RAPID and Wizard Easy Programming on the ABB robot system, is designed in a modular structure. The requirements for the environment are that the modern production line can have products, inspection criteria, or detection models which may change over time. By separating core functionalities into dedicated modules, the system can be updated or extended.

The structure of the Main Environment is shown in Figure 23 and acts as the central controller of the inspection process. This is implemented using RAPID and Wizard Easy Programming from the robot system, coordinating three core functional modules:

- Inspection-Positions: This module defines the predefined positions of the robot for each inspection task. These positions can be updated directly on the Flex Pendant either by jogging the robot manually or using the HG feature. This makes the process intuitive and adaptable, allowing quick reconfiguration without modifying the core program structure.
- Server/Client-Communication: This module manages the data exchange between the robot which is acting as a server, and the vision system which is acting as a client. Based on the inspection results from the vision system, the robot executes the appropriate next action.
- Human Machine Interface (HMI)-Communication: This part enables communication through a visual HMI interface with the software AppStudio from ABB Ltd. on the Flex Pendant or a potential HMI in a production setting, allowing the human to start, stop, or reset the inspection process.

Figure 23 shows the modular architecture of the control logic, where the Main Environment coordinates and exchanges information with the other components. The modularity supports future extension or reconfiguration such as changing inspection positions or updating communication logic without affecting the entire system.

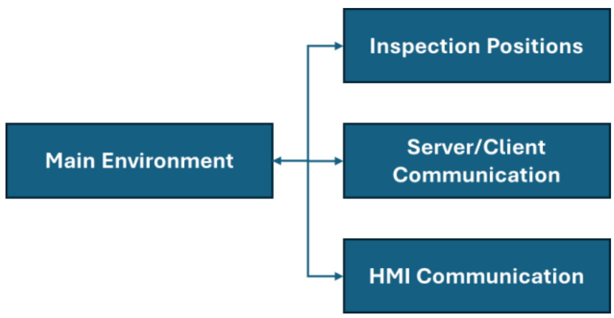

Figure 23 Modular structure of the robot-based inspection environment, illustrating the interaction between the Main Environment and the key components which are the Inspection Positions, Server/Client Communication, and Human Machine Interface (HMI) Communication. The setup is implemented using RAPID and Wizard Easy Programming on the ABB Flex Pendant.

4.4.2 Collaboration Type and Operational Design in a PFL-Based HRC Workstation

The integration of the robotic system requires a robust definition of the HRI to enable a safe collaboration. The HRC design in this thesis uses an industrial robot with PFL strategies as the collaboration technology. PFL strategies allow the robot to work safely near humans without needing safety fences, as long as the impact stays within the biomechanical limits for force and pressure of the defined body parts. These limits are defined in the international guideline ISO/TS 15066:2016 [18] and the updated safety standard ISO 10218-2:2025 [3]. This design follows these standards, along with the Machinery Regulation [4], to ensure that the design meets necessary safety requirements for HRC.

The robot and the human in this setup work in a coexistence mode which fits into the second level of HRI from Subchapter 2.1.3. This means the human and robot work in different workspaces and perform different tasks at the same time. In this design the robot works automatically without specific human intervention or collaboration. The human can watch over the process and step in the workspace if needed.

During inspection, the AGV stops at the station, and the robot performs the inspection tasks. Each inspection point is assigned a defined position, which can easily be adjusted if needed. The robot can either be moved manually using the Flex Pendant interface or guided using the HG function to the desired position. The new position can be stored directly into the robot program. After the inspection is done, the robot returns to a safe position, the home position and the AGV continues along the line. This setup reduces the chance of unsafe interactions and helps to keep tasks running smoothly. Because the human does not need to stand next to the robot during operation, this adds flexibility to how the workstation can be designed and used.

Once this setup shows a safe HRC workstation, there is the possibility of expanding the HRI level to sequential collaboration or cooperation. The key advantage of this workstation is the possibility to have a safe HRC workspace without having the complete need of a human in the same workspace and then afterwards introducing the shared work tasks, by additionally adding guidelines for the human on how to operate in the HRC environment. For example, the human could take over surface inspection tasks or work more closely with the robot, moving towards sequential collaboration or even cooperation. This would require updating the safety design and interaction rules.

4.4.3 Workspace Configuration and Safety Considerations

The collaborative workspace is designed to allow safe interactions between the human and the robot. The space is divided into clearly defined zones in which the robot has different rules depending on the configuration allowing controlled interaction. These safe zones are a virtual boundary created using the configuration tool SafeMove. A built-in safety functionality which allows the robot to operate in a fenceless or partially restricted environment while complying with functional safety standards.

SafeMove integrates safety supervision directly into the robot controller. The safety logic responds dynamically to the position, force and speed of the tool and the robot joints. The safety logic can be implemented as different virtual zones or globally for every movement position. The most relevant SafeMove functionalities used in the context of this thesis include:

- Tool Speed Supervision: This feature sets a maximum allowable speed for the tool centre point. If the speed is exceeding the threshold the controller will automatically reduce the speed or stop the motion within safe limits. This ensures the robot moves carefully in the shared zones or when operating near the human.

- Tool Force Supervision: This monitors the external forces acting on the tool centre point of the robot. By exceeding a defined threshold, the protective stop is triggered. Therefore, once a contact event occurs the external forces increases rapidly.
- Tool Position Supervision: With this function a specific safe zone and workspace can be defined. The robot can be allowed or denied moving in this zone. This prevents the robot from moving in restricted zones or to collide with infrastructure and the human.
- Human Contact Supervision: This function is the combination of the Tool Speed Supervision and the Tool Force Supervision by applying the biomechanical limits from ISO/TS 15066:2016 [18].

These functionalities are configured using RobotStudio and validated on the Flex Pendant. By using SafeMove, the behaviour of the robot becomes predictable and compliant with ISO/TS 15066:2016 [18] and ISO 10218-2:2025 [3].

The use of SafeMove in this application supports the thesis aim of designing a safe and efficient collaborative workstation. This allows the robot to adapt to different tasks within the designed safety features while minimizing physical risks to the human. This SafeMove and the implementation is the result of initial Risk Assessments which is described in the following sections.

5 Safety Analysis and Risk Assessment

The design and integration of a collaborative robot system requires a structured and standard-compliant risk assessment process. In this thesis, the risk analysis is conducted in accordance with the ISO 12100:2010 [1] framework, which defines a systematic approach through the key phases from the Subchapter 2.2.5 on page 15. These are the identified scope with the intended use and the following risk identification, risk estimation, risk evaluation, risk reduction and risk validation. This chapter outlines the methodology and practical implementation of each phase which are applied in this collaborative workstation in the Smart Factory Lab at Scania CV AB. Complementary standards such as ISO 10218-2:2025 [3], ISO/TS 15066:2016 [18], and the Machinery Regulation [4] are used to guide the design of the workstation and the implemented safety functions. The ABB SafeMove toolset is employed to enforce motion constraints in accordance with the defined risk mitigation strategies.

5.1 The intended use of the HRC Workstation

The intended use and the scope of this HRC workstation needs to be defined in the beginning of the risk assessment process to ensure a smooth and thorough process, as defined in ISO 12100:2010 [1]. The layout and use are shown in Figure 24. The HRC workstation performs a quality inspection in the Flexible Assembly Line of the Smart Factory Lab with the preassembled product. There are no takt time constraints, there can be a live demo where visitors are standing and walking around as in Figure 24, and the operation is a partly automated operation which requires a manual start. However, at the time of the thesis, the overall communication system is not yet fully developed or operational. As a result, the operator must manually trigger the signal on the Flex Pendant to start the automated process. This is by pressing the start button on the HMI

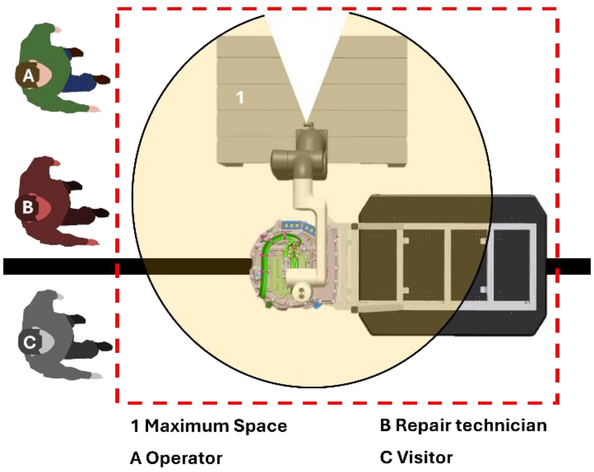

Figure 24 Top-down view of the HRC workstation illustrating defined safety and interaction zones. The red dashed box marks the maximum safety space, while the circular area indicates the operational range of the robot. Three user roles are defined as the operator, repair technician, and visitor, each representing different interaction and access levels within the station layout.

and therefore does not need specific training. The operational inspection limits are defined in Subchapter 4.1.3 on page 32 and the spatial limits are shown in Figure 24. The layout shows the maximum space of the robot and an operator, repair technician and visitors which can be present in the workstation. The humans can be present but should not necessarily be in the operating environment of the robot since the tasks and the inspection process of the robot are automated.

5.2 Risk Identification

The first phase involves systematically identifying all potential hazards associated with the interaction between the human, the ABB GoFa CRB 15000-10/1.52 robot, and the workstation environment. In the overall layout the risks are identified and classified into different subgroups which are the mechanical hazards, hazards arising from the design and reliability of the control system, additional non-mechanical hazards, maintenance and lack of adequate operational information or warnings. In accordance with ISO 12100:2010 [1] Chapter 5.3 and ISO 10218-2:2025 chapter 5.5, several hazards and risks have been identified in the workstation involving the AGV and the robot system. The complete risk identification for the whole workstation can be seen in Appendix A.

The following section outlines the risks associated with the collaborative inspection operation, including additional task-specific hazards which are identified. These relate to the robot configuration, the motion parameters, and the physical arrangement of the workstation. The following risks are assessed in accordance with ISO 12100:2010 [1] Chapter 5.3 and 6.2, ISO 10218-2:2025 [3] Chapter 5.3, 5.5, 5.7, 5.9 and Annex M as well as ISO 13854:2017 [34]:

- Maximum Operating Height: The maximum operating height must be restricted to prevent the robot from exceeding to a head height.
- Minimum Distance to Objects: The minimum operating distance to the closest object should be determined to eliminate any risk of clamping.
- Maximum Operating Space: The maximum operating space needs to be limited to the intended use of the workstation to prevent future changes from introducing a not considered hazard.
- Robot Base Height: The robot base position on a table is too high and needs to be lowered. The height should be as low as possible to prevent the robot from exceeding to a head height.
- Tool Speed Supervision: The speed of the robot can exceed a reasonable value and needs therefore be limited to minimize the possibility of the risk and harm.
- Tool Force Supervision: The force of the robot can exceed a reasonable value and therefore needs to be limited to minimize the possibility of the risk and harm.

With the relevant hazards identified and categorized, the next step involves evaluating the likelihood and severity of each potential risk. The following section provides a detailed estimation of these risks based on established safety standards and practical assessment methods.

5.3 Risk Estimation

The risk estimation is assessed using risk tables and guidelines from ISO 12100:2010 [1] supported by injury classification data and exposure thresholds from Annex C of

ISO 10218-2:2025 [3]. The risk estimation in this thesis is differentiated in the severity of potential harm, the frequency and duration of human exposure, the probability of occurrence of a hazardous event and possibility of hazard avoidance or limiting the damage. This ensures conformity with Annex C from ISO 10218-2:2025 [3], which is a normative section of the standard and therefore mandatory for compliance.

In reference to ISO 12100:2010 [1] where the factors are the severity of harm, exposure frequency, and possibility of avoidance are used to determine the necessary safety performance. Therefore, the possibility of avoidance in ISO 12100:2010 [1] is divided into the probability of occurrence of a hazardous event and the possibility of avoidance in Annex C from ISO 10218-2:2025 [3] which is also used in this thesis.

The process in this thesis classifies the interaction with the human and the collaborative inspection workstation as group A in Annex C from ISO 10218-2:2025 [3]. This is characterized by occasional and non-cyclic human presence. For example, tasks such as visual inspection or temporary manual intervention can fall under this category.

The severity of harm based on ISO 10218-2:2025 [3] is evaluated on the scale from minor to catastrophic which is shown in Table 2. This leads from mild pinching or bruising to permanent impairment or severe internal injuries.

Table 2. Classification of severity of harm (S) based on ISO 10218-2:2025 Annex C [3], ranging from minor to catastrophic injuries, this table categorizes potential harm.

Ranges	Explanation
S1 - Minor	Bruising, mild pinching, or temporary discomfort, no medical treatment required or may involve soft tissue compression without lasting effects.
S2 - Moderate	Superficial cuts, light sprains, or temporary injuries requiring basic first aid or no long-term impairment but some work interruption.
S3 - Serious	Bone fractures, deep lacerations, or injuries requiring medical attention and recovery time or potential for short-term disability.
S4 - Catastrophic	Permanent impairment, loss of limb, severe internal injury, or fatal outcome or high-level impact on human safety and system design requirements.

In addition to severity, the exposure E to hazards is a function of the frequency F of exposers in 48 hours, the duration D of each single exposure and the number of persons N_r which are exposed. Based on ISO 10218-2:2025 [3] each exposure to hazard can be estimated by

$$E = F \cdot D \cdot N_r$$

where the result is the exposure in minutes per 48 hours. The results are classified based on ISO 10218-2:2025 [3] as defined in Table 3 in either high or low. High exposure is defined as a frequency of more than four interactions per hour or more than 144 minutes over a 48-hour period, while low exposure refers to fewer than four interactions per hour or less than 144 minutes over the same period.

Table 3. Classification of frequency and duration of exposure (E) according to ISO 10218-2:2025 Annex C [3], based on interaction frequency and duration over a 48-hour period.

Ranges	Explanation
E1 - Low	$E < \frac{144\ minutes}{48\ hours}$ or $F < \frac{4\ interactions}{1\ hour}$
E2 - High	$E > \frac{144\ minutes}{48\ hours}$ or $F > \frac{4\ interactions}{1\ hour}$

The next factor considers the likelihood, a hazardous event will occur based on environmental conditions, system designs and the task complexity. This results in Table 4 to the probability of occurrence which is categorized based on ISO 10218-2:2025 [3]. The probability ranges from low which indicates a rare event under controlled conditions, to high where the hazard will likely or frequently occur due to the design of the process and the environment.

Table 4. Classification of the probability of occurrence of a hazardous event (O) according to ISO 10218-2:2025 Annex C [3], based on environmental conditions, system design, and task complexity.

Ranges	Explanation
O1 - Low	Rare event under controlled conditions or when fail-safes are in place
O2 - Medium	Occasional event, influenced by task, human error, or system complexity
O3 - High	Likely or frequent event due to environmental, design, or process factors

Finally, the ability of the human to avoid or mitigate the hazard is evaluated. This considers how visible and predictable the hazard is and how much time is available for the human to react. The possibility of avoidance based on ISO 10218-2:2025 [3] in Table 5 is the human ability to perceive and avoid the hazard in time. Indicating a not avoidable event which is sudden or hidden due to the operational constraints until an avoidable event which is clearly visible and can be easily avoided.

Table 5. Classification of the possibility of avoidance (A) according to ISO 10218-2:2025 Annex C [3], based on hazard visibility, predictability, and available reaction time.

Ranges	Explanation
A1 - Avoidable	Hazard is clearly visible and can be avoided easily with minimal effort or awareness.
A2 - Reasonably Avoidable	Hazard may be avoided if the human is alert and responds appropriately.
A3 - Not Avoidable	Hazard is sudden, hidden, or unavoidable due to operational constraints or limited reaction time.

The risk evaluation related to the collaborative operation in this thesis is summarized in the following Table 6. The estimation is based on a robot without any implemented limitations regarding force, speed, or height, and is therefore assessed under worst-case assumptions.

A robot operating over 1.5 meters from the ground at a high speed is classified as a catastrophic severity, where potential injuries might include a severe internal injury, or fatal outcome or high-level impact on the human safety. The frequency is less than four interactions per hour or less than 144 minutes over a 48-hour period since the human should not necessarily be there. The probability is considered high, which is a likely or frequent event due to environmental, design, or process factors. However, since the robot is moving at a high speed, the possibility of avoidance is not avoidable since the hazard is sudden, hidden, or unavoidable due to operational constraints or limited reaction time. The robot is operating at a head height with a high speed and is therefore a high risk.

Operating at a very low distance to an object is classified as serious severity, where potential injuries might include bone fractures, deep lacerations, or injuries requiring medical attention and recovery time. The frequency is less than four interactions per hour or less than 144 minutes over a 48-hour period since the human should not necessarily be there. The probability is considered high, which is a likely or frequent event due to environmental, design, or process factors. The possibility is classified as not avoidable because the hazard is sudden, hidden, or unavoidable due to limited visibility and reaction time. The robot can clamp the human with a high force and speed and is therefore a high risk.

Exceeding the maximum operating space outside of the intended use is considered serious severity, where potential injuries could include bone fractures or serious impacts requiring medical recovery. The frequency is less than four interactions per hour or less than 144 minutes over a 48-hour period. The probability is high due to a likely or frequent event when the robot moves outside controlled areas. Avoidance is classified as not avoidable since unintended motion outside of expected areas is sudden and may leave little opportunity for the human reaction. Exceeding the space is not within the intended use and is therefore not considered in this risk assessment and a high risk.

A robot positioned too high and unstable is classified as catastrophic severity, where injuries might involve permanent impairment, loss of limb, or fatal outcome. The frequency is less than four interactions per hour or less than 144 minutes over a 48-hour period since the human should not necessarily be there. The probability is high due to a likely or frequent event influenced by system design and operational instability. The possibility of avoidance is considered not avoidable because sudden robot movement on a high height would leave limited time for human reaction.

The tool speed exceeding reasonable limits is classified as catastrophic severity, where potential injuries might include a severe internal injury or a fatal outcome. The frequency is less than four interactions per hour or less than 144 minutes over a 48-hour period since the human is not part of the operating sequence. The probability is considered high, as the speed could be programmed as high as possible, and the events can frequently occur due to no implemented safety features. The hazard is considered not avoidable because high-speed tool movement is sudden and hidden, giving limited time for a human to react.

A tool force exceeding acceptable thresholds is classified as catastrophic severity, where possible injuries might include severe internal injury, permanent impairment, or fatal outcomes. The frequency is less than four interactions per hour or less than 144 minutes over a 48-hour period under normal working conditions with a low manual interaction. The probability is considered high, since excessive force can occur frequently when the limits have no implemented safety features and are not monitored. Avoidance is classified as not avoidable because a high force application is often sudden, and the human has little to no time to respond appropriately.

The complete risk estimation for the collaboration part of this workstation is shown in Appendix C. The risk estimations for all identified risks are due to time limits and constraints not carried out in this thesis.

Table 6. Summary of risk estimation for identified hazards in the collaborative workstation according to ISO 10218-2:2025 Annex C [3], categorizing each hazard by severity of harm (S), exposure (E), probability of occurrence (O), and possibility of avoidance (A) to support prioritization of risk reduction measures.

Hazard	S	E	O	A
Maximum Operating Height	S4 - Catastrophic	E1 - Low	O3 - High	A3 - Not Avoidable
Minimum Distance to Objects	S3 - Serious	E1 - Low	O3 - High	A3 - Not Avoidable
Maximum Operating Space	S3 - Serious	E1 - Low	O3 - High	A3 - Not Avoidable
Robot Base Height	S4 - Catastrophic	E1 - Low	O3 - High	A3 - Not Avoidable
Tool Speed Supervision	S4 - Catastrophic	E1 - Low	O3 - High	A3 - Not Avoidable
Tool Force Supervision	S4 - Catastrophic	E1 - Low	O3 - High	A3 - Not Avoidable

The initial identification together with the estimation of the risks results in a function which is not specifically stated in a standard but ISO 12100:2010 [1] defines the risk level as a function of the severity of potential harm S, the frequency and duration of human exposure E, the probability of occurrence of a hazardous event O and the possibility of hazard avoidance or limiting the damage A. The combined risk can therefore be estimated by using.

$$Risk\ Level = S \cdot E \cdot O \cdot A.$$

This expression is not explicitly found in any standard but serves as a practical interpretation for assessing risk levels. This provides a systematic basis to prioritize which risks require additional protective measures or functional safety features in the subsequent risk evaluation. This expression helps to prioritize which risks require additional protective measures or functional safety features in the following risk evaluation.

5.4 Risk Evaluation

The process of the risk evaluation decides the necessary risk reduction measures, such as the system needs a complete design change, change the way of using, the need for safety measures, additional information or can remain without measures. To further structure the interpretation of the risk scores, the overall distribution of the overall possible calculated scores is analysed and modelled. Therefore, all possible parameter combinations are multiplied, resulting in a distribution of risk scores. This distribution is illustrated in Figure 25 as a background histogram, showing where most scores are concentrated and where fewer occur.

The evaluation and how to categorize the necessary risk reduction measures are not specifically stated in ISO 12100:2010 [1] or ISO 10218-2:2025 [3]. Therefore, this thesis uses a practical interpretation of these standards, which is shown in the following method.

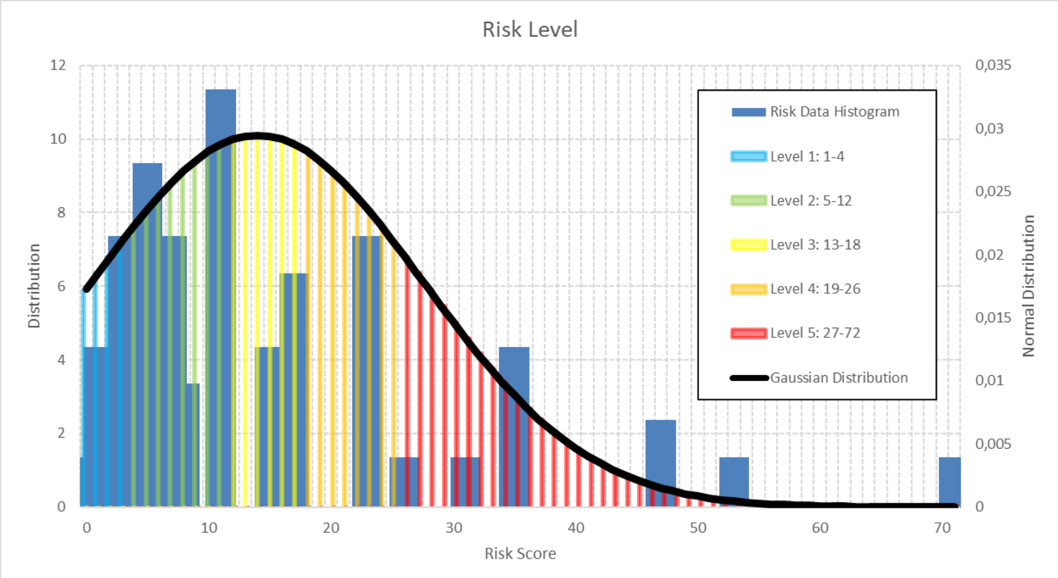

Figure 25 Risk score distribution and fitted Gaussian curve illustrating the categorization into five risk levels. Coloured bands represent different risk ranges, with level 1 to level 5 progressing from low to high risk.

The following levels are the possible levels based on the possible parameter combinations. A Gaussian normal distribution is also shown in Figure 25 and is used to assess the spread of the scores. The corresponding probability density function is defined as

$$f(x) = \frac{1}{\sigma \cdot 2 \cdot \pi} \cdot e^{-\frac{(x-\mu)^2}{2 \cdot \sigma^2}}$$

where μ represents the mean and σ the standard deviation of the distribution. The distribution of the histogram in Figure 25 resulted in $\mu = 15$ and in $\sigma = 13.54$. This statistical approach reflects the observation that the function to calculate the risk levels in the risk estimation, results in most hazards which are expected to exhibit moderate risk values, while very high or very low risks occur less frequently. Therefore, the distribution needs to be considered to ensure higher risk scores are not underrepresented in the final categorization.

Based on this model, the range of possible risk scores from 1 to 72 is subdivided into the predefined five risk levels. The boundaries between these levels are determined by selecting thresholds at regular cumulative probability intervals, specifically at the 20%, 40%, 60%, and 80% quantiles of the normal distribution which are represented in the different colours in Figure 25. This ensures a balanced classification across the full range of possible scores. The exact calculations are shown in Appendix B.

This method does not simply reflect the natural clustering of most hazards around moderate risk values but instead applies a structured approach that ensures each risk level contains an equal proportion of the possible risk score range. Although very high or very low risk scores may occur less frequently, this method prevents them from being underrepresented by dividing the fitted Gaussian distribution into equal cumulative probability intervals of 20%. This allows the higher risk scenarios to be given an appropriate weight in the evaluation. As a result, the classification supports a more balanced and systematic prioritization of risks. Therefore, Table 7 summarizes the final risk level categorization of the possible parameter combinations in the risk level function and the associated recommended actions.

Table 7. Classification of final risk levels based on calculated risk scores from the risk level model, using a Gaussian distribution to define thresholds at cumulative probability intervals in accordance with a structured interpretation of ISO 12100:2010 [1] and ISO 10218-2:2025 [3], supporting prioritization of appropriate risk reduction actions.

Range	Risk Level	Recommended Action
1-4	Level 1	Can remain without measures
5-12	Level 2	Can be mitigated by information
13-18	Level 3	Needs to implement safety measures
19-26	Level 4	Change the way of using
27-72	Level 5	Needs a design change

Following this methodology, the previously estimated risks for the industrial robot used in the collaborative application are assessed and assigned specific risk scores and corresponding risk levels, as shown in Table 8. The hazards result in the highest evaluated risk scores, falling into level 5, indicating critical areas requiring immediate redesign measures to ensure compliance with safety requirements and to achieve acceptable risk levels. The complete risk evaluation for the collaboration part of this workstation is shown in Appendix C.

Table 8. Risk level evaluation for the defined hazards in the collaborative workstation, assigning each identified hazard to a risk level based on the risk level scoring model and corresponding Gaussian-based categorization, supporting the selection of appropriate mitigation actions in alignment with ISO 12100:2010 [1] and ISO 10218-2:2025 [3].

Hazard	Risk Level	Recommended Action
Maximum Operating Height	Level 5	Needs a design change
Minimum Distance to Objects	Level 5	Needs a design change
Maximum Operating Space	Level 5	Needs a design change
Robot Base Height	Level 5	Needs a design change
Tool Speed Supervision	Level 5	Needs a design change
Tool Force Supervision	Level 5	Needs a design change

The risk evaluations for all identified risks are due to time limits and constraints not carried out in this thesis. Therefore, in the following the risk reductions for the collaboration part is analysed and is implemented.

5.5 Risk Reduction

The final phase involves selecting and implementing appropriate safety measures to reduce the identified and evaluated risks. The illustration of the risk reductions can be seen in Appendix D. These measures are categorized into passive and active strategies which are implemented in this thesis. The passive risk reduction measures can be categorized to:

- Rounded mechanical design of the robot arm and custom end-effector.
- The new layout introduces a "pallet" or small "stage" on which the robot is mounted, creating a subtle elevation that acts as a barrier without being a physical obstruction. The robot is positioned 100 millimetre above ground level. The risk of tripping of the robot platform is low, and the forces and torques involved are minimal, making this setup sufficient and acceptable for the intended use case.

- Spatial separation and marked floor zones to limit unnecessary overlap.
- Defined home position to prevent idle arm extension into human space where the robot is unfolding and going to the inspection positions.

Whereas the active risk reduction measures implemented via the ABB SafeMove can be concluded as:

- Tool Position Supervision: Which constrains the robot movement with safe zones. The maximum operating height is limited to 1.5 meter. In accordance with ISO 10218-2:2025 [3] and ISO 13854:2017 [34], the operating distance from the object is restricted to 180 millimetre at the top and 230 millimetre at the sides to ensure no clamping risks.
- Tool Speed Supervision: Enforcing speed limits dynamically during tasks. In accordance with ISO 10218-2:2025 [3] from Annex C, reducing the operating speed of the robot to 150 millimetre per second minimizes the possibility of the risk and harm. Outside of the work zones the speed is globally set to 250 millimetre per second.
- Tool Force Supervision: Detecting abnormal forces and triggering protective stops. In accordance with Annex M from ISO 10218 [3], reducing the operating force from the robot to under 65 newton minimizes the possibility of the risk and harm. This needs validation that the force and pressure is not exceeding. According to Table H.1 from ISO 10218:2025-2 [3]. Outside of the work zones the force are globally set to 65 newtons. This also needs validation that the pressure is not exceeding. According to Table H.1 from ISO 10218:2025-2 [3].

All implemented measures align with ISO 10218-2:2025 [3] requirements for an industrial robot which is used in collaborative application and are tested under realistic operating conditions in the Smart Factory Lab setup.

5.6 Risk Validation

Following the iterative risk reduction process defined in ISO 12100:2010 [1], the final step is to validate that all remaining risks have been sufficiently mitigated. For industrial robots in a collaborative application using PFL strategies, this involves biomechanical validation in accordance with ISO 10218-2:2025 [3]. Specifically, the industrial robot must demonstrate that any unintentional contact with a human remains below defined safety thresholds for force and pressure, ensuring human safety during the workspace operation. The validation process can be done by calculations and measurements.

The biomechanical limits and calculations are based on Annex N and M, which are informative sections of ISO 10218-2:2025 [3], which provide example values for different body regions during quasi-static and transient contact. Except for the skull, forehead, and face, the allowed limits for transient contact are generally at least twice as high as for the quasi-static contact.

These biomechanical values originate from research conducted by the University of Mainz to estimate human pain thresholds for robots in a collaborative application. The study represents current but limited research within this field on which the validation process is built on. The tests are conducted on 100 healthy adults where the pressure limits correspond to the 75th percentile of the recorded values. Showing that 75% of the participants experienced discomfort at this level.

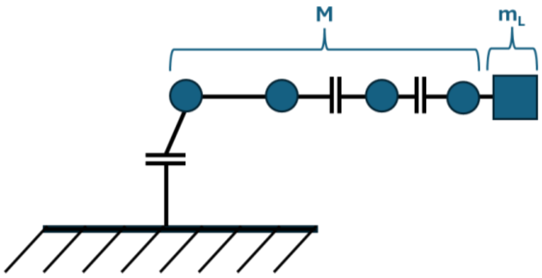

Figure 26 Schematic representation of a robot arm indicating the mass distribution relevant for the biomechanical validation. The moving mass M of the robot and the mass of the load or the end-effector m_L is contributing to the impact forces during a contact, based on ISO 10218-2:2025 [3].

To calculate the force and pressure of the robot used in a collaborative application the system can be simplified as in Figure 26 which illustrates the moving mass of the robot along with the end-effector. Since the end-effector is located at the farthest point from the robot base, a high proportion of the mass is considered in the calculation. In contrast, the moving mass of the robot arm is assumed to act at the midpoint of the lever arm, simplifying the effect to half the total arm length.

Therefore, with the simplified two-body system in Figure 26 based on ISO 10218-2:2025 [3] and the resulting formula

$$m_R = \frac{M}{2} + m_L$$

the moving mass m_R of the robot can be calculated with the total mass M of the robot arm and the mass m_L of the end-effector. The transient contact force F_T based on ISO 10218-2:2025 [3] can be calculated with

$$F_T = v_{rel} \cdot \sqrt{\frac{k}{\frac{1}{m_H} + \frac{1}{m_R}}}$$

which is using the moving mass m_R of the robot together with the velocity v_{rel} as well as the effective mass m_H and spring constant k of the body region of the human. Dividing the same formula by the contact area A leads to the transient pressure in

$$p_T = \frac{v_{rel}}{A} \cdot \sqrt{\frac{k}{\frac{1}{m_H} + \frac{1}{m_R}}}$$

where A is the smallest contact area on either the human or the robot side. According to the relationship between pressure and force defined in Annex N of ISO 10218-2:2025 [3] a large padded machine surface with a relative large surface area could lead to low pressures and could lead therefore to the force values which could be the limiting factor. The design of the workstation as well as the end-effector in this thesis considers the recommendation of the standard that the application should have a high contact surface areas as possible [3]. To ensure these values are in fact below the thresholds the workstation needs additional measurements to the calculations.

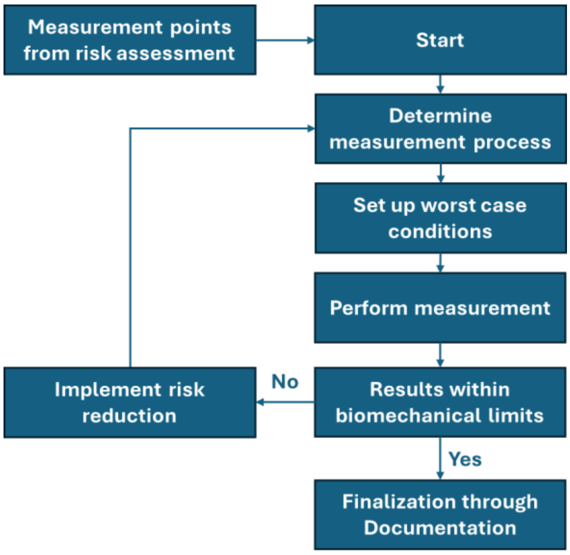

Figure 27 Measurement procedure for potential contact events according to ISO 10218-2:2025 [3], illustrating the iterative workflow for validating biomechanical compliance under worst-case conditions and guiding necessary risk reduction and documentation steps.

The measurement validation process, illustrated in Figure 27, begins with identifying the relevant measurement points derived from the comprehensive risk assessment. These points indicate where human-robot contact is most likely or critical. Based on these risk-relevant areas, a suitable measurement process is defined, including the selection of tools, test procedures, and impact conditions.

To ensure safety under realistic but challenging scenarios, the system is tested under worst-case conditions, which may include maximum robot speed, contact with rigid components, or edge-based collisions. The measurements in this thesis cover both quasi-static and transient contact events to reflect different types of potential human-robot interactions.

The measured data are then analysed to verify that the resulting forces and pressures remain below the biomechanical limits specified in Annex M and N, which are informative sections of ISO 10218-2:2025 [3]. The process from ISO 10218-2:2025 [3] includes measurements for both quasi-static and transient contact scenarios. These provide threshold values based on current biomechanical research and are used here to assess compliance.

If all measured values are within the defined safety limits, the process concludes with proper documentation to finalize the validation. However, if any values exceed these limits, risk reduction measures must be implemented. This may include adjustments to robot speed, contact surface materials, or end-effector geometry. The process is iterative, meaning that after implementing improvements, the measurement cycle must be repeated until full compliance is achieved. This structured approach ensures that the collaborative system meets safety expectations through a clear, repeatable validation loop grounded in international standards.

Since the design and operating sequence is explicitly designed to prevent any clamping conditions only the transient contact event will be validated. The risk verification and validation process can be performed using a commercially available Pressure and Force Measurement Device (PFMD), as outlined in Annex N of ISO 10218-2:2025 [3]. In this setup, the PFMD solution CoboSafe from the German company GTE Industrieelektronik GmbH is used.

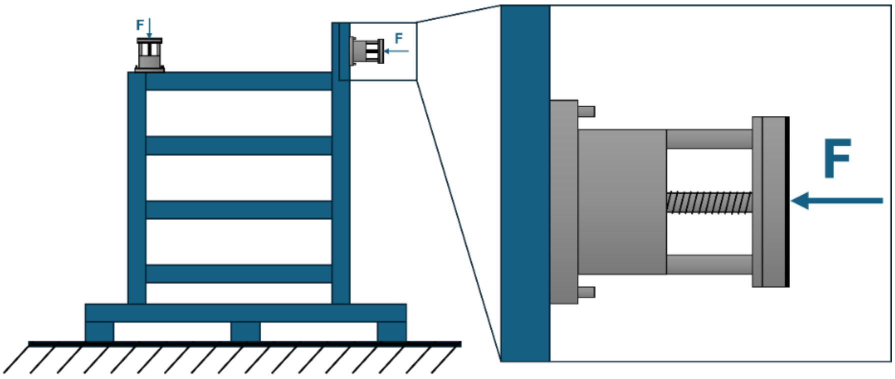

Figure 29 Experimental setup for biomechanical validation of contact forces using a PFMD and a test stand to simulate the worst-case scenarios. The enlarged view illustrates the device used to measure the contact, based on ISO 10218-2:2025 [3]

The configuration of the PFMD, shown in Figure 29, follows the principles and guidelines provided in Annex N of ISO 10218-2:2025 [3]. To guarantee accurate measurements, the procedure needs to simulate realistic worst-case scenarios within the collaborative workspace. According to Annex N of ISO 10218-2:2025 [3], the use of personal protective equipment or materials beyond standard clothing is not considered. Therefore, during the measurement process, only a thin fibre cloth can be used to simulate the real-world conditions. The measurement stand, shown in Figure 29, is constructed on a pallet using Bosch Rexroth profiles to minimize errors caused by a system movement. The structure must be rigid and stable to prevent displacement from impact forces, while also being portable enough to accommodate measurements at various heights and orientations.

The measurement results are displayed in a diagram similar to Figure 28, illustrating both the transient and quasi-static contact forces with the PFMD. The quasi-static contact typically occurs during slow movements, where a body part may be pinched or clamped between the robot and another object. This type of contact is generally more predictable and easier to control. In contrast, transient contact involves sudden, high-speed impacts which are less predictable and potentially more dangerous especially for

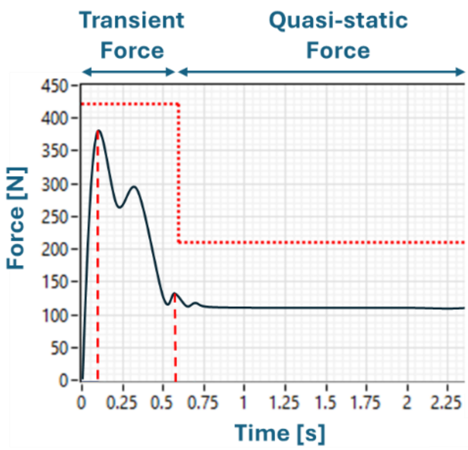

Figure 28 Example force-time curve showing the distinction between transient and quasi-static contact forces measured with the PFMD. The black line represents the recorded force over time, while the red dotted lines indicate the biomechanical threshold values. Transient force occurs during the initial high-impact phase, followed by a stabilized quasi-static force level.

sensitive areas such as the skull and forehead. In these situations, relying on human reflexes or quick reaction times is not sufficient to prevent injury, highlighting the importance of strict force limitation and accurate validation.

To assess pressure distribution across contact surfaces, this thesis uses Fujifilm Prescale Film. This film is designed to visualize pressure variations through changes in colour intensity. This set-up consists of two polyester-based sheets an A-film that contains microencapsulated colour forming material, and a C-film coated with a colour developing layer. When pressure is applied between the two sheets, the microcapsules rupture and react with the developer to produce a red coloration. The density of the colour correlates with the magnitude of the applied pressure, enabling qualitative and semi-quantitative evaluation.

The films are cut to fit the geometry of the contact area. The A-film and C-film are aligned so their active surfaces face each other and are placed between the contacting components. After pressure is applied, the films are removed, and the pressure distribution is observed directly from the developed image. This method offers a simple and effective way to measure contact pressure patterns in real time.

Measurement points derived from the comprehensive risk assessment are selected based on the body regions which are most exposed to potential contact events during the collaborative application. The standard requires each of these points be individually validated to ensure contact forces remain below the defined safety threshold limits.

As illustrated in Figure 30 the selected measurement points focus on the upper body part regions such as the neck, shoulders, chest, back and abdomen. These areas are considered as a potential contact point due to their alignment with the typical operating height of the robot, ranging from 1.2 to 1.35 meters above the ground. For the lower body, the pelvis and upper legs are also considered as relevant contact areas. These areas are highlighted in red in Figure 30 to indicate their higher potential for a contact event during the normal operation. In contrast, the face, skull, and forehead are classified as contact areas only under unreasonably foreseeable misuse. However, including these areas in the measurements can provide valuable additional insights. The measurements are documented in appendix F, G, H, I and the results are shown and validated in Section 6.4 based on the already described process.

The standard also states that alternative test conditions could lead to varying results therefore the measurement needs to be put in perspective to summarize the comprehensive risk assessment process.

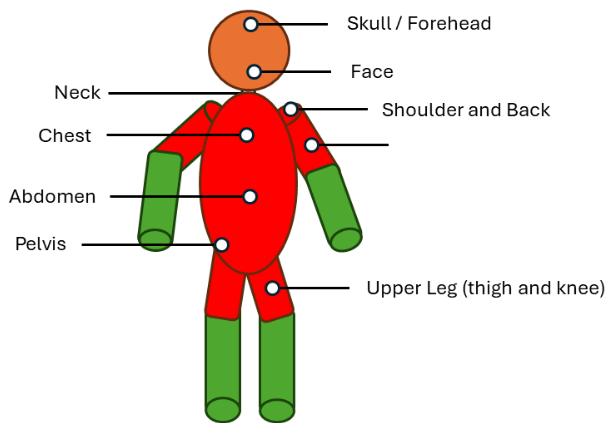

Figure 30 The specific human body regions which can be a potential contact area, the red areas show the likely contact zones during normal operation, while orange areas are considered only in cases of foreseeable misuse, based on ISO 10218-2:2025 [3]

6 System Validation

This section presents the achieved outcomes of the workstation design, implementation, and initial validation, following the objectives of creating a safe, efficient, and flexible HRC system for vision-based quality inspections.

6.1 System Design for a Collaborative Vision-Based Inspection

This section presents the achieved results regarding the design and implementation of the HRC workstation, developed to meet the objectives of creating a safe, efficient, and flexible system for vision-based quality inspections.

The workstation consists of an ABB GoFa CRB 15000-10/1.52 industrial robot equipped with an Intel RealSense Depth Camera D435. The robot is mounted on a fixed inspection stage, while an AGV autonomously delivers assembled parts into the inspection zone. The hardware structure is designed for modular expansion allowing adaptation to future system updates without extensive redesign.

The software architecture is developed using ABB RobotStudio, with the robot program written in RAPID and Wizard Easy Programming to maintain modularity and user-friendly operation. The Server-Client-Communication is established via TCP/IP to integrate the robot system with the external vision processing node. An HMI provides the human with the ability to initiate the automated inspection sequence, monitor the system status, and manage exceptions through an HMI.

Based on the HRI levels reviewed in the previous Subsection 2.1.3 on page 9, the workstation operates at HRI Level 2 in coexistence. In this configuration, the robot autonomously performs inspection tasks while the human supervises the operation and can intervene if necessary. This interaction level is chosen to balance the robotic autonomy together with the safety requirements. The task allocation follows a function-based division, with the industrial robot responsible for repetitive, objective inspection activities such as verifying the presence of brackets with screws and a red tape indicator while the human initiates the operation and monitors the performance and handles any high decision cases or manual checks if required.

In the initial development phase, the vision system is built around a fully manual data pipeline using the YOLO11 object detection model. This process involves manual collection and labelling of the training data, building the training model from scratch, and would need to conduct extensive hyperparameter tuning. While the manually created dataset is diverse, incorporating multiple viewing angles and component variations, the manual approach proves to be highly time consuming and resource intensive. Labelling, augmenting, and optimizing the dataset require considerable effort, limiting scalability and slowing down the overall system development.

Due to these challenges, the development process transitions to an AI assisted workflow using the Intel Geti platform. This alternative approach significantly accelerates the generation of the datasets and object detection models through assisted labelling and training. In this setup, the object detection model is switched to the YOLOX-TINY architecture, a robust and earlier version of the YOLO frameworks, which is supported by the Intel Geti platform. Although YOLOX-TINY is not the latest available model, the system provides reliable performance for the intended quality inspection tasks under the time constraints.

Throughout the development process of the object detection models, several key observations are made. The manually labelled dataset remains relatively small but diverse, covering different product orientations and small visual changes. Automated labelling using Intel Geti improves the volume and quality of the dataset and the time for annotations, introducing faster model iteration. However, both manual and AI-trained models demonstrate some sensitivity to changing conditions where the detection accuracy occasionally is affected by shadows, reflections, or abrupt illumination changes typical in an industrial setting. Therefore, the possibility of the model to generalize well to different unseen cases remains a challenge.

The transition to a pipeline based on Intel Geti enables faster deployment and a more efficient retraining process, supporting the goal of creating a flexible and scalable quality control workstation. For most of the inspected components, the final YOLOX-TINY-based models achieve good detection certainty rates, providing a sufficient confidence threshold for the industrial intermediate inspection application. Most models reach almost 100% accuracy after training, while still missing sometimes some labels. Therefore, indicating the model is overfitting and is not as good in generalization.

Overall, the modular hardware configuration, the possibility of a scalable software design, and the adaptive vision system demonstrate a good feasibility of deploying a HRC workstation for a vision-based quality inspection. The implementation of the vision system, using YOLO-based object detection, is successfully trained and validated in an industrial-like environment, exceeding the expectations set in the initial research scope.

6.2 Functional Safety and Risk Evaluation

Where applicable, safety functions are evaluated against the predefined performance level listed in Table C.1 of Annex C in ISO 10218-2:2025 [3]. The overall PFL strategies as a safety function is required to meet at least performance level d, which is fulfilled by the ABB GoFa CRB 15000-10/1.52 [35]. In cases where the performance level cannot be applied the risk assessment needs to be done. By systematically identifying hazards, estimating and evaluating risks, and applying protective measures based on established actions.

After the risk mitigation in most scenarios the risk estimation needs to be done again for the updated risks which is shown in Table 9. All the hazards are either a minor or moderate severity level which is based on the expected contact force and the system as well as the human reaction time. This includes cases such as minor crushing of extremities or bruises, assuming low impact pressures and sufficient reaction space. The frequency of exposure of all hazards are assessed as low since these are not exceeding four interactions per hour, and a total exposure time is remaining below the 144-minute threshold over a 48-hour span, in accordance with ISO 10218-2:2025 [3]. The probability of occurrence of a hazardous event is generally assessed as low to medium throughout the hazards. This corresponds to a rare event under controlled conditions, or an occasional event influenced by the task, human error, or system complexity. Finally, the possibility of avoidance is considered high in all the cases due to the visible robot motion paths, the safety-rated speed limitations, and the ability of the human to move away before a hazardous event can cause harm. This is supported by implementing the speed and force limits defined in Annex C of ISO 10218-2:2025 [3].

The risk evaluation based on the methodology from Section 5.4 on page 50 concluded all hazards into Level 1 where no additional safety measures are required as listed in Table 9.

Table 9. Risk assessment summary for key hazards associated with the collaborative application, evaluated using severity (S), exposure (E), occurrence (O), and avoidance (A) criteria as defined in ISO 10218-2:2025 [3]. All assessed hazards fall within risk level 1, indicating that no additional safety measures are required under the defined operating conditions.

Hazard	S	E	O	A	Risk Level
Maximum Operating Height	S2 Moderate	E1 Low	O2 Medium	A1 Avoidable	Level 1
Minimum Distance Objects	S1 Minor	E1 Low	O2 Medium	A1 Avoidable	Level 1
Maximum Operating Space	S1 Minor	E1 Low	O1 Low	A1 Avoidable	Level 1
Robot Base Height	S2 Moderate	E1 Low	O1 Low	A1 Avoidable	Level 1
Tool Speed Supervision	S1 Minor	E1 Low	O2 Medium	A1 Avoidable	Level 1
Tool Force Supervision	S1 Minor	E1 Low	O2 Medium	A1 Avoidable	Level 1

The complete risk assessment for the collaborative application is presented in Appendix C and concludes that the application can be inferred as safe. However, as explained in Subchapter 2.2.5 on page 15, the final step is to verify and validate the PFL strategies to confirm this safety. This aligns with the procedures outlined in Annex H of ISO 10218-2:2025 [3] which define the necessary methods for validating the collaborative safety measures. These include:

- Design Validation: Ensuring the PFL strategy is designed to adequately reduce injury risks by keeping forces and pressures below the biomechanical thresholds. This is validated through practical tests, measurements, application-specific documentation reviews, and analysis of safety-related software and task-based risk assessments [3].
- Contact Parameter Verification: Force and pressure values for all identified contact points are verified through physical testing and measurements [3].
- Safety Function Validation: Safety functions are confirmed to be active and correctly configured, ensuring the robot reacts appropriately to limit injury risk. This is verified through measurements [3].
- Contact Classification: All potential contact events are classified as either quasi-static or transient by analysing physical tests and reviewing system layouts and motion paths [3].
- Risk Reduction Confirmation: The severity and likelihood of contact events are minimized via implemented safeguards, and this is substantiated through testing, simulation models, task-based risk assessments, and virtual commissioning tools [3].

- Head and Face Region Considerations: Additional analysis is performed to evaluate hazards associated with collisions to the skull, forehead, and face, using observations, simulations, and task-based reviews [3].

This process results in biomechanical calculations and measurements which are required as per Annex M and N of ISO 10218-2:2025 [3] and will be presented in the following subchapters. However, due to time constraints, a complete assessment and validation of all identified risks, is also not fully executed leaving these hazards as a consisting risk.

6.3 Safety Threshold Evaluation Through Analytical Calculations

The calculations for the risk validation are conducted using a robot moving mass $m_R = 10.5\,kg$, a relative operating velocity of $v_{rel} = 150\,\frac{mm}{s}$ and the contact area $A = 1\,cm^2$. These values are combined with the effective mass m_H and the biomechanical spring constant k of the human body region which get selected based on Annex N of ISO 10218-2:2025 [3]. The specific calculations of the transient force values can be seen in Appendix E. The results are summarized in the following subsections and compared to the safety thresholds from Annex M of ISO 10218-2:2025 [3].

6.3.1 Upper Body Force and Pressure Calculations

In the risk assessment the important upper body part areas are defined as the neck, chest, shoulders, upper arm, elbows and the back. The specific calculations for the transient contact force and transient pressure are provided in Appendix E and the results are summarized in Table 10. For all these regions, the calculated values remain below their respective safety thresholds, indicating compliance with safety requirements during the standard operation.

In addition, the analysis includes transient force and pressure values for the skull, forehead and face. Although these areas are not specified within the defined scope of the risk assessment, they are included for informational purposes if the workstation operates at a head height. Since the verification and validation based on Annex H of ISO 10218-2:2025 [3], collisions involving the head and face regions must be taken into account. The transient force value for the face exceeds the defined safety threshold, while the values for the skull and forehead remain slightly below the limit. Compared to the other body part areas, the transient pressure values for the skull, forehead, and face are closer to their respective safety thresholds and with minor changes in the impact area, which leads to exceeding thresholds.

These results based on the calculations confirm all upper-body regions relevant to the intended operation remain within the allowable limits for both force and pressure. The skull, forehead, and face area, while exceeding the force and pressure threshold in one case, provide important insight into design considerations for an operation on a head height. The half of the impact area leads to double of the pressure values and therefore exceeds the head height safety thresholds.

Table 10. Transient force and pressure values of the calculation for the upper body regions, compared to the safety thresholds defined in ISO 10218-2:2025 [3]. All regions relevant to the intended operation remain within safe limits. Additional values for the skull, forehead, and face are included for reference.

Body Part Area	Transient Force Calculation in $[N]$	Transient Force Threshold in $[N]$	Transient Pressure Calculation in $[\frac{N}{cm^2}]$	Transient Pressure Threshold in $[\frac{N}{cm^2}]$
Skull and Forehead	102.3	130	102.3	110
Face	72.3	65	72.3	110
Neck	34.8	300	34.8	280
Shoulders	80.9	420	80.9	320
Chest	68.4	280	68.4	240
Upper Arm and Elbows	39.7	300	39.7	380

These values suggest if the system operates at head height, additional safety measures may be necessary. The risk assessment identifies the lower body region as an additional area where the normal operation would operate. Therefore, the results of the corresponding calculations are presented in the following.

6.3.2 Lower Body Force and Pressure Calculations

In the risk assessment the important lower body part areas are defined as the back, abdomen, pelvis, thighs and knees. The specific calculations for the transient contact forces and pressures are provided in Appendix E. The results are summarized in Table 11 where in all cases the transient force and pressure values are much lower than the defined safety threshold for these areas.

Table 11. Transient force and pressure values of the calculation for the lower body regions, compared to the safety thresholds defined in ISO 10218-2:2025 [3]. All calculated values remain well below the respective limits.

Body Part Area	Transient Force Calculation in $[N]$	Transient Force Threshold in $[N]$	Transient Pressure Calculation in $[\frac{N}{cm^2}]$	Transient Pressure Threshold in $[\frac{N}{cm^2}]$
Back	80.9	420	80.9	420
Abdomen	43.2	220	43.2	280
Pelvis	68.4	360	68.4	420
Thighs and Knees	101.8	440	101.8	440

These results confirm that the HRC workstation remains for all assessed lower body part areas within the safety thresholds. This indicates that the upper body may pose a risk, which requires validation through measurements, as specified by the verification and validation procedures in Annex H of ISO 10218-2:2025 [3].

6.4 Experimental Risk Validation Through Contact Measurements

Following the calculations for the risk validations the most relevant body part areas are selected for the validation through measurements. These are for the operation process including the neck, shoulders and chest which needs to be measured. Additionally measuring the skull, forehead and face can bring additional information to represent the risks, if the system would operate at a head height. Since the verification and validation are based on Annex H of ISO 10218-2:2025 [3] collision with the head and face region need to considered.

The measurement process and the results for every test used for the biomechanical risk validation is provided in Appendix F, G and H. The programmed robot motion remains the same for each test to ensure comparability. The robot moves from the home position to an intermediate approach position at the height of 1.3 meter above the ground. Afterwards, continuing a linear movement with full speed to the final position on the same height. The PFMD is placed in the middle of a long path to guarantee that the robot is not accelerating or decelerating. A fibre cloth is placed between the sensor and the robot as permitted by Annex N from ISO 10218-2:2025 [3], to simulate a realistic contact condition.

This configuration enables repeatable, controlled measurements of the transient contact forces and pressures. Annex N from ISO 10218-2:2025 [3] recommends a movable system, which is not used here. movable system refers to a test setup in which the measurement device or dummy can yield or recoil during contact, better simulating real human body responses during transient interactions. Without this mobility, the contact is artificially rigid, resulting in higher measured peak forces and pressures. Because of that, the measured values in this thesis are likely higher than they would be with the proper setup. Studies such as Fischer et al. [36] are exploring methods to calculate a conversion factor, which can be used to estimate transient forces from quasi-static measurements. The results of these measurements are presented in the following sections and compared with the biomechanical limits with Annex M from ISO 10218-2:2025 [3] to evaluate compliance.

ISO 10218-2 Annex N [3] recommends taking three measurements per test case and ensuring that the variance remains within 10% to ensure reliable results. This process follows this specification and maintains the required variance by selecting the worst-case measurement from the validated set. The limited availability of different effective spring constants for various body regions means the results are not always fully representative and used to provide approximate values under the given conditions. Additionally, the PFMD is calibrated by the test set provider, with a stated measurement uncertainty of $\pm\ 15\ N$ for the force and $\pm\ 25\,\frac{\mathrm{N}}{\mathrm{cm}^2}$ for the pressure measurements.

Therefore, for the skull, forehead, face and shoulders the correct damping material with the corresponding effective spring constant, as specified in Annex N from ISO 10218-2:2025 [3], is used to measure the following force and pressure values.

The measurement value for the neck is not fully representative. While the correct damping material is used, the correct effective spring constant is not applied. As a result, the effective spring constant $\mathrm{k} = 75\,\frac{\mathrm{N}}{\mathrm{mm}}$ is used instead of $\mathrm{k} = 50\,\frac{\mathrm{N}}{\mathrm{mm}}$, which likely leads to higher values than would be expected with a properly matched spring constant. Additionally, the measurement value for the chest is also not fully representative. While the correct damping material is used, the correct effective spring constant is not applied. As a result, the effective spring constant $\mathrm{k} = 35\,\frac{\mathrm{N}}{\mathrm{mm}}$ is used instead of $\mathrm{k} = 25\,\frac{\mathrm{N}}{\mathrm{mm}}$, which is likely to lead to higher values than would be expected with a properly matched spring constant.

6.4.1 First Measurement the Contact with the End-Effector Edge

In these measurements the contact event happens with the edge of the end-effector and the surface of the PFMD. The measurements for the transient contact forces over time are provided in Appendix F. The same measurement procedure also produces the pressure values based on the same motion sequence. Each plot in Appendix F shows the pressure distribution measured by the PFMD for the specific upper body region. In this test set-up the robot speed is $v_{rel} = 150 \frac{mm}{s}$ and the tool speed supervision is set to $F = 38$ N.

A comparison of the final results in Table 12 shows the measured forces and pressures as well as the defined safety thresholds specified in Annex M from ISO 10218-2:2025 [3]. For the neck, shoulders, and chest, the measured transient forces and pressures remain below the defined safety limits. Although the measurements for the neck and chest are carried out using an approximate spring constant rather than the exact specified values, the results would likely be lower with full accuracy. Therefore, the results from the collision with the edge of the end-effector suggest that all upper-body regions relevant to the intended operation remain within the acceptable safety limits for both force and pressure.

The measured transient force for the skull and forehead is below the safety threshold, while the force for the face exceeds the defined limit. The measured pressures for the skull, forehead, and face are all above the corresponding thresholds. These values are obtained using the correct spring constants and damping materials, making them reliable indicators. These values suggest if the system operates at head height, where contact with the head and the edge of the end-effector is possible, additional safety measures should be considered to reduce the risk of injury. The end-effector is designed with very round edges but likely due to the composed material the pressure exceeds the safety threshold.

Table 12. Measured transient contact forces and pressures for the upper body regions during contact with the edge of the end-effector. Values are compared to the corresponding safety thresholds defined in ISO 10218-2:2025 [3]. While force values remain within safe limits for most regions, pressure values for the skull, forehead and face exceed the recommended thresholds, highlighting potential safety concerns in head-height interactions.

Body Part Area	Transient Force Measurement in [N]	Transient Force Threshold in [N]	Transient Pressure Measurement in $[\frac{N}{cm^2}]$	Transient Force Threshold in $[\frac{N}{cm^2}]$
Skull and Forehead	109 ± 15	130 N	132 ± 25	110
Face	105 ± 15	65 N	179 ± 25	110
Neck	105 ± 15	300 N	179 ± 25	280
Shoulders	96 ± 15	420 N	130 ± 25	320
Chest	83 ± 15	280 N	63 ± 25	240

In the risk assessment the collision with the end-effector is selected as one worst-case scenario but also colliding with the robot head is selected as an additional worst-case scenario, which is tested in the following.

6.4.2 Second Measurement the Contact with the Robot Head

In these measurements the contact event happened with the robot head and the surface of the PFMD. Specifically, the spot for mounting the screw is selected because this point is the most worst-case scenario which can happen at a contact event which is also in accordance with ISO 10218-2:2025 [3]. The measurements for the transient contact forces over time are provided in Appendix G. The same measurement procedure also produces the pressure values based on the same motion sequence. Each plot in Appendix G shows the pressure distribution measured by the PFMD for the specific upper body region. In this test set-up the robot speed is $v_{rel} = 150 \frac{mm}{s}$ and the tool speed supervision is set to $\mathrm{F} = 38\ \mathrm{N}$.

A comparison of the final results in Table 13 show the measured forces and pressures as well as the defined safety thresholds specified in Annex M from ISO 10218-2:2025 [3]. For the shoulders and chest, the measured transient force and pressure stay below the safety limits. For the neck the measured forces are also below the limit, however the pressures are higher than the threshold. Since the correct spring constants are not used for the chest, the actual values would likely be lower if the proper setup would be applied. This means the results from the collision with the edge of the robot head still support that the upper-body regions used during normal operation are within the safe range for both force and pressure. The values for the neck and chest should be seen as estimates and would likely meet the safety limits with accurate test conditions.

For the skull and forehead, the measured forces are below the limits, but the face exceeds the safety threshold. The measured pressures for the skull, forehead, and face are higher than the safety limits. These tests used the correct spring constants and damping materials, so the results are reliable. These values suggest that if the robot works at head height and there is a chance of contact with the worst-case of the edge of the robot head, extra safety measures should be taken.

Table 13. Measured transient contact force and pressure values for the upper body regions compared to safety thresholds defined in ISO 10218-2:2025 [3]. The values are based on contact with the edge of the robot head under standard test conditions. Pressure values for the skull, forehead, face, neck, and chest exceed the respective thresholds, indicating potential safety concerns in head-height operation.

Body Part Area	**Transient Force Measurement in $[N]$**	**Transient Force Threshold in $[N]$**	**Transient Pressure Measurement in $[\frac{N}{cm^2}]$**	**Transient Force Threshold in $[\frac{N}{cm^2}]$**
Skull and Forehead	102 ± 15	130 N	268 ± 25	110
Face	105 ± 15	65 N	283 ± 25	110
Neck	105 ± 15	300 N	283 ± 25	280
Shoulders	100 ± 15	420 N	259 ± 25	320
Chest	88 ± 15	280 N	137 ± 25	240

A collision with the end-effector was selected as one worst-case scenario, while a collision with the robot head was included as an additional critical case and tested accordingly. The measurements for the robot head collision showed that contact with the neck exceeded the safety threshold during normal operation. Although this value remained below the threshold in the previous test, in this measurement the value exceeds the limit. Furthermore, pressure values for the face, skull, and forehead exceed the threshold in both measurements. As a result, additional mitigation measures are tested, with the skull and forehead used as examples for pressure reduction strategies.

6.4.3 Third Measurement the Mitigation Strategies for Pressure Reduction

In this test the contact event with the robot head and the surface of the PFMD is repeated. In this measurement additional actions to reduce these forces and pressures are being tested. Therefore, the test is repeated without any additional action but a collision with the rounded edge of the robot head, with added soft padding, with reduced speed and no padding, and with both reduced speed and force but no padding.

In this setup the correct damping material for the skull and forehead is used with the corresponding effective spring constant, as specified in Annex N from ISO 10218-2:2025 [3], to measure the force and pressure values for the worst-case. The measurements are provided in Appendix H and the results together with the thresholds for the transient contact forces and pressures are displayed in Table 14.

In comparison in Table 14, all tests remain below the force threshold values specified in Annex M from ISO 10218-2:2025 [3]. These results highlight that adding soft padding slightly reduces the transient force. Reducing the speed and further reducing both speed and force of the robot, leads to an even greater decrease in the measured transient contact force.

In comparison in Table 14, the measured transient pressures without additional actions, with reduced speed and with reduced speed and force exceeds the safety threshold. Additional padding of the robot is the only action that reduces the pressure drastically under the threshold values, specified in Annex M from ISO 10218-2:2025 [3].

Table 14. Measured transient forces and pressures for a head height contact scenario under different safety configurations, compared to the ISO 10218-2:2025 [3] threshold for the skull and forehead. All configurations remain within the force limits, but only the use of additional soft padding successfully reduces pressure below the safety threshold. These results highlight the effectiveness of padding in mitigating impact risk, particularly when operating at standard speeds.

Risk Reduction Actions on the Collision with the Skull and Forehead	Transient Force Measurement in $[N]$	Transient Force Threshold in $[N]$	Transient Pressure Measurement in $[\frac{N}{cm^2}]$	Transient Force Threshold in $[\frac{N}{cm^2}]$
Without Additional Action	94 ± 15	130	162 ± 25	110
Additional Soft Padding	64 ± 15	130	25 ± 25	110
With Reduced Speed	45 ± 15	130	202 ± 25	110
With Reduced Speed and Force	39 ± 15	130	272 ± 25	110

These measurements highlight a slower movement and show that a more sensitive system can improve the transient force and pressure. Moreover, the measurements show that the movement needs to be much lower than $v_{rel} = 50\frac{mm}{s}$ and a tool speed supervision which is lower than $\mathrm{F} = 25\ \mathrm{N}$ must be implemented. Keeping the robot speed at $v_{rel} = 150\frac{mm}{s}$ and the tool speed supervision also at $\mathrm{F} = 38\ \mathrm{N}$ with additional padding, the transient pressure significantly decreases. Even increasing the speed to $v_{rel} = 250\frac{mm}{s}$ showed only a slight increase in the transient force and pressure. These results can be adapted to the collision with the neck in the previous test. With the correct spring constant, the pressure values can still exceed the safety threshold and therefore slightly reducing the speed and the tool force supervision is one option to make the system more sensitive. The other option is to improve the soft padding of the complete moving robot arm with the end-effector.

As shown in the tests with the end-effector in Appendix I, where changes to the robot settings are tested. The speed has a big effect on force and pressure. Therefore, lowering the tool force supervision is beneficial, but reducing the speed or improving the robot by soft padding have the best results. Since speed is a key factor and tool force supervision cannot be reduced too much without causing unnecessary stops, soft padding is the most effective way to improve safety.

6.5 Potential Industrial Integration and Expert Validation

To understand how the developed collaborative robot setup can be used in a real production environment, feedback is collected from professionals at Scania CV AB. An Automation Competence Leader agreed with the design approach and confirmed that the setup followed the safety principles discussed. Several Safety Engineers and Automation Engineers also gave positive feedback. All of them said that all important safety measures had been taken and that no further risks from the HRC process could be identified.

The safety engineers also noted the common practice in production of using an AGV with adjustable height, allowing the system to accommodate the varying heights of different humans. This helps to reduce the chance of risky contact with the robot at an uncomfortable height to reduce the height of the AGV and therefore the operating height. If the operating height together with the adjustable AGV is still too high in some cases, the Safety Engineer suggests in using warning signs and floor markings to make the potential risk more visible to the human.

Appendix C includes suggestions for how the system could be safely used in a real factory. These include adjusting the AGV and part height, adding weight to the robot base to avoid tipping, and clearly defining the workspace of the robot on the ground. If new tasks are added that change how the robot moves a new risk assessment must be done. If the takt time allows, the speed and force of the robot can be even more limited to improve safety. ISO 10218-2:2025 [3] supports reducing the speed of the robot to 150 millimetre per second in working zones and setting a global limit of 250 millimetre per second outside those zones. However, if a shorter takt time is required, the speed may need to be increased accordingly with a new risk assessment.

7 Results and Discussion

This chapter discusses the results of the HRC workstation in the context of the research aims, related literature, and the industrial application. This reflects the practical performance of the system, the safety-enabling features, and the broader implications of the findings. The discussion is structured to evaluate the feasibility of the solution in a real production environment, assess the compliance with relevant safety standards, and identify both the strengths and limitations of the approach.

7.1 Interpretation of Results

This section interprets key findings of this thesis in relation to the initial research questions and the theoretical background discussed in earlier chapters. The interpretation of the results evaluates whether the developed HRC workstation meets the criteria of safety, flexibility and practical implementation in an industrial-like context. The quantitative results from the risk assessment together with the risk validation and the qualitative design choices and engineer feedback are discussed to assess the relevance and implications to this thesis.

7.1.1 Design of the HRC Workstation

The implementation of a modular and safety-compliant HRC workstation demonstrates that vision-based quality inspection tasks can be feasibly automated without compromising human safety. The integration of a YOLO model enables efficient detection of missing components, addressing the research aim of enhancing intermediate quality control processes. This thesis demonstrates that the training process is compatible with Intel Geti's automated framework, offering a viable path for future iterations where time constraints or rapid prototyping are critical. The successful training and application of the vision system not only validated the technical feasibility but also demonstrated the adaptability and performance of modern AI-based inspection tools within robots which are used in a collaborative application.

To ensure an efficient integration of the vision system within the HRC workstation, the Python environment is designed in a modular structure. This modularity supports adaptability, maintainability, and scalability. The importance is that the modern production line can have products, inspection criteria, or detection models which may change over time. By separating core functionalities into dedicated modules, the system can be updated or extended with minimal impact on the overall structure.

The reference to PFL strategies and ISO standards fulfils the requirement of ensuring safety in the collaborative application, aligning with both legal frameworks and industrial practices. The successful use of ABB SafeMove functionalities confirms the ability of the system to create dynamic, non-fenced safe workspaces, supporting flexible production needs.

The selected task allocation in this thesis not only reduces cognitive load on the human but also aligns with ergonomic principles by minimizing exposure to repetitive, low-value tasks, which is one of the key motivations for adopting HRC systems in manufacturing as highlighted by Proia et al. [22]. Musculoskeletal injuries can be caused by high repetition, excessive effort or high precision by standing in uncomfortable position for a long time [11]. These inspection tasks are repetitive and require high accuracy, making a good fit for an automation using a not fenced robot in a HRC application. Adding a vision system helps the robot in handling the inspection work, reducing the receptiveness as well as the demands on the humans while keeping the needed flexibility for changing production conditions. This approach also aligns with ISO 10218-2:2025 [3] in Annex H where the severity and probability of occurrence for the contact events need to be reduced to a safe minimum.

The comparative insights by A. Gisginis [9] and Bindel [26] demonstrate that while fixed and semi-fixed vision systems provide reliable results in static or narrowly defined environments, these system often lack the adaptability required for flexible, human-centred production lines. The integration of the vision systems directly onto a flexible position, such as an industrial robot which is used in a collaborative application, offers a promising approach by enabling dynamic repositioning, better angle coverage, and easier adaptation to design or product changes. This thesis builds on that direction by combining the flexibility of an industrial robot with a vision system in a collaborative application, overcoming the rigidity of fixed systems and addressing flexibility and usability demands in future-ready manufacturing environments. This design ensures a flexible, user-friendly, and reliable setup suited for the inspection task in this thesis.

Moreover, the design of this workstation supports rapid redeployment and adaptation to new inspection tasks, fulfilling one of the aims of this thesis to improve flexibility and reduce stress on the human. This makes the setup highly flexible and user-friendly, especially during system setup or when inspection targets change. In earlier systems, the robot and vision parts are often treated as separate. In this thesis, they are fully integrated. This makes programming easier, saves space, and improves coordination between tasks. Also supporting the goal of designing a safe, flexible, and effective collaborative workstation, as outlined in the thesis aims.

One of the core principles of Scania CV AB is providing the highest quality to the customers and is therefore the fundamental thinking of a zero-defect manufacturing, by aiming to prevent failures in the production environment by ensuring every component is made perfectly from the beginning [23].

In addition to physical layout, ergonomic factors such as human reach, standing position, and line-of-sight are considered during station layout. The home position of the robot ensures there is no arm extension into the human zone during idle states, minimizing psychological stress and perceived risk which is an often overlooked aspect discussed in ISO 12100:2010 [1] and addressed in the updated Machinery Regulation [4], which emphasizes reducing mental strain in collaborative applications.

The human needs to feel safe when collaborating with the industrial robot. The feeling of safety can be achieved by trusting the industrial robot and essentially the algorithms that are designed for HRC. The level of effectiveness of HRC is designed for and can be achieved by a safe collaboration, when the human worker does not feel endangered. The trust can be earned by explainable, predictable, and understandable industrial robot actions which should be addressed by smart bidirectional communication between the human and the industrial robot.

7.1.2 Safety Analysis and Risk Assessment

The safety solution presented in this thesis includes both mechanical and control-based measures to reduce risks during HRC. The end-effector is designed as a lightweight structure made from a micro carbon fibre filled nylon material with rounded edges to lower the risk of injury in the event of a contact. In the case of a head collision or another worst-case scenario this material needs softening either by a material change or an additional soft padding. The physical design of this system is supported by PFL strategies which monitor and control the movement of the robot, force, and energy output.

This approach addresses several key risk factors described in ISO 12100:2010 [1]. These include the time and frequency of human presence in potentially hazardous zones, the likelihood of interaction between the human and the robot, and the speed and predictability of the movements of the robot. Each of these factors are significantly reduced through careful system design, supervised motion, and spatial planning. The collaborative type of the application is defined through a structured risk assessment during the system design process. The ISO 10218-2:2025 [3] gives a guideline on how to assess the biomechanical limits in an informative approach and can only guide the process. Instead, the biomechanical limits provided are based on ongoing research and serve as practical safety guidelines. Engineers are encouraged to adopt a conservative approach when applying these limits to maintain a high level of safety for humans.

The results of the risk validation show that the calculated forces for the upper body closely match the measured values. Although there are small differences, the values are in a similar range. This suggests that the calculations are a reliable way to estimate forces and can support the safety assessment of the system.

The test results from collisions with the edge of the end-effector support the conclusion that the system can operate safely under normal conditions. However, collisions with the edge of the robot head can create very high pressure on certain body regions in a worst-case situation. This shows that sharp edges are a critical safety concern and should be avoided or minimized as much as possible.

In addition, pressure at head height is often the main safety concern. If the robot operates on a height above the ground, which is considered a head height, extra safety measures are needed to reduce the risk of injury. These may include reducing the speed and limiting the tool force of the robot. While both actions help lower the force and pressure, the most effective method is to add soft padding to the robot and the end-effector. The risk assessment always considers the worst-case scenario with the lowest impact area and therefore not only the end-effector needs to be padded.

The force and pressure values used in this thesis are based on conservative estimates found in the standard [3]. The measurements taken in this thesis are also estimates, which are limited in number, but they strongly support the conclusion that the workstation is safe if it does not operate at a head height.

While the system operates within safe parameters, the close physical proximity to the human still presents possible risks such as collisions or entrapment. In addition, the end-effector used is not originally developed for certified collaborative systems and may not meet all formal safety requirements [12]. Since no commercially available solution fully met the specific needs of this application, a custom tool was designed as part of this thesis to better align with the safety and functional requirements of the HRC workstation. To further improve the system for industrial use, future work should consider the integration of certified collaborative tools that meet safety standards for human interaction or to certify the tool from this thesis.

7.1.3 Link to Research Aims and Literature Gaps

The selected application is directly tied to the overarching aims presented in Chapter 1, particularly the real-world application, improved safety measures, user-friendly design, and the efficient human-robot task sharing. Therefore, this thesis is moving beyond theoretical models to implement an HRC workstation in an actual production-like setting, relying exclusively on PFL strategies to ensure safety during the HRI. Additionally, conducting a comprehensive risk assessment and ensuring compliance with ISO 10218:2011 [16, 17], ISO 10218:2025 [2, 3] and ISO/TS 15066 [18] by implementing safety measures and risk mitigation actions. Furthermore, this thesis is incorporating HG features, such as those in the ABB GoFa CRB 15000-10/1.52 which is allowing easy reprogramming and task adjustments. Finally, this thesis is enabling humans to delegate repetitive inspection tasks to the industrial robot which is used in a collaborative application while focusing on critical quality control tasks.

Concluding to that, this thesis is addressing key research questions related to safety design, vision integration, and feasibility in industrial collaborative applications. As identified in Chapter 2.6, current literature often neglects the safety-validation of industrial robots used in a collaborative application, particularly in vision-based inspection tasks. Most implementations remain in simulation or prototype stages in a Lab without full safety evaluation or user-oriented deployment.

The implementation shown in Figure 31 exemplifies the practical and safety-validated approach in this thesis. This setup demonstrates a real-world, safety-validated application of PFL strategies for the vision-based quality control. Designed for user-friendly operation and the workstation enables easy task reprogramming through HG features and reduces human workload by automating repetitive inspection tasks. This practical deployment addresses key literature gaps by moving beyond simulations to a tested and ISO standard compliant solution in a production-like environment.

Figure 31 Implementation of the HRC workstation developed in this thesis, featuring the ABB GoFa CRB 15000 with a custom vision-integrated end-effector and an AGV simulating an industrial part flow.

7.2 Safety-Enabling Design Features and Risk Mitigation Benefits

This HRC workstation offers several key advantages that contribute to its safety, efficiency, and readiness for industrial use:

- Improved Safety through Controlled Contact: The robot maintains a safe distance from the inspected object, which significantly reduces the risk of clamping or entrapment. As a result, only transient contact is possible, aligning well with the safety requirements specified in ISO 10218-2:2025 [3].
- Natural Barriers and Spatial Separation: The AGV and the inspected object themselves act as physical barriers, limiting the likelihood that a human will enter the operating space of the robot. Additionally, the robot operates below head height, meaning that upper-body regions are the primary areas at risk. In a real production environment, the AGV could further lower the object height, reducing this risk even more.
- Minimized Human Involvement: Since this is a semi-automated quality inspection station, the human has limited interaction with the object. This lowers both the frequency and the probability of HRI, keeping exposure to a minimum in line with the ISO 10218-2:2025 [3] risk assessment criteria.
- Partial Physical Separation: The robot is mounted on a raised platform, which serves as a small but effective physical separation. While this is not a full safety barrier, this naturally limits how close a person can get to the robot.
- Low Operating Speed and Force Supervision: In this application, the robot operates at low speeds and with limited tool force. According to ISO 10218-2:2025 [3], this allows the risks to be considered avoidable and supports a lower overall risk level in the formal risk assessment.

When combined with the formal risk assessment, the biomechanical calculations, and the validation through physical measurements, these features create a strong foundation for defining the workstation as a safe collaborative environment. However, an important note is that any significant change to one of these features, such as exceeding the robot speed, tool design, layout, or interaction frequency, would require a new risk assessment. The safety of a collaborative application depends on the system as a whole, and modifying one element can impact the overall risk level.

These design choices not only enhance safety but also move the system closer to meeting CE conformity requirements. Although full CE certification is not completed within the scope of this thesis, the workstation incorporates many principles that support future compliance.

7.3 Academic and Industrial Implications

This thesis demonstrates the practical implementation of a vision-based HRC workstation that complies to modern safety standards while maintaining flexibility for dynamic production environments. The approach holds value both for academic research and for industrial stakeholders such as Scania CV AB.

7.3.1 Insights for Research

Researchers can draw several key lessons from this study. First, this thesis highlights the feasibility of integrating vision systems into a collaborative application without compromising safety. The successful application of PFL strategies, validated through both calculations and measurements, provides a replicable method for biomechanical risk assessment in future studies. Moreover, the combination of modular software, real-world feedback, and risk evaluation based on current standards fills an important gap in current HRC literature, where many systems remain limited to simulation or lab prototypes. The research also underscores the importance of physical validation through pressure and force measurements, which is often overlooked in purely theoretical work. Defining a completely safe HRC workstation has a high demand on additional feedback from Safety Engineers and is always influencing the feasibility of the workstation and the technical implementation. The safety considerations are often limiting factors to prevent the workstation and the robot from creating a hazardous environment.

PFL works well and is tested successfully, but other safety methods like soft covers or flexible materials are not explored. These could help reduce risk even more, especially in the upper part of the robot arm or at the tool, where the highest forces during collisions occur.

The system reduces manual work and supports safer inspections, but this thesis does not measure time savings, cost reduction, or energy use. Future research can focus on these aspects to show how HRC improves both efficiency and environmental performance. Connecting safety, speed, cost, and sustainability makes the design more useful for real production.

7.3.2 Applications for Scania and Similar Companies

For Scania CV AB, this project serves as a validated use case for deploying an industrial robot in a collaborative application in a quality control task. The workstation meets the demands of modern assembly lines by enabling safe, efficient, and flexible inspection of a part without the need for physical fencing. This supports the goal of Scania CV AB of achieving zero-defect manufacturing while reducing ergonomic strain on humans. Key features such as safe motion control, automated object detection using YOLO, and minimal human involvement align with Industry 5.0 goals, emphasizing human-centric automation.

In addition, the modularity of the system makes this suitable for future adaptation to different tasks or product variants. Scania CV AB can apply this solution in various stations by adjusting vision models or changing the robot program, as long as the risk assessment is updated accordingly. The study also emphasizes the need for careful tool and layout design, particularly to avoid unsafe operations on a head height, which is a valuable insight for broader deployment. Additionally, if the system would operate at a head height the additional risk mitigations are presented and show additional soft padding can drastically reduce the transient pressure values.

Safety and technology always go together. Safety design shapes the layout, movement and the whole system. The setup supports goals of Industry 4.0 and Industry 5.0 by helping humans, not replacing them. The robot handles repetitive tasks and lowers stress for humans.

The workstation also fits well in flexible production systems like cellular manufacturing. This system can be adapted for new tasks or products if safety is checked again. This helps Scania CV AB and similar companies to stay efficient, reduce waste, and work in a more human-centred way.

The system contributes to the vision of Scania CV AB in having a zero-defect manufacturing by detecting assembly anomalies early and avoiding downstream waste.

This thesis also supports environmental and continuous improvement goals by minimizing rework and reducing unnecessary human workload.

The safety design and system layout are not limited to ABB robots. As long as force and torque parameters are available and programmable, the same concept can be applied to other industrial robot brands, such as KUKA, FANUC, or Universal Robots, following the same risk assessment procedures. This makes the solution highly transferable across different robotic platforms in the industry.

7.4 Critical Reflection

The design research methodology in this thesis combines the system design with the risk assessment and safety validation. This proves an effective way of addressing key challenges in designing a safe HRC workstation. One major strength is the integration of the standard ISO 10218-2:2025 [3] together with the corresponding normative and informative appendices. This provides a structure and practical framework for evaluating the safety of the HRI. The feedback from Scania CV AB further strengthens the relevance of the system in a real-world industrial context.

Despite the main advantages highlighted in the earlier sections some limitations in the application of the methodology are still present. The number of measurements taken during the risk validation is limited to one operation height. Measurements on different heights and distances as well as joint positions needs to be done to get a complete overview of the whole workstation. Since research like Fischer et al. [36] show that these factors have an impact on the system.

Additionally, time constraints and limited equipment availability restricted broader data collection and contributed to measurement uncertainty. Although the calculated and measured values remain closely aligned, an important note is that every measurement carries inherent uncertainty which can come from different factors such as the calibration of the PFMD, the pressure film accuracy, the robot behaviour and variability, due to test setup inconsistency and the environmental conditions which are temperature and humidity [36]. These factors are always present and influence the measurements, meaning the results can provide informative insights but cannot definitively confirm that the workstation is entirely safe. As described in ISO 10218-2:2025 [3] applying biomechanical limits is essential to maintain a high level of human safety. However, these limits should be viewed in context and adapted appropriately to the specific application.

From a technical standpoint this workstation serves as a good foundation for future implementation in the Flexible Assembly Line of the Smart Factory Lab at Scania CV AB. The machine vision application uses not the latest YOLO model. However, this process with Intel Geti is very stable and fast in deploying models which serves as a good foundation for a fast and accurate machine vision implementation. Although the end-effector has rounded edges the pressure threshold can exceed when the robot is operating at a head height. In this workstation and in the risk assessment this is not the case and can therefore be considered as safe in this collaborative application.

Some assumptions in the system design may also influence the outcome. The chosen speed and tool force supervision settings reflect safe operation for this specific task but may not be directly transferable to other applications. Additionally, the exclusive use of PFL strategies limits the scope to one interaction mode, although other safeguards can also be implemented without increasing the complexity by keeping the system flexible and efficient.

7.5 Limitations

Several limitations arise during the development and technical evaluation of the workstation. The generalizability of the vision system remains limited. Although the object detection models perform well under controlled conditions, these models show signs of overfitting. Variations in lighting and changes in viewing angles occasionally reduce detection accuracy, which may affect performance in a dynamic production environment. Therefore, additional lightning on the end-effector may be necessary to guarantee better conditions which can introduce new safety risks and needs therefore be considered in a new risk assessment. While the machine vision process demonstrates potential for automation, the initial stages, such as model training, data labelling, and tuning, still require significant manual effort. The transition to the Intel Geti platform significantly improves efficiency and reduces the time required to develop detection models. However, full system connectivity is not implemented in this thesis, resulting in a semi-automated workstation.

Limitations also exist in the risk assessment and validation process. Although the initial risk identification is comprehensive and addresses all areas relevant to the workstation, the full process from assessment to final validation is not completed due to time constraints. As a result, the thesis focuses primarily on safety considerations related to the collaborative application itself. Operations on a head height are not included in the validated risk scenarios, as the robot does not operate at a height typically considered hazardous to the head. However, the exact definition of a head height is not clearly specified in the standards, leaving room for interpretation. Lastly, the selected robot velocity and tool force settings are tailored to this specific application. Different tasks or working environments would require parameter adjustments and a new risk assessment. The system meets safety requirements within the scope of this thesis, but does not undergo a full CE certification, which would be required for deployment in a real factory setting.

8 Conclusion and Future Work

This thesis presents the design, implementation, and validation of an industrial robot which is used in a collaborative application for a vision-based quality inspection. The primary focus of this thesis relies on the safety, flexibility, and industrial applicability. Through a combination of the risk assessments as well as expert feedback, the workstation meets key safety requirements in a fenceless HRC environment. The conclusion reflects both, the achievements and the further directions for research and development.

8.1 Summary of Contributions

This thesis advances the field of industrial robots used in a collaborative application by demonstrating that a vision quality inspection can be safely and efficiently implemented in an industrial-like setting at Scania CV AB without physical barriers. The workstation integrates a modular vision pipeline and an industrial robot with PFL strategies. Safety is validated using ISO 12100:2010 [1], ISO 10218:2011 [16, 17] and ISO 10218:2025 [2, 3] and through both calculations and physical testing of transient contact forces and pressures. The use of expert feedback from Scania CV AB strengthens the real-world relevance of the design and supports the potential future deployment. The system also contributes to the ongoing evolution of Industry 5.0 by prioritizing human safety, ergonomic design, and adaptable technology. The integration of a YOLO-based detection model, combined with the flexibility of robot-guided inspection, addresses core requirements of modern production systems while reducing repetitive strain.

8.2 Critical Discussion

This thesis reflects a learning experience in combining safety engineering, automation, and AI-driven vision systems. One key insight is the complexity of translating standards like ISO 10218:2011 [16, 17] and ISO 10218:2025 [2, 3] into practical testing and measurements. The physical validation of forces and pressures proves that this process is more challenging and nuanced than expected, especially with limitations in sensor setup and time for repeated measurements. The collaboration with Scania CV AB provides a valuable context for real-world implementation and reinforces how important practical feedback is in shaping a safe and usable system. At times, working within safety constraints limits the performance of the system potential, but still, these boundaries serve as a necessary foundation for a safe automation. Balancing safety with efficiency is an ongoing challenge in any HRC application.

8.3 Generalization of the result

While the workstation is developed for a specific intermediate inspection task at Scania CV AB, the methods and safety strategies applied are generalizable. The risk assessment process, the approach in validating safety thresholds, and the modular design of both hardware and software can be adapted to other collaborative tasks in the manufacturing, particularly those involving vision-based quality control. However, the biomechanical validation results are scenario-specific and need re-evaluation when changes occur in the robot, tool, task, or workspace layout. Additionally, the design of the inspected part is limited by the robot reach and is therefore not generalizable to parts which are greater than the robot reach. This study is unique in combining a fully implemented vision-guided robot system with a structured risk validation process supported by compliant testing based on current ISO standards. This system remains a prototype in a lab environment and should be seen as a foundation for future adaptation and industrial CE certification. The proposed safety concept is not tied to any specific robot manufacturer. While tested with an ABB robot, the approach can be adapted to other brands that allow speed, force, and collision settings to be monitored and controlled, as required by the ISO standards.

8.4 Future Work and Research Directions

While this thesis presents a validated and safety-compliant collaborative workstation for vision-based quality inspections, several areas remain open for future research and development. The first area is having broader defect detection capabilities. This thesis focuses on detecting missing components, but future developments could include expanded vision capabilities for surface inspection, dimensional measurement, and anomaly detection. Enhancing the robustness of object detection models under changing lighting and environmental conditions also remain as a key challenge. This highlights the need for additional lighting to be integrated into the end-effector design, which needs a new risk assessment with the changed equipment to ensure safety.

Going further to the second area the real-time adaptability through AI. The current system relies on static task programming and retrained models. Future work can explore the integration of adaptive AI algorithms that enable real-time decision-making, autonomous trajectory planning [25], and dynamic model updates based on real-world feedback. For example implementing the work from Jafari-Tabrizi et al. [25] for an autonomous trajectory planning to get a more intuitive model. This would support continuous learning and improved performance in changing production environments and increases the possibility of an integration in a continuously moving line.

The third area are the full CE certification and industrial integration. Although this thesis follows ISO 12100:2010 [1], ISO 10218:2025 [2, 3] and the Machinery Regulation [4] the full CE conformity is still pending. This process includes thorough documentation, creating technical files, and a complete risk assessment and mitigation outside of the collaboration part of this thesis. These are essential next step for deployment in a live production setting. Future research could focus on the certification process and the practical challenges involved as well as a standardized risk validation process for simplification.

Finally, the last area of future work and research are human factors and ergonomic studies. The workstation design emphasizes physical safety, but further studies can investigate user acceptance, perceived safety, and the reduction in the long-term ergonomic impact. For instance, psycho-social risks such as isolation from colleagues or difficulty matching the pace of the robot during a collaboration are highlighted in literature Madzharova-Atanasova and Shakev [11] and should be considered to improve trust and cooperation in HRC. Additionally, a study can be conducted to determine to what extent a human can be brought into the collaboration without requiring major changes to the safety measures or risk assessment. By addressing these research directions, future work can move closer to realizing flexible, human-centric, and industry-ready collaborative systems, supporting the evolution toward Industry 5.0 manufacturing principles.

9 References

[1] *Safety of machinery - General principles for design - Risk assessment and risk reduction,* ISO 12100:2010, 2010.

[2] *Robotics - Safety requirements - Part 1: Industrial robots,* ISO 10218-1:2025, 2025.

[3] *Robotics - Safety requirements - Part 2: Industrial robot applications and robot cells,* ISO 10218-2:2025, 2025.

[4] *Regulation (EU) 2023/1230 on machinery*, Official Journal of the European Union, 2023.

[5] E. Matheson, R. Minto, E. G. G. Zampieri, M. Faccio, and G. Rosati, "Human–Robot Collaboration in Manufacturing Applications: A Review," *Robotics*, vol. 8, no. 4, pp. 1–25, 2019, doi: 10.3390/robotics8040100.

[6] T. Brito, J. Queiroz, L. Piardi, L. A. Fernandes, J. Lima, and P. Leitão, "A Machine Learning Approach for Collaborative Robot Smart Manufacturing Inspection for Quality Control Systems," *Procedia Manufacturing*, vol. 51, pp. 11–18, 2020, doi: 10.1016/j.promfg.2020.10.003.

[7] A. Papavasileiou, G. Michalos, and S. Makris, "Quality control in manufacturing – review and challenges on robotic applications," *International Journal of Computer Integrated Manufacturing*, vol. 38, no. 1, pp. 79–115, 2025, doi: 10.1080/0951192X.2024.2314789.

[8] Grand View Research, *Collaborative Robots Market Size, Share & Trends Analysis 2023-2030.* [Online]. Available: https://www.grandviewresearch.com/industry-analysis/collaborative-robots-market### [Accessed: Feb. 23, 2025].

[9] A. Gisginis, *Production line optimization featuring cobots and visual inspection system*. Bachelor's thesis, Dept. of Mechanical Eng., Blekinge Inst. of Technol., Karlskrona, Sweden, 2021. [Online]. Available: https://urn.kb.se/resolve?urn= urn:nbn:se:bth-21752## [Accessed: Jan. 27, 2025]].

[10] *Directive 2006/42/EC on machinery*, Official Journal of the European Union, 2006.

[11] K. Madzharova-Atanasova and N. Shakev, "Intelligence in Human-Robot Collaboration – Overview, Challenges and Directions," in *2023 International Conference Automatics and Informatics (ICAI)*, Varna, Bulgaria, 2023, pp. 190–194.

[12] Z. M. Bi, C. Luo, Z. Miao, B. Zhang, W. J. Zhang, and L. Wang, "Safety assurance mechanisms of collaborative robotic systems in manufacturing," *Robotics and Computer-Integrated Manufacturing*, vol. 67, p. 102022, 2021, doi: 10.1016/j.rcim.2020.102022.

[13] J. Edward, W. Wannasuphoprasit, and M. Peshkin, "Cobots: Robots For Collaboration With Human Operators," Northwestern Univ., Evanston, IL, USA, Tech. Rep., 1999.

[14] ABB Ltd., *SafeMove.* [Online]. Available: https://new.abb.com/products/robotics/controllers/safemove## [Accessed: Mar. 11, 2025].

[15] M. Dhanda, B. A. Rogers, S. Hall, E. Dekoninck, and V. Dhokia, "Reviewing human-robot collaboration in manufacturing: Opportunities and challenges in the context of industry 5.0," *Robotics and Computer-Integrated Manufacturing*, vol. 93, p. 102937, 2025, doi: 10.1016/j.rcim.2024.102937.

[16] *Robots and robotic devices - Safety requirements for industrial robots - Part 1: Robots,* ISO 10218-1:2011, 2011.

[17] *Robots and robotic devices - Safety requirements for industrial robots - Part 2: Robot systems and integration,* ISO 10218-2:2011, 2011.
[18] *Robots and robotic devices - Collaborative robots,* ISO/TS 15066:2016, 2016.
[19] KUKA AG, *KUKA.SafeOperation.* [Online]. Available: https://www.kuka.com/en-us/products/robotics-systems/software/hub-technologies/kuka_safeoperation## [Accessed: Mar. 16, 2025].
[20] C. Emeric, D. Geoffroy, and D. Paul-Eric, "Development of a new robotic programming support system for operators," *Procedia Manufacturing*, vol. 51, pp. 73–80, 2020, doi: 10.1016/j.promfg.2020.10.012.
[21] J. Arents, V. Abolins, J. Judvaitis, O. Vismanis, A. Oraby, and K. Ozols, "Human–Robot Collaboration Trends and Safety Aspects: A Systematic Review," *JSAN*, vol. 10, no. 3, p. 48, 2021, doi: 10.3390/jsan10030048.
[22] S. Proia, R. Carli, G. Cavone, and M. Dotoli, "Control Techniques for Safe, Ergonomic, and Efficient Human-Robot Collaboration in the Digital Industry: A Survey," *IEEE Trans. Automat. Sci. Eng.*, vol. 19, no. 3, pp. 1798–1819, 2022, doi: 10.1109/TASE.2021.3131011.
[23] A. Villalonga, Y. J. Cruz, D. Alfaro, R. E. Haber, J. L. Martínez-Lastra, and F. Castaño, "Enhancing Quality Inspection in Zero-Defect Manufacturing Through Robotic-Machine Collaboration," in *2024 7th Iberian Robotics Conference (ROBOT)*, Madrid, Spain, 2024, pp. 1–6.
[24] *Safety of machinery - Integrated manufacturing systems - Basic requirements,* ISO 11161:2007, 2007.
[25] A. Jafari-Tabrizi, D. P. Gruber, and A. Gams, "Exploiting image quality measure for automatic trajectory generation in robot-aided visual quality inspection," *Int J Adv Manuf Technol*, vol. 132, 9-10, pp. 4885–4901, 2024, doi: 10.1007/s00170-024-13609-5.
[26] S. Bindel, *Robotics in the era of digitalisation: 47th International Symposium on Robotics : June 21-22, 2016, Messe München, Entrance East, Munich, Germany*. Berlin, Offenbach: VDE Verlag, 2016.
[27] C.-C. J. Hsu, P.-J. Hwang, W.-Y. Wang, Y.-T. Wang, and C.-K. Lu, "Vision-Based Mobile Collaborative Robot Incorporating a Multicamera Localization System," *IEEE Sensors J.*, vol. 23, no. 18, pp. 21853–21861, 2023, doi: 10.1109/JSEN.2023.3300301.
[28] K. Säfsten and M. Gustavsson, *Research methodology 2.0 : For engineers and other problem-solvers,* 2nd ed. Lund: Studentlitteratur AB, 2024.
[29] *Application manual - Force control Standard for GoFa*, Document ID: 3HAC083267-001, ABB Ltd., 2019.
[30] Intel Corporation, *Intel® RealSense™ Depth Camera D435.* [Online]. Available: https://www.intelrealsense.com/depth-camera-d435/## [Accessed: Apr. 12, 2025].
[31] *Application manual - Controller software IRC5*, Document ID: 3HAC050798-001, ABB Ltd., 2025.
[32] Ultralytics Ltd., *Ultralytics YOLO11.* [Online]. Available: https://docs.ultralytics.com/models/yolo11/## [Accessed: Apr. 14, 2025].
[33] Ultralytics Ltd., *Machine Learning Best Practices and Tips for Model Training.* [Online]. Available: https://docs.ultralytics.com/guides/model-training-tips/#other-techniques-to-consider-when-handling-a-large-dataset## [Accessed: Apr. 14, 2025].

[34] *Safety of machinery - Minimum gaps to avoid crushing of parts of the human body,* ISO 13854:2017, 2017.

[35] ABB Ltd., *GoFa CRB 15000 Datasheet: Go far with your new helping hand.* [Online]. Available: https://search.abb.com/library/Download.aspx?DocumentID=9AKK107991A8564&LanguageCode=en&DocumentPartId=&Action=Launch## [Accessed: Apr. 27, 2025].

[36] C. Fischer, M. Neuhold, M. Steiner, T. Haspl, M. Rathmair, and S. Schlund, "Collision Tests in Human-Robot Collaboration: Experiments on the Influence of Additional Impact Parameters on Safety," *IEEE Access*, vol. 11, pp. 118395–118413, 2023, doi: 10.1109/ACCESS.2023.3327301.

A. Full risk identification

According to ISO 12100:2010 [1] Clause 5.3, 6.2 and ISO 10218-2:2025 [3] Clause 5.5 and 5.6, the following design related hazards are identified:

- Risk of loss of stability: The transported part on the AGV may have an uneven weight distribution or extend significantly beyond the AGV base. This could shift the centre of gravity, increasing the risk of tipping or loss of stability during movement or braking.
- Risk due to sharp surfaces, edges, or angles: Components of the workstation, including the robot, AGV, and surrounding structures, may contain sharp edges. These present potential risks of cuts, punctures, or abrasions upon contact.
- Risk arising from moving parts: Mechanical movement of the robot arm, AGV platform, or end-effector introduces a risk of entrapment, impact, or crushing. There is also a risk that speed and force settings could be altered unintentionally or without adequate restriction, resulting in unsafe operating conditions if the values are higher than intended.
- Risk of uncontrolled movements: There is a potential hazard in cases where emergency stop or safety inputs are activated, but the system fails to respond correctly for instance, if the AGV enters the zone and the robot initiates motion unexpectedly due to communication failure or logic error.

According to ISO 12100:2010 [1] Clause 6.2 and ISO 10218-2:2025 [3] Clause 5.6, the following control related hazards are identified:

- Safety and reliability of control systems: There is a risk of unintended robot movement due to software faults, logic errors, or loss of communication with the higher-level system. If control logic fails, hazardous motion may occur without warning. Repair technicians entering the station must manually trigger an emergency stop to ensure no system is active during access.
- Control devices: The teach pendant is currently the only control device. This introduces the risk of limited redundancy in control access and emergency intervention. This must be clarified whether this single device is sufficient for safe operation under all conditions.
- Start function: A false signal from the upper system may cause the robot to start without the AGV being present, introducing a serious hazard. The control logic must ensure that such accidental starts are impossible through proper interlocks and logic conditions.
- Normal stop function: There is a potential hazard if pressing the stop button does not result in an immediate stop. The behaviour of the robot after pressing the stop, whether the system halts immediately or continues to the end of the current motion must be defined. Additionally, behaviour following reset or restart must be safely controlled, and the assigned stop category should be clearly documented.
- Operational stop: An operational stop is only acceptable if restarting and continuing motion can be done safely and predictably. Poor design here increases the risk of unpredictable motion during recovery from a stop.

- Emergency stop: At least one emergency stop device must be available outside the risk area. If the teach pendant serves this function, the placement must allow access without entering hazardous zones.
- Assembly of machinery: If any process in the line triggers an emergency condition, this must cause the robot to halt as well. The same applies in reverse. A lack of synchronization between systems presents a high risk of uncontrolled interaction.
- Selection of control/operating mode: The transition between manual and automatic modes must be protected by secure access, such as a password or operator code, to prevent unauthorized or accidental switching. Similar access control is needed for enabling/disabling safety functions.
- Failure of power supply: In the event of a power loss or emergency stop, there must be a guaranteed safe condition for the robot. Scenarios such as a person being trapped between the robot and another object must be considered that there should be a way to safely release or move the robot in such cases.

In line with ISO 12100 [1] Clause 5.5, additional non-mechanical hazards are identified:

- Errors in fitting: Improper installation or insecure attachment of the AGV or its payload may result in movement instability, increasing the risk of tipping or collision.
- Noise and radiation: The workstation must comply with legal exposure limits for noise and radiation in a production environment. Excessive noise or radiation may introduce health risks to operators or technicians.
- Risk of entrapment: There is a significant risk of entrapment between the robot and the part, or between the AGV and structures such as tables. These areas must be marked clearly, and design measures such as sloped barriers or physical separation should be considered to prevent human presence in these danger zones. Additionally, signals or sensors could be used to confirm safe clearance before motion.

According to ISO 12100 [1] Clause 6.2 and ISO 10218-2:2025 [3] Clause 5.9, maintenance related risks include:

- Access to servicing points: Maintenance personnel must have the ability to safely access components without risk of activation. This includes physical protection such as lockable covers or transparent shields.
- Isolation of energy sources: During maintenance or emergency stops, the system must isolate all forms of stored energy. In addition, the control logic must prevent any unintentional restart, including accidental start commands from the upper system. The design must ensure that the robot cannot resume motion unless all safety conditions are actively met.

Lack of adequate operational information or warnings is a safety risk as defined in ISO 12100 [1] Clause 6.4:

- Warning devices: There is currently no clear visual indication of the operating state. Proper signalling is essential to always inform nearby personnel of the system status.
- Information and safety markings: The machine lacks necessary instructional and safety labelling. Warnings must be visible in both local language and English and should include pictograms where possible. Additionally, CE marking, operating instructions, and safety principles in accordance with standards are missing and must be provided for regulatory compliance and operator safety.

B. Full risk evaluation calculations

S	E	O	A	Risk Score	Mean	Deviation	Risk from 1 to 72	The distribution of the score	Normal Distribution	Cumulative Normal Distribution	Levels	Percentage	Threshold Value	Level Score Range
1	1	1	1	1	15	13,54006	1	1	0,01726	0,15058	Level 1	20%	4	1,0 - 4,0
1	1	1	2	2			2	4	0,01858	0,16850	Level 2	40%	12	5,0 - 12,0
1	1	1	3	3			3	3	0,01989	0,18774	Level 3	60%	18	13,0 - 18,0
1	1	2	1	2			4	7	0,02118	0,20828	Level 4	80%	26	19,0 - 26,0
1	1	2	2	4			5	0	0,02243	0,23009	Level 5	99%	46	27,0 - 72,0
1	1	2	3	6			6	9	0,02362	0,25312				
1	1	3	1	3			7	0	0,02474	0,27731				
1	1	3	2	6			8	7	0,02578	0,30258				
1	1	3	3	9			9	3	0,02671	0,32884				
1	2	1	1	2			10	0	0,02752	0,35596				
1	2	1	2	4			11	0	0,02821	0,38384				
1	2	1	3	6			12	11	0,02875	0,41233				
1	2	2	1	4			13	0	0,02914	0,44129				
1	2	2	2	8			14	0	0,02938	0,47056				
1	2	2	3	12			15	0	0,02946	0,50000				
1	2	3	1	6			16	4	0,02938	0,52944				
1	2	3	2	12			17	0	0,02914	0,55871				
1	2	3	3	18			18	6	0,02875	0,58767				
2	1	1	1	2			19	0	0,02821	0,61616				
2	1	1	2	4			20	0	0,02752	0,64404				
2	1	1	3	6			21	0	0,02671	0,67116				
2	1	2	1	4			22	0	0,02578	0,69742				
2	1	2	2	8			23	0	0,02474	0,72269				
2	1	2	3	12			24	7	0,02362	0,74688				
2	1	3	1	6			25	0	0,02243	0,76991				
2	1	3	2	12			26	0	0,02118	0,79172				
2	1	3	3	18			27	1	0,01989	0,81226				
2	2	1	1	4			28	0	0,01858	0,83150				
2	2	1	2	8			29	0	0,01726	0,84942				
2	2	1	3	12			30	0	0,01595	0,86603				
2	2	2	1	8			31	0	0,01466	0,88133				
2	2	2	2	16			32	1	0,01340	0,89536				
2	2	2	3	24			33	0	0,01218	0,90814				
2	2	3	1	12			34	0	0,01101	0,91973				
2	2	3	2	24			35	0	0,00990	0,93018				
2	2	3	3	36			36	4	0,00885	0,93954				
3	1	1	1	3			37	0	0,00787	0,94790				
3	1	1	2	6			38	0	0,00696	0,95531				
3	1	1	3	9			39	0	0,00612	0,96185				
3	1	2	1	6			40	0	0,00536	0,96758				
3	1	2	2	12			41	0	0,00466	0,97259				
3	1	2	3	18			42	0	0,00403	0,97693				
3	1	3	1	9			43	0	0,00347	0,98068				
3	1	3	2	18			44	0	0,00297	0,98389				
3	1	3	3	27			45	0	0,00253	0,98664				
3	2	1	1	6			46	0	0,00214	0,98897				
3	2	1	2	12			47	0	0,00180	0,99094				
3	2	1	3	18			48	2	0,00151	0,99260				
3	2	2	1	12			49	0	0,00126	0,99398				
3	2	2	2	24			50	0	0,00104	0,99513				
3	2	2	3	36			51	0	0,00086	0,99608				
3	2	3	1	18			52	0	0,00070	0,99686				
3	2	3	2	36			53	0	0,00057	0,99750				
3	2	3	3	54			54	1	0,00047	0,99801				
4	1	1	1	4			55	0	0,00038	0,99843				
4	1	1	2	8			56	0	0,00030	0,99877				
4	1	1	3	12			57	0	0,00024	0,99904				
4	1	2	1	8			58	0	0,00019	0,99925				
4	1	2	2	16			59	0	0,00015	0,99942				
4	1	2	3	24			60	0	0,00012	0,99956				
4	1	3	1	12			61	0	0,00009	0,99966				
4	1	3	2	24			62	0	0,00007	0,99974				
4	1	3	3	36			63	0	0,00005	0,99980				
4	2	1	1	8			64	0	0,00004	0,99985				
4	2	1	2	16			65	0	0,00003	0,99989				
4	2	1	3	24			66	0	0,00002	0,99992				
4	2	2	1	16			67	0	0,00002	0,99994				
4	2	2	2	32			68	0	0,00001	0,99995				
4	2	2	3	48			69	0	0,00001	0,99997				
4	2	3	1	24			70	0	0,00001	0,99998				
4	2	3	2	48			71	0	0,00001	0,99998				
4	2	3	3	72			72	1	0,00000	0,99999				

Figure 32 Tabulated values of the standard normal distribution function showing the cumulative probability for the corresponding score. This table is typically used in statistical analysis to determine the probability that a standard normal variable falls below a given score.

C. Full Risk Assessment

Risk Identification			Risk Estimation				Risk Evaluation		Risk reduction	
No	Source of risk	Description (what is it that generates the risk) and what can happen	S	E	O	A	Risk Level	Recommended action	Prioritising	Implemented actions
1. Collaboration										
1	Maximum Operating Height	The maximum operating height must be restricted to prevent it from being exceeded.	4	1	3	3	36	Design change	High	The maximum operating height is limited to 1.5 m.
2	Minimum Operating Height	The minimum operating height should be determined in accordance with ISO 13854 to eliminate any risk of clamping.	3	1	3	3	27	Design change	High	In accordance with ISO 10218 and ISO 13854, the relative operating height is restricted in distance to the object to 180 mm at the top and 230 mm at the sides to ensure no clamping risks.
3	Maximum Operating Space	The maximum operating space must be restricted to prevent it from being exceeded. No unwanted and not considered motions outside of the intended areas	3	1	3	3	27	Design change	High	The maximum operating space is limited to the intended motion
4	Robot Height	The robot's base position on a table or stand is too high and needs to be lowered.	4	1	3	3	36	Design change	High	The new layout introduces a "pallet" or small "stage" on which the robot is mounted, creating a subtle elevation that acts as a barrier without being a physical obstruction. The robot is positioned 10 cm above ground level. The risk of errors in fitting of the robot to the base is low, and the forces and torques involved are minimal, making this setup sufficient and acceptable for the intended use case.
5	Tool Speed Supervision	The robot's speed can exceed a reasonable value and needs therefore be limited to minimize the possibility of the risk and harm.	4	1	3	3	36	Design change	High	In accordance with ISO 10218 Annex C, reducing the robot's operating speed to 150 mm/s minimizes the possibility of the risk and harm. Outside of the work zones the speed are globally set to 250 mm/s
6	Tool Force Supervision	The robot's force can exceed a reasonable value and needs therefore be limited to minimize the possibility of the risk and harm.	4	1	3	3	36	Design change	High	In accordance with ISO 10218 Annex M, reducing the robot's operating force to under 65 Newton minimizes the possibility of the risk and harm. (Needs validation that the pressure is not exceeding) Outside of the work zones the force are globally set to 65 Newton. (Needs validation that the pressure is not exceeding)

Figure 33 Risk assessment table for the collaborative robotic application, showing identified hazards, risk estimation using severity (S), exposure (E), occurrence (O), and avoidance (A) criteria, and the resulting risk level. Recommended mitigation actions are based on ISO 10218-2:2025 [3] and ISO 13854:2017 [34] guidelines. All risks are prioritized as high, and corresponding actions have been implemented to ensure safe operation within biomechanical and spatial limits.

Risk Identification			Risk Estimation				Risk Evaluation		Risk reduction		Potential Production Implementation	
No	Source of risk	Description (what is it that generates the risk) and what can happen	S	E	O	A	Risk Level	Recommended action	Acceptable risk after risk reduction	Action introduced (sign and date)	Prioritising	Recommended action or actions
1.8 Collaboration												
1	Maximum Operating Height	The maximum operating height must be restricted to prevent it from being exceeded.	2	1	2	1	4	Can remain without measures	Yes		High	The height must account for foreseeable misuse during production, which requires considering typical operator body positions. In the production the AGV needs to be able to adjust the height of the object for the difference operating heights for different humans. Therefore, the AGV and part height will be able to operate at a lower position reducing the risk of foreseeable misuse during production
2	Minimum Operating Height	The minimum operating height should be determined in accordance with ISO 13854 to eliminate any risk of clamping.	1	1	2	1	2	Can remain without measures	Yes		High	This "pallet" or small "stage" setup requires a heavier base in production, as the forces and torques involved can be higher. This added weight helps reduce the risk of tripping.
3	Maximum Operating Space	The maximum operating space must be restricted to prevent it from being exceeded. No unwanted and not considered motions outside of the intended areas	1	1	1	1	1	Can remain without measures	Yes		High	The current workspace depends on the task and how the robot moves. When the task changes, the movement can also change, which may affect the level of risk. That's why the workspace is only valid for the current motion. If a new type of motion is added, like for quality inspection, and it is not part of the original setup, then a new risk assessment and safety check are needed. Limited to the intended use
4	Robot Height	The robot's base position on a table or stand is too high and needs to be lowered.	2	1	1	1	2	Can remain without measures	Yes		High	If the takt time allows this speed, then the possibility of the risk and harm is minimized to the minimum.
5	Tool Speed Supervision	The robot's speed can exceed a reasonable value and needs therefore be limited to minimize the possibility of the risk and harm.	1	1	2	1	2	Can remain without measures	Yes		High	In accordance with ISO 10218 Annex C, reducing the robot's operating speed to 150 mm/s minimizes the possibility of the risk and harm. Outside of the work zones the speed are globally set to 250 mm/s
6	Tool Force Supervision	The robot's force can exceed a reasonable value and needs therefore be limited to minimize the possibility of the risk and harm.	1	1	2	1	2	Can remain without measures	Yes		High	If the takt time allows this force, then the possibility of the risk and harm is minimized to the minimum.

Figure 34 Updated risk assessment for collaborative operation, showing reduced risk levels after mitigation actions. Each risk is evaluated based on severity (S), exposure (E), occurrence (O), and avoidance (A), followed by risk reduction measures and production implementation notes. All risks are rated as acceptable after mitigation and include practical considerations for real-world deployment, including AGV adjustments, workspace limitations, and process safety boundaries.

D. Full risk mitigation

This appendix provides visual documentation of the design elements and safety zoning implemented in the collaborative robotic workstation. The images demonstrate how physical layout, zone configuration, and control logic work together to achieve a fully mitigated risk environment in accordance with ISO 10218-2:2025 [3].

Figure 35 End-effector with rounded geometry used in the collaborative workstation to minimize injury risk during contact events. The design reduces the likelihood of sharp-edge impacts and clamping, supporting safer interaction in accordance with biomechanical safety guidelines outlined in ISO 10218-2:2025 [3].

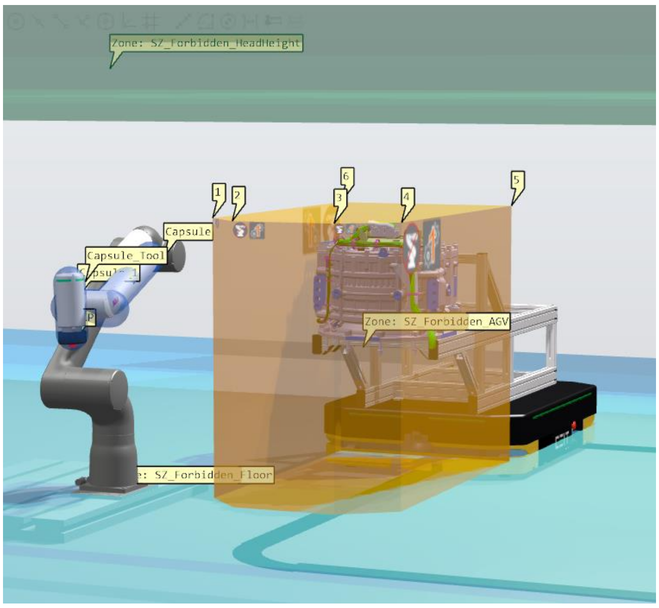

Figure 36 Configured safety zones around the robot and AGV during operation. The zones define dynamic boundaries based on robot motion and task type, enforcing safe distances and triggering speed or force limitations where necessary. This supports real-time risk reduction and spatial awareness in the collaborative environment.

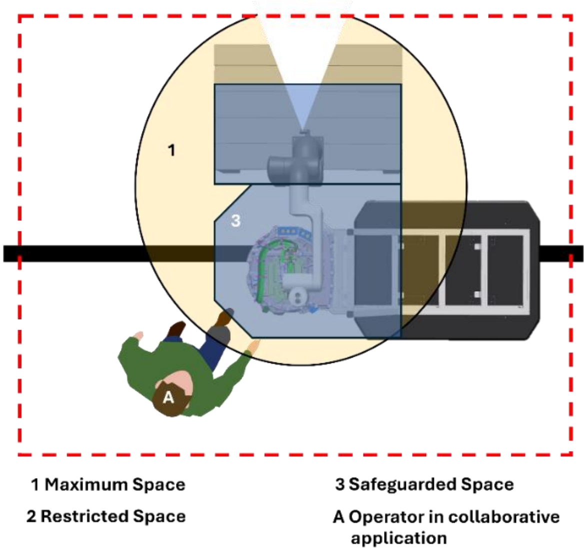

Figure 37 Top-down layout of the collaborative workspace, highlighting operator position, robot range, and inspection area. Visual zoning supports controlled movement and risk avoidance. The illustration helps assess potential human-robot interactions and validates field-of-view coverage for the vision system.

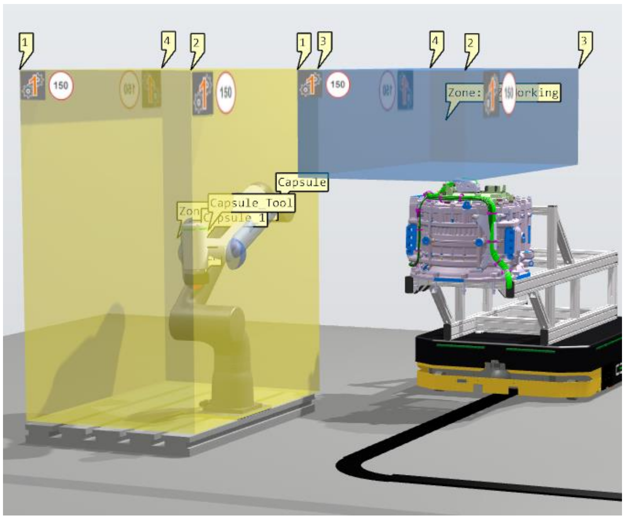

Figure 38 Finalized safety zoning by combining speed and force supervision with task-specific work areas. Dynamic capsule zones adjust according to robot activity, ensuring compliance with the guidelines outlined in ISO 10218-2:2025 [3]. Visual markers and speed limits contribute to a fully mitigated collaborative setup.

E. Risk Validation Calculations

The risk validation calculations can be done with the following formula

$$F_T = v_{rel} \cdot \sqrt{\frac{k}{\frac{1}{m_H} + \frac{1}{m_R}}}$$

to calculate the transient force for different body areas were

- F_T is the transient force,
- v_{rel} is the relative velocity of the robot,
- k is the stiffness coefficient for the respective body region from Table M.3 in ISO 10218-2:2025 [3],
- m_H is the effective human body mass for that region from Table M.3 in ISO 10218-2:2025 [3],
- m_R is the moving mass of the robot.

The moving mass of the robot needs to be determined with

$$m_R = \frac{M}{2} + m_L$$

where M is the moving mass of the robot arm and m_L the mass of the end-effector. Since the base of the robot is the heaviest component and remains fixed, the value needs to be excluded from the moving mass calculation. The ABB GoFa CRB 15000-10/1.52 has a total weight of 51 kilograms [35]. Given the high reach of the robot, the moving mass of the robot arm is estimated at 40% of the total weight, resulting in $M = 20.4\ kg$. The mass of the end-effector can be measured by the ABB GoFa CRB 15000-10/1.52 through calibration and results in 300 grams. Leading to a total weight of the moving mass to

$$m_R = \frac{M}{2} + m_L$$

$$m_R = \frac{20.4\ kg}{2} + 0.3\ kg$$

$$m_R = 10.5\ kg.$$

The relative highest operating velocity of the robot is set to

$$v_{rel} = 150 \frac{mm}{s}$$

with the values from Table M.3 in ISO 10218-2:2025 [3]. To calculate the transient pressure p_T with

$$p_T = \frac{F_T}{A}$$

the transient force F_T is divided by the contact area A which is simplified to $A = 1\ \text{cm}^2$ in these calculations.

The calculation begins with the upper body regions, using the respective values from Table M.3 of ISO 10218-2:2025 [3]. Calculating for the Skull and forehead

$$F_T = v_{rel} \cdot \sqrt{\frac{k}{\frac{1}{m_H} + \frac{1}{m_R}}}$$

$$F_T = 150\frac{mm}{s} \cdot \sqrt{\frac{150\frac{N}{mm}}{\frac{1}{4.4\ kg} + \frac{1}{10.5\ kg}}}$$

$$F_T = 102.3\ N$$

and

$$p_T = \frac{F_T}{A}$$

$$p_T = 102.3\frac{N}{cm^2}$$

the face

$$F_T = v_{rel} \cdot \sqrt{\frac{k}{\frac{1}{m_H} + \frac{1}{m_R}}}$$

$$F_T = 150\frac{mm}{s} \cdot \sqrt{\frac{75\frac{N}{mm}}{\frac{1}{4.4\ kg} + \frac{1}{10.5\ kg}}}$$

$$F_T = 72.3\ N$$

and

$$p_T = \frac{F_T}{A}$$

$$p_T = 72.3\frac{N}{cm^2}$$

the neck

$$F_T = v_{rel} \cdot \sqrt{\frac{k}{\frac{1}{m_H} + \frac{1}{m_R}}}$$

$$F_T = 150\frac{mm}{s} \cdot \sqrt{\frac{50\frac{N}{mm}}{\frac{1}{1.2\ kg} + \frac{1}{10.5\ kg}}}$$

$$F_T = 34.8\ N$$

and

$$p_T = \frac{F_T}{A}$$

$$p_T = 34.8 \frac{N}{cm^2}$$

the back and shoulders

$$F_T = v_{rel} \cdot \sqrt{\frac{k}{\frac{1}{m_H} + \frac{1}{m_R}}}$$

$$F_T = 150 \frac{mm}{s} \cdot \sqrt{\frac{35 \frac{N}{mm}}{\frac{1}{40\ kg} + \frac{1}{10.5\ kg}}}$$

$$F_T = 80.9\ N$$

and

$$p_T = \frac{F_T}{A}$$

$$p_T = 80.9 \frac{N}{cm^2}$$

the upper arm and elbow

$$F_T = v_{rel} \cdot \sqrt{\frac{k}{\frac{1}{m_H} + \frac{1}{m_R}}}$$

$$F_T = 150 \frac{mm}{s} \cdot \sqrt{\frac{30 \frac{N}{mm}}{\frac{1}{3\ kg} + \frac{1}{10.5\ kg}}}$$

$$F_T = 39.7\ N$$

and

$$p_T = \frac{F_T}{A}$$

$$p_T = 39.7 \frac{N}{cm^2}$$

the chest

$$F_T = v_{rel} \cdot \sqrt{\frac{k}{\frac{1}{m_H} + \frac{1}{m_R}}}$$

$$F_T = 150\frac{mm}{s} \cdot \sqrt{\frac{25\frac{N}{mm}}{\frac{1}{40\ kg} + \frac{1}{10.5\ kg}}}$$

$$F_T = 68.4\ N$$

and

$$p_T = \frac{F_T}{A}$$

$$p_T = 68.4\frac{N}{cm^2}$$

The calculation continue with the lower body regions, using the respective values from Table M.3 of ISO 10218-2:2025 [3]. Calculating for the abdomen

$$F_T = v_{rel} \cdot \sqrt{\frac{k}{\frac{1}{m_H} + \frac{1}{m_R}}}$$

$$F_T = 150\frac{mm}{s} \cdot \sqrt{\frac{10\frac{N}{mm}}{\frac{1}{40\ kg} + \frac{1}{10.5\ kg}}}$$

$$F_T = 43.25\ N$$

and

$$p_T = \frac{F_T}{A}$$

$$p_T = 43.25\frac{N}{cm^2}$$

the pelvis

$$F_T = v_{rel} \cdot \sqrt{\frac{k}{\frac{1}{m_H} + \frac{1}{m_R}}}$$

$$F_T = 150\frac{mm}{s} \cdot \sqrt{\frac{25\frac{N}{mm}}{\frac{1}{40\ kg} + \frac{1}{10.5\ kg}}}$$

$$F_T = 68.4\ N$$

and

$$p_T = \frac{F_T}{A}$$

$$p_T = 68.4\frac{N}{cm^2}$$

the upper leg with thighs and knees

$$F_T = v_{rel} \cdot \sqrt{\frac{k}{\frac{1}{m_H} + \frac{1}{m_R}}}$$

$$F_T = 150 \frac{mm}{s} \cdot \sqrt{\frac{50 \frac{N}{mm}}{\frac{1}{75\ kg} + \frac{1}{10.5\ kg}}}$$

$$F_T = 101.8\ N$$

and

$$p_T = \frac{F_T}{A}$$

$$p_T = 101.8 \frac{N}{cm^2}.$$

F. First Measurement

This appendix presents the test setup, motion sequence, and results of the initial measurement used to validate safety compliance in a collaborative HRI scenario. The purpose of this test is to evaluate whether the contact forces and pressures during a worst-case scenario remain within the biomechanical limits defined by ISO 10218-2:2025 [3].

Therefore, Figure 39 shows the programmed motion path of the robot from the home position to the contact point. The left diagram illustrates the linear approach used during testing, while the right image depicts the actual test environment where the end-effector of the robot makes contact with the measurement area. A fibre cloth is placed between the sensor and the end-effector to simulate realistic contact conditions. The robot is operated at a height of 1300 mm from the ground, with a speed of $150 \frac{\text{mm}}{\text{s}}$ and tool force supervision set to 38 N.

The measurements are conducted three times with a maximum of 10% variance and the worst-case scenario is taken to obtain reliable estimates. Due to time constraints, repeated trials and broader statistical sampling are not performed. Additionally, the limited availability of different effective spring constants for various body regions means the results are not always fully representative and used to provide approximate values under the given conditions.

Therefore, for the skull, forehead, face and shoulders the correct damping material with the corresponding effective spring constant, as specified in Annex N from ISO 10218-2:2025 [3], is used to measure the following force and pressure values.

The measurement value for the neck is not fully representative. While the correct damping material is used, the correct effective spring constant is not applied. As a result, the effective spring constant $k = 75 \frac{\text{N}}{\text{mm}}$ is used instead of $k = 50 \frac{\text{N}}{\text{mm}}$, which likely leads to higher values than would be expected with a properly matched spring constant. Additionally,

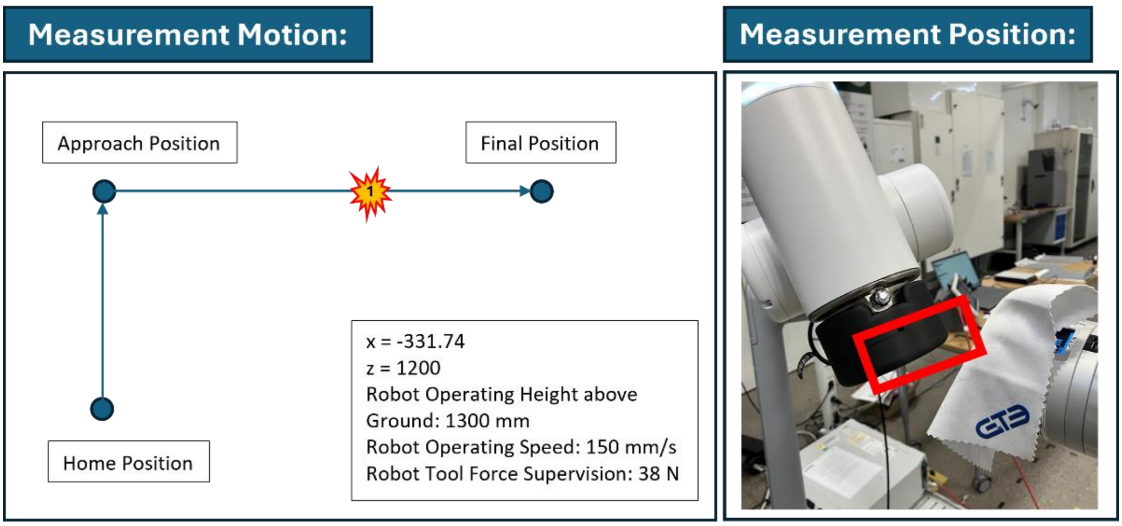

Figure 39 Test setup and robot trajectory used for force measurement. The left image shows the programmed motion from the home position to the contact point. The right image displays the physical setup, where the end-effector makes contact with the PFMD sensor covered with a fibre cloth to simulate realistic conditions.

the measurement value for the chest is also not fully representative. While the correct damping material is used, the correct effective spring constant is not applied. As a result, the effective spring constant $k = 35\frac{N}{mm}$ is used instead of $k = 25\frac{N}{mm}$, which likely leads to higher values than would be expected with a properly matched spring constant.

The force measurements for different body regions are recorded and visualized in Figure 40. These plots illustrate the transient contact force behaviour over time. Each measurement starts with a sharp force increase caused by the transient impact and then converges to a quasi-static force level. The red dotted line on each plot represents the safety threshold for the respective body region, as outlined in Annex N of ISO 10218-2:2025 [9].

The results demonstrate the following:

- Skull and Forehead: Peak transient force remains below the $130\ N$ threshold.
- Face and Neck: The measured force for the face exceeds the $65\ N$ threshold, whereas the neck force stays below the $300\ N$ respective limit.
- Back and Shoulders: Measured values are safely below the $420\ N$ threshold.
- Chest: The transient force remains well within the $280\ N$ safety limit.

These measurements provide a reference for assessing biomechanical compliance and identifying critical areas where further risk reduction may be required. The pressure measurements for different body regions are recorded and visualized in Figure 41. Each plot illustrates the spatial distribution of contact pressure during a transient impact event, as recorded by the PFMD sensor. The peak pressure values are noted at the centre of each distribution, offering insight into the severity of the impact on each body area. The results demonstrate the following:

- Skull and Forehead: Peak transient pressure exceeds the $110\frac{N}{cm^2}$ threshold.
- Face and Neck: The measured pressure for the face exceeds the $110\frac{N}{cm^2}$ threshold, whereas the neck pressure stays below the $280\frac{N}{cm^2}$ limit.

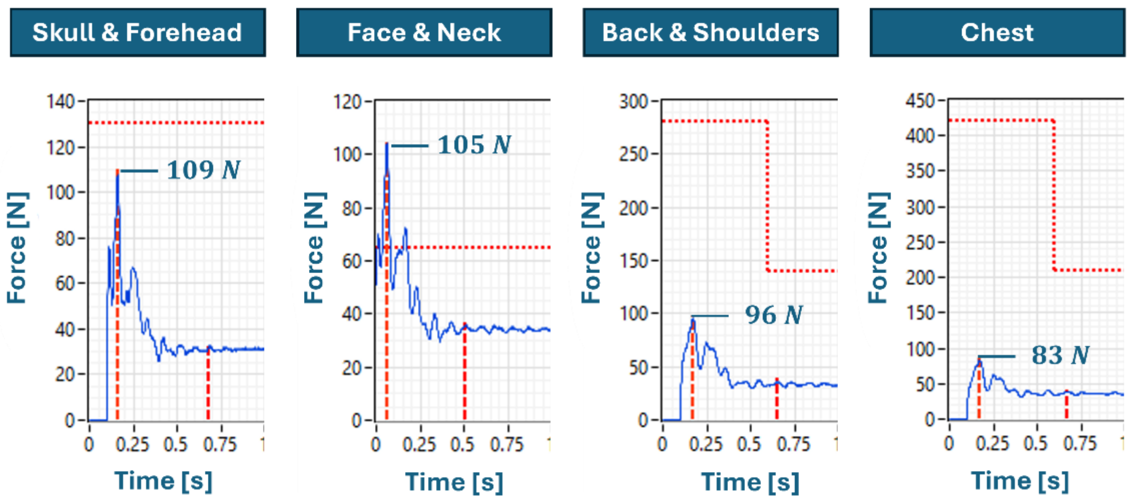

Figure 40 Transient contact force profiles for various upper body regions during initial impact. Each plot shows a rapid rise in force upon contact, followed by a stabilization phase reflecting the quasi-static force. The red dotted line indicates the biomechanical safety threshold for each respective body region as outlined in Annex N of ISO 10218-2:2025 [9]. These curves help to evaluate the safety compliance of the physical interactions.

- Back and Shoulders: The measured pressure for the shoulders stays below the $320\,\frac{\mathbf{N}}{\mathbf{cm^2}}$ threshold, as well as the back pressure which stays below the $420\,\frac{\mathbf{N}}{\mathbf{cm^2}}$ limit.
- Chest: The transient pressure remains well within the $240\,\frac{\mathbf{N}}{\mathbf{cm^2}}$ safety limit.

These measurements provide a reference for assessing biomechanical compliance and identifying critical areas where further risk reduction may be required.

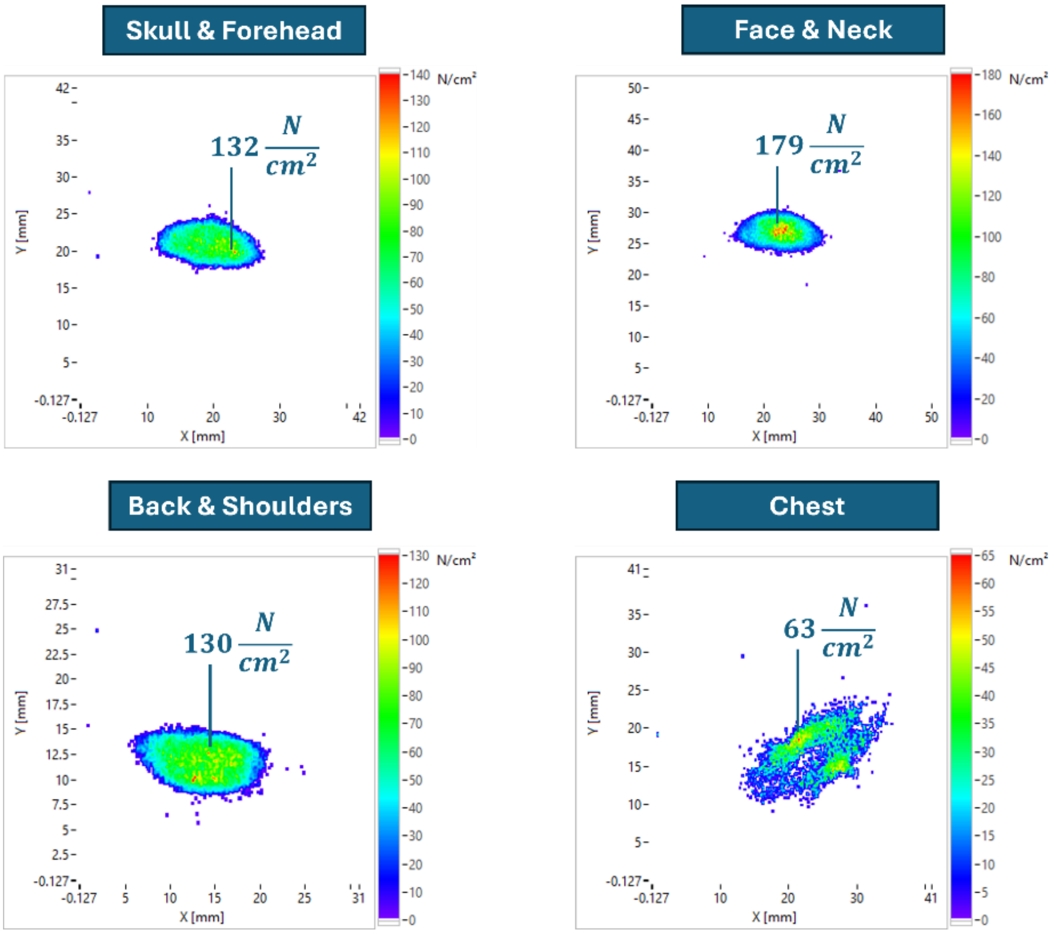

Figure 41 Spatial distribution of transient contact pressure for different upper body regions. The visualizations show the pressure intensity at the contact point with the maximum values annotated for each region. The colour gradient represents pressure intensity, from low (blue) to high (red), enabling identification of critical areas that may exceed biomechanical thresholds as defined in Annex N of ISO 10218-2:2025 [9]. These measurements highlight potential risk zones, especially at head-height impact areas.

G. Second Measurement

This appendix presents the test setup, motion sequence, and results of the second measurement used to validate safety compliance in a collaborative HRI scenario. The purpose of this test is to evaluate whether the contact forces and pressures during an additional worst-case scenario remain within the biomechanical limits defined by ISO 10218-2:2025 [3].

Therefore, Figure 42 shows the programmed motion path of the robot from the home position to the contact point. The left diagram illustrates the linear approach used during testing, while the right image depicts the actual test environment where the head of the robot makes contact with the measurement area. Particularly at the location where the screw is mounted on the robot head, the risk of high contact pressure is most pronounced. A fibre cloth is placed between the sensor and the contact area to simulate realistic contact conditions. The robot is operated at a height of $1300\ \mathrm{mm}$ above the ground, with a speed of $150\ \frac{\mathrm{mm}}{\mathrm{s}}$ and tool force supervision set to $38\ \mathrm{N}$.

The measurements are conducted three times with a maximum of 10% variance and the worst-case scenario is taken to obtain reliable estimates. Due to time constraints, repeated trials and broader statistical sampling are not performed. Additionally, the limited availability of different effective spring constants for various body regions means the results are not always fully representative and used to provide approximate values under the given conditions.

Therefore, for the skull, forehead, face and shoulders the correct damping material with the corresponding effective spring constant, as specified in Annex N from ISO 10218-2:2025 [3], is used to measure the following force and pressure values.

The measurement value for the neck is not fully representative. While the correct damping material is used, the correct effective spring constant is not applied. As a result, the

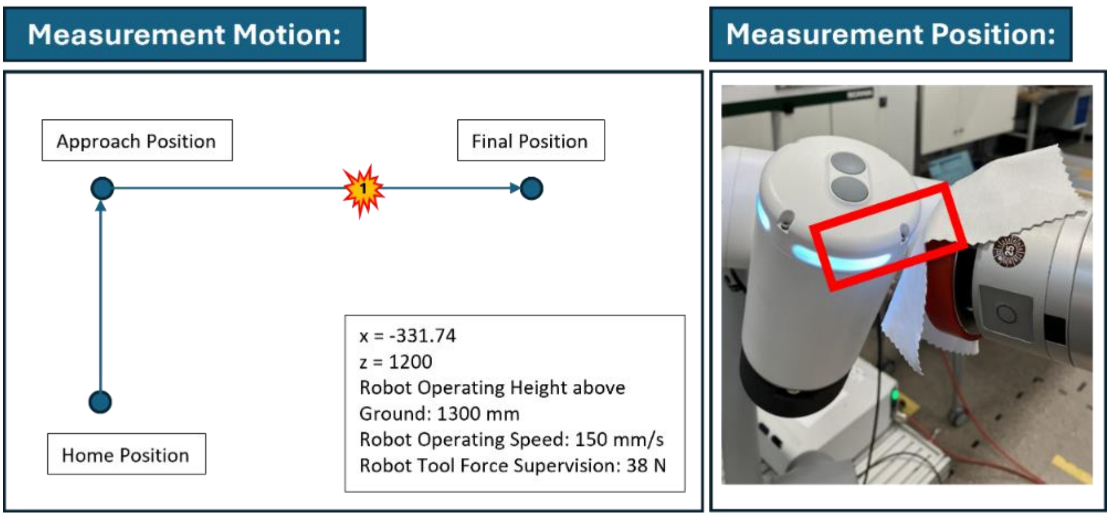

Figure 42 Test setup and robot trajectory used for force measurement. The left image shows the programmed motion from the home position to the contact point. The right image displays the physical setup, where the robot head makes contact with the PFMD sensor covered with a fibre cloth to simulate realistic conditions.

effective spring constant $k = 75 \frac{N}{mm}$ is used instead of $k = 50 \frac{N}{mm}$, which likely leads to higher values than would be expected with a properly matched spring constant. Additionally, the measurement value for the chest is also not fully representative. While the correct damping material is used, the correct effective spring constant is not applied. As a result, the effective spring constant $k = 35 \frac{N}{mm}$ is used instead of $k = 25 \frac{N}{mm}$, which likely leads to higher values than would be expected with a properly matched spring constant.

The force measurements for different body regions are recorded and visualized in Figure 43. These plots illustrate the transient contact force behaviour over time. Each measurement starts with a sharp force increase caused by the transient impact and then converges to a quasi-static force level. The red dotted line on each plot represents the safety threshold for the respective body region, as outlined in Annex N of ISO 10218-2:2025 [9]. The results demonstrate the following:

- Skull and Forehead: Peak transient force remains below the $130\ N$ threshold.
- Face and Neck: The measured force for the face exceeds the $65\ N$ threshold, whereas the neck force stays below the $300\ N$ respective limit.
- Back and Shoulders: Measured values are safely below the $420\ N$ threshold.
- Chest: The transient force remains well within the $280\ N$ safety limit.

These measurements provide a reference for assessing biomechanical compliance and identifying critical areas where further risk reduction may be required. The pressure measurements for different body regions are recorded and visualized in Figure 44. Each plot illustrates the spatial distribution of contact pressure during a transient impact event, as recorded by the PFMD sensor. The peak pressure values are noted at the centre of each distribution, offering insight into the severity of the impact on each body area. The results demonstrate the following:

- Skull and Forehead: Peak transient pressure exceeds the $110 \frac{N}{cm^2}$ threshold.

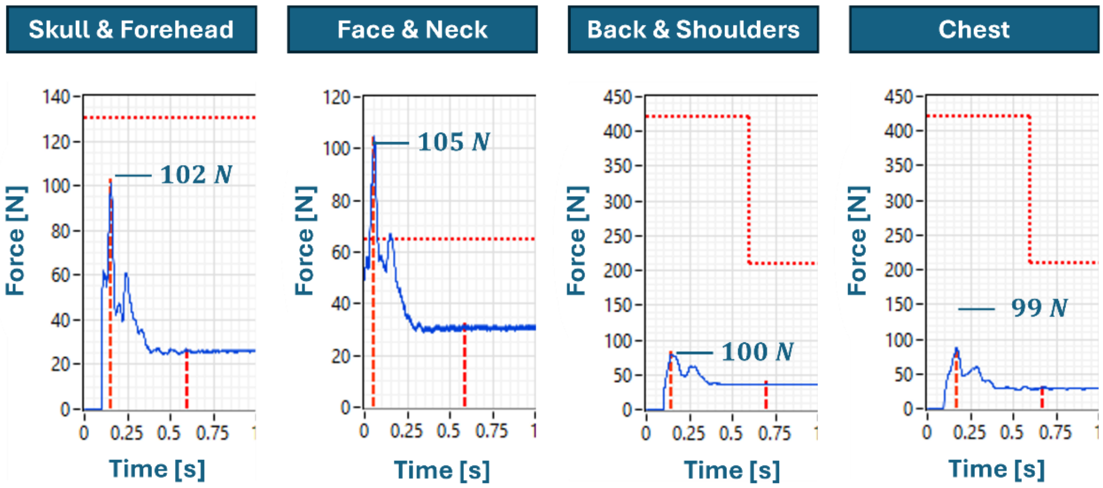

Figure 43 Visualization of transient contact force over time for different upper body regions. Each plot displays a sharp force peak at the moment of contact, followed by a gradual stabilization into the quasi-static force level. The measured peak force is annotated in each subplot. The red dotted line indicates the biomechanical force threshold as defined in Annex N of ISO 10218-2:2025 [9], allowing assessment of safety compliance during robot-human contact scenarios.

- Face and Neck: The measured pressure for the face exceeds the $110\,\frac{N}{cm^2}$ threshold, as well as the neck pressure which exceeds the $280\,\frac{N}{cm^2}$ limit.
- Back and Shoulders: The measured pressure for the shoulders exceeds the $320\,\frac{N}{cm^2}$ threshold, whereas the back pressure stays below the $420\,\frac{N}{cm^2}$ limit.
- Chest: The transient pressure for the chest exceeds the $240\,\frac{N}{cm^2}$ safety limit.

These measurements provide a reference for assessing biomechanical compliance and identifying critical areas where further risk reduction may be required.

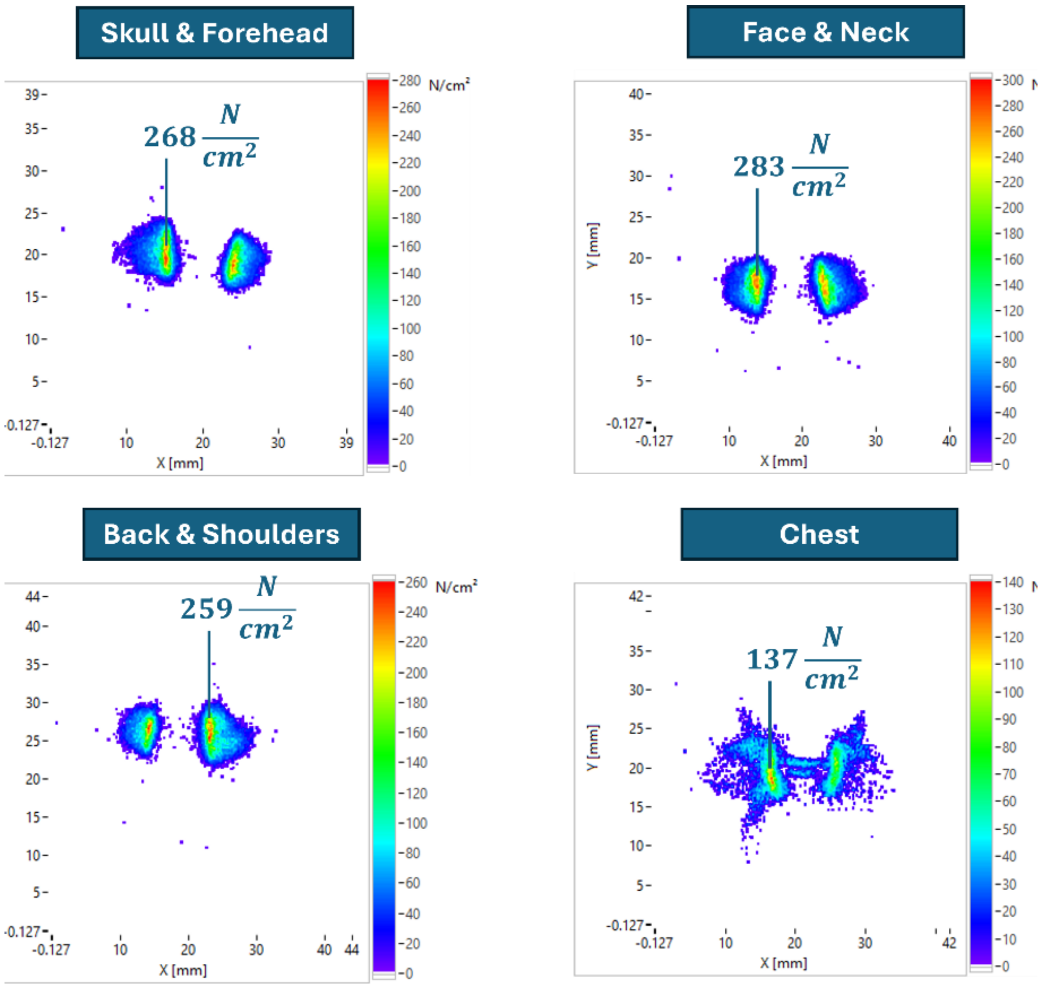

Figure 44 Pressure distribution maps for different upper body regions following contact with the robot head. The colour scale indicates pressure intensity with peak values labelled in each subplot. The data visualize the concentration and spread of pressure during transient impact events, revealing that all measured values exceed biomechanical safety thresholds defined in Annex N of ISO 10218-2:2025 [9]. These results highlight the critical need for additional safety measures in head-height operations.

H. Third Measurement

This appendix presents the test setup, motion sequence, and results of the third measurement used to validate safety compliance in a collaborative HRI scenario. The purpose of this test is to evaluate whether the contact forces and pressures during a worst-case scenario remain within the biomechanical limits defined by ISO 10218-2:2025 [3].

Therefore, the programmed motion path of the robot stays the same as the previous tests for the home position to the contact point. In the test environment the head of the robot makes contact with the measurement area. Particularly at the location where the screw is mounted on the robot head, the risk of high contact pressure is most pronounced. A fibre cloth is placed between the sensor and the contact area to simulate realistic contact conditions. The robot is operated at a height of $1300\ \text{mm}$ from the ground, and with the robot operating parameters as outlined in Figure 45. There the robot is evaluated on how a collision with the rounded edge of the robot head, additional soft padding and reduced speed and force is influencing the transient force and pressure values. Therefore, the reduced speed is $50\,\frac{\text{mm}}{\text{s}}$ and the reduced tool force supervision is set to $25\ \text{N}$.

The measurements are conducted three times with a maximum of 10% variance and the worst-case scenario is taken to obtain reliable estimates. Due to time constraints, repeated

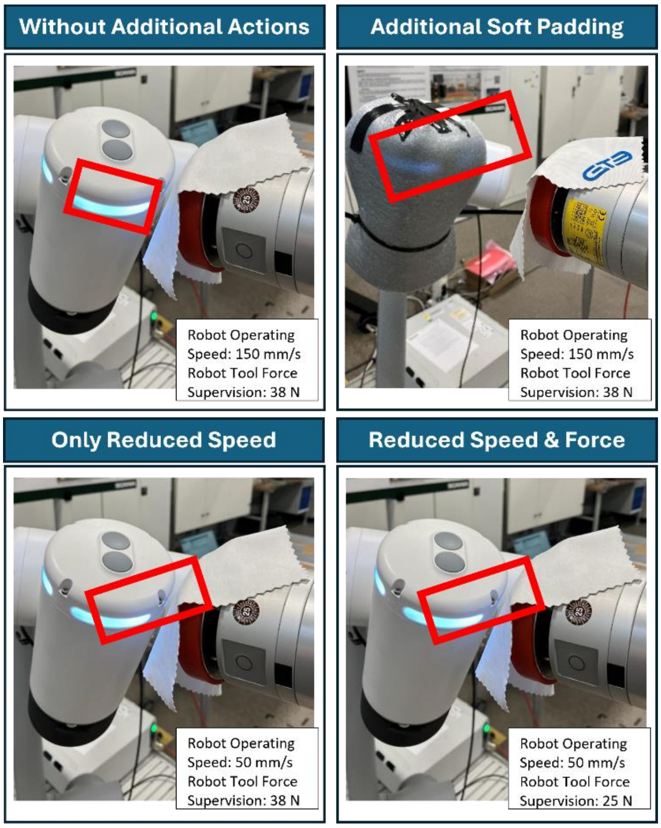

Figure 45 Visualization of the physical setup, where the robot head makes contact with the PFMD sensor covered with a fibre cloth to simulate realistic conditions. The different robot parameter conditions where the rounded edge, additional soft padding as well as reducing the speed and tool force supervision are tested.

trials and broader statistical sampling are not performed. Therefore, for the skull and forehead the correct damping material with the corresponding effective spring constant, as specified in Annex N from ISO 10218-2:2025 [3], is used to measure the following force and pressure values.

The force measurements for different parameter conditions are recorded and visualized in Figure 46. These plots illustrate the transient contact force behaviour over time. Each measurement starts with a sharp force increase caused by the transient impact and then converges to a quasi-static force level. The red dotted line on each plot represents the safety threshold for the skull and forehead, as outlined in Annex N of ISO 10218-2:2025 [9]. The results demonstrate the following:

- Without additional Actions: The measured force for the collision with the rounded robot head remains slightly below the $130\ \mathrm{N}$ threshold but due to the uncertainties of the PFM the value could also exceed the threshold.
- Additional Soft Padding: The measured force for the additional soft padding with the speed of $150\,\frac{\mathrm{mm}}{\mathrm{s}}$ and the tool force supervision stays $38\ \mathrm{N}$ which decreases the transient force and remains below the $130\ \mathrm{N}$ threshold.
- Only Reduced Speed: The measured force for the collision with no soft padding but only reduced speed to $50\,\frac{\mathrm{mm}}{\mathrm{s}}$ and the tool force supervision stays $38\ \mathrm{N}$ which further decreases the transient force and remains far below the $130\ \mathrm{N}$ threshold.
- Reduced Speed and Force: The measured force for the collision with no soft padding but reduced speed to $50\,\frac{\mathrm{mm}}{\mathrm{s}}$ and reduced tool force supervision to $25\ \mathrm{N}$ the transient force reaches the minimum of the measurements and remains far below the $130\ \mathrm{N}$ threshold.

These measurements provide a reference for assessing biomechanical compliance and identifying critical areas where further risk reduction may be required. The pressure measurements for different parameter conditions are recorded and visualized in Figure 47.

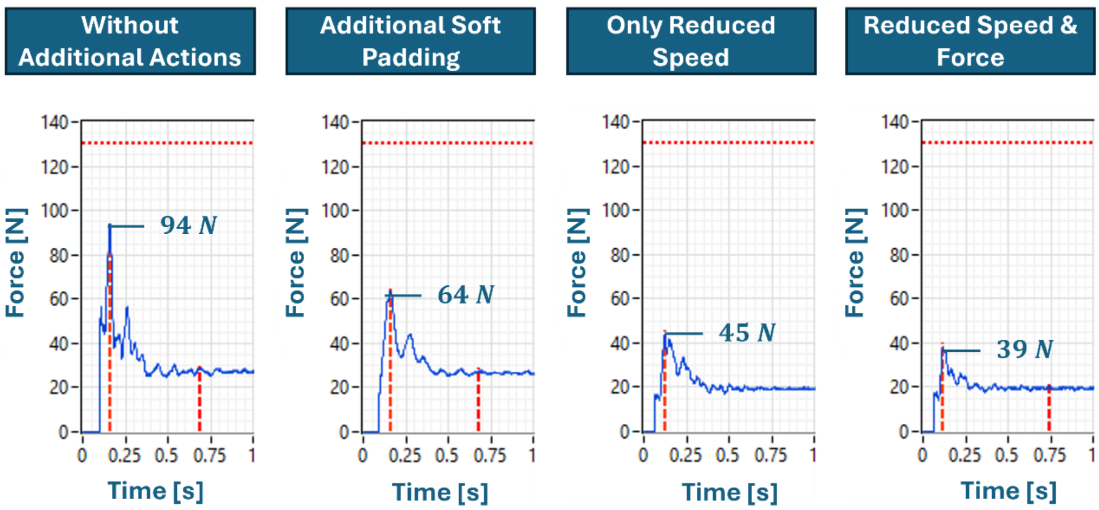

Figure 46 Visualization of transient contact force over time for different robot operating parameter. Each plot displays a sharp force peak at the moment of contact, followed by a gradual stabilization into the quasi-static force level. The measured peak force is annotated in each subplot. The red dotted line indicates the biomechanical force threshold as defined in Annex N of ISO 10218-2:2025 [9], allowing assessment of safety compliance during robot-human contact scenarios.

Each plot illustrates the spatial distribution of contact pressure during a transient impact event, as recorded by the PFMD sensor. The peak pressure values are noted at the centre of each distribution, offering insight into the severity of the impact on each body area. The results demonstrate the following:

- Without additional Actions: The measured pressure for the collision with the rounded robot head exceeds the $110\,\frac{\mathbf{N}}{\mathbf{cm^2}}$ threshold.
- Additional Soft Padding: The measured pressure for the additional soft padding with the speed of $150\,\frac{\mathrm{mm}}{\mathrm{s}}$ and the tool force supervision stays $38\ \mathrm{N}$ stays far below the $110\,\frac{\mathbf{N}}{\mathbf{cm^2}}$ threshold.
- Only Reduced Speed: The measured pressure for the collision with no soft padding but only reduced speed to $50\,\frac{\mathrm{mm}}{\mathrm{s}}$ and the tool force supervision stays $38\ \mathrm{N}$ remain below the $110\,\frac{\mathbf{N}}{\mathbf{cm^2}}$ threshold.
- Reduced Speed and Force: The measured pressure for the collision with no soft padding but reduced speed to $50\,\frac{\mathrm{mm}}{\mathrm{s}}$ and reduced tool force supervision to $25\ \mathrm{N}$ exceeds slightly the $110\,\frac{\mathbf{N}}{\mathbf{cm^2}}$ safety limit but due to the uncertainties of the PFM the value could also be closer the threshold.

These initial measurements provide a reference for assessing biomechanical compliance and identifying critical areas where further risk reduction may be required.

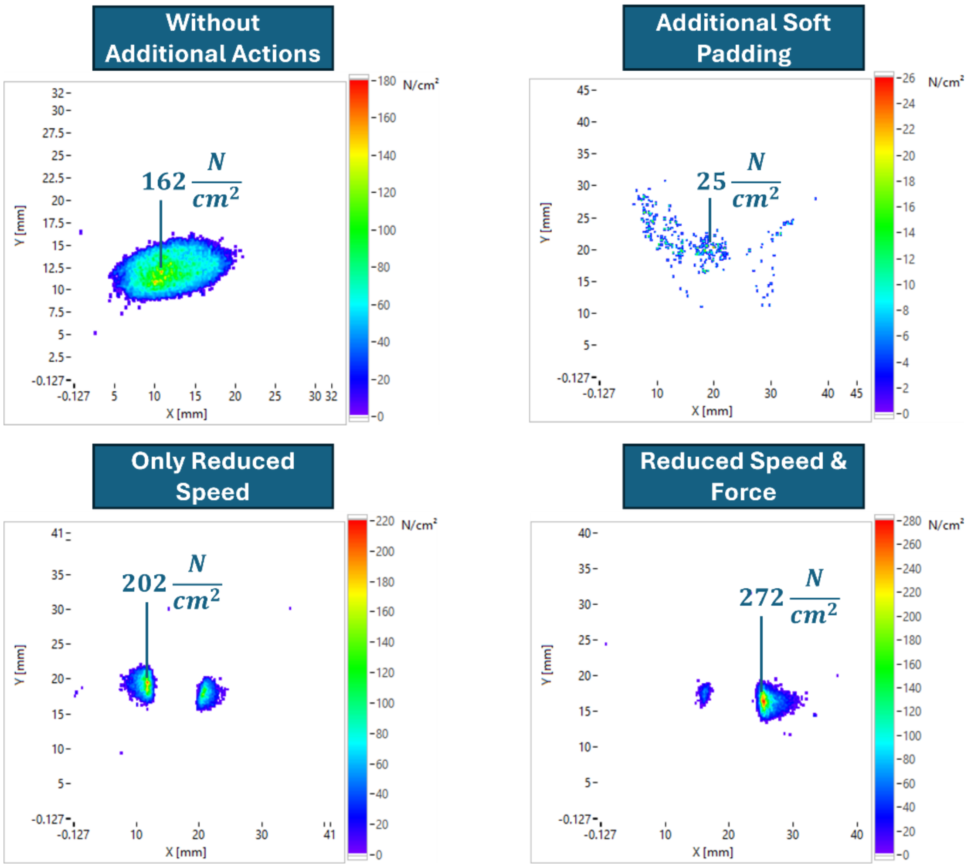

Figure 47 Pressure distribution maps for different robot operating conditions during contact with the PFMD. The peak pressure values are shown for the skull and forehead. These measurements reflect localized contact pressure during transient impact events.

I. Fourth Measurement

This appendix presents the test setup, motion sequence, and results of the measurement used to validate safety compliance in a collaborative HRI scenario. The purpose of this test is to evaluate whether the contact forces and pressures during a worst-case scenario remain within the biomechanical limits defined by ISO 10218-2:2025 [3].

Therefore, the programmed motion path of the robot stays the same as the previous tests for the home position to the contact point. In the test environment the end-effector is in contact with the measurement area. A fibre cloth is placed between the sensor and the contact area to simulate realistic contact conditions. The robot is operated at a height of $1300\ \mathrm{mm}$ from the ground, and with the different robot operating parameters as outlined in Figure 48. There the robot is evaluated on how a collision with the reduced speed and force as well as additional soft padding is influencing the transient force and pressure values. Therefore, the maximum reduced speed is $50\,\frac{\mathrm{mm}}{\mathrm{s}}$ and the maximum reduced tool force supervision is set to $25\ \mathrm{N}$.

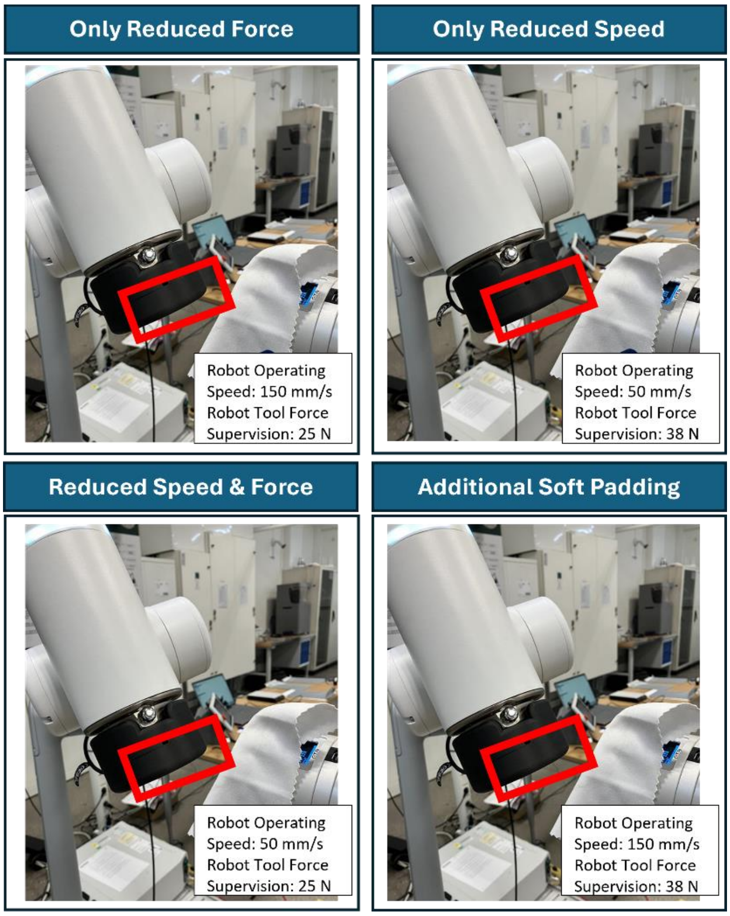

Figure 48 Visualization of the physical setup, where the end-effector makes contact with the PFMD sensor covered with a fibre cloth to simulate realistic conditions. The different robot parameter conditions where additional soft padding as well as reducing the speed and tool force supervision are tested.

The measurements are conducted three times with a maximum of 10% variance and the worst-case scenario is taken to obtain reliable estimates. Due to time constraints, repeated trials and broader statistical sampling are not performed. Therefore, for the skull and forehead the correct damping material with the corresponding effective spring constant, as specified in Annex N from ISO 10218-2:2025 [3], is used to measure the following force and pressure values.

The force measurements for the different parameter conditions are recorded and visualized in Figure 49. These plots illustrate the transient contact force behaviour over time. Each measurement starts with a sharp force increase caused by the transient impact and then converges to a quasi-static force level. The red dotted line on each plot represents the safety threshold for the respective body region, as outlined in Annex N of ISO 10218-2:2025 [9]. The results demonstrate the following:

- Only reduced Force: The measured force for the collision with no soft padding and the speed at $150 \frac{\text{mm}}{\text{s}}$ but with a reduced tool force supervision to $25\ \text{N}$ the transient force remains below the $130\ \text{N}$ threshold but stays high in comparison to the others.
- Only reduced Speed: The measured force for the collision with no soft padding and a reduced speed to $50 \frac{\text{mm}}{\text{s}}$ but with a tool force supervision of $38\ \text{N}$ the transient force remains far below the $130\ \text{N}$.
- Reduced Speed and Force: The measured force for the collision with no soft padding but reduced speed to $50 \frac{\text{mm}}{\text{s}}$ and reduced tool force supervision to $25\ \text{N}$ the transient force even decreases and remains far below the $130\ \text{N}$ threshold.
- Additional Soft Padding: The measured force for the additional soft padding with the speed of $150 \frac{\text{mm}}{\text{s}}$ and the tool force supervision stays $38\ \text{N}$ the transient force remains below the $130\ \text{N}$ threshold but slightly increases.

These initial measurements provide a reference for assessing biomechanical compliance and identifying critical areas where further risk reduction may be required. The pressure measurements for different parameter conditions are recorded and visualized in Figure 50.

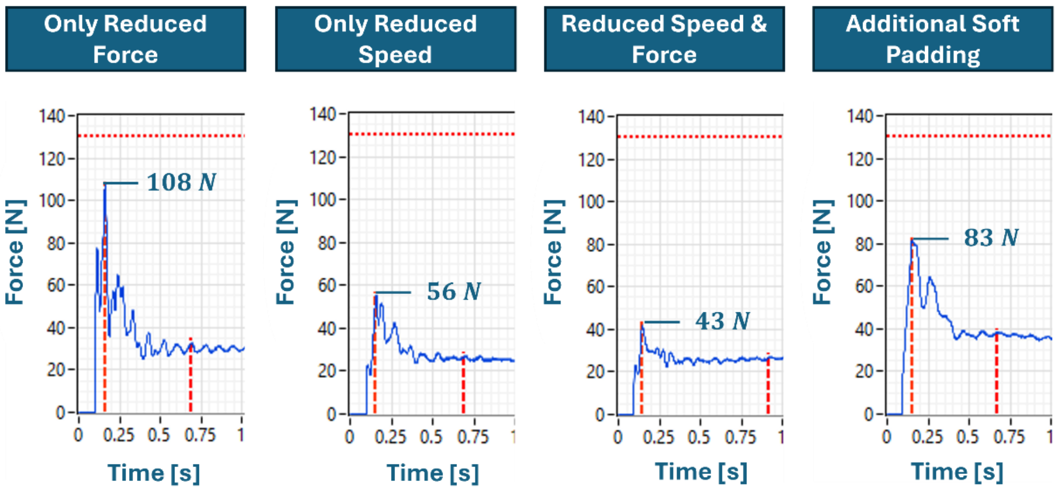

Figure 49 Visualization of transient contact force over time for different robot parameter conditions. Each plot displays a sharp force peak at the moment of contact, followed by a gradual stabilization into the quasi-static force level. The measured peak force is annotated in each subplot. The red dotted line indicates the biomechanical force threshold as defined in Annex N of ISO 10218-2:2025 [9], allowing assessment of safety compliance during robot-human contact scenarios.

Each plot illustrates the spatial distribution of contact pressure during a transient impact event, as recorded by the PFMD sensor. The peak pressure values are noted at the centre of each distribution, offering insight into the severity of the impact on each body area. The results demonstrate the following:

- Only reduced Force: The measured pressure for the collision with no soft padding and the speed at $150\,\frac{\mathrm{mm}}{\mathrm{s}}$ but with a reduced tool force supervision to $25\,\mathrm{N}$ the transient pressure exceeds the $110\,\frac{\mathbf{N}}{\mathbf{cm^2}}$ threshold.
- Only reduced Speed: The measured pressure for the collision with no soft padding but only reduced speed to $50\,\frac{\mathrm{mm}}{\mathrm{s}}$ and the tool force supervision stays $38\,\mathrm{N}$ remain below the previous measurement but exceeds the $110\,\frac{\mathbf{N}}{\mathbf{cm^2}}$ threshold.
- Reduced Speed and Force: The measured pressure for the collision with no soft padding but reduced speed to $50\,\frac{\mathrm{mm}}{\mathrm{s}}$ and reduced tool force supervision to $25\,\mathrm{N}$ stays between the previous measurements and also exceeds the $110\,\frac{\mathbf{N}}{\mathbf{cm^2}}$ safety limit but due to the uncertainties of the PFM the value could also be closer the threshold.
- Additional Soft Padding: The measured pressure for the additional soft padding with the speed of $150\,\frac{\mathrm{mm}}{\mathrm{s}}$ and the tool force supervision stays $38\,\mathrm{N}$ stays far below the $110\,\frac{\mathbf{N}}{\mathbf{cm^2}}$ threshold.

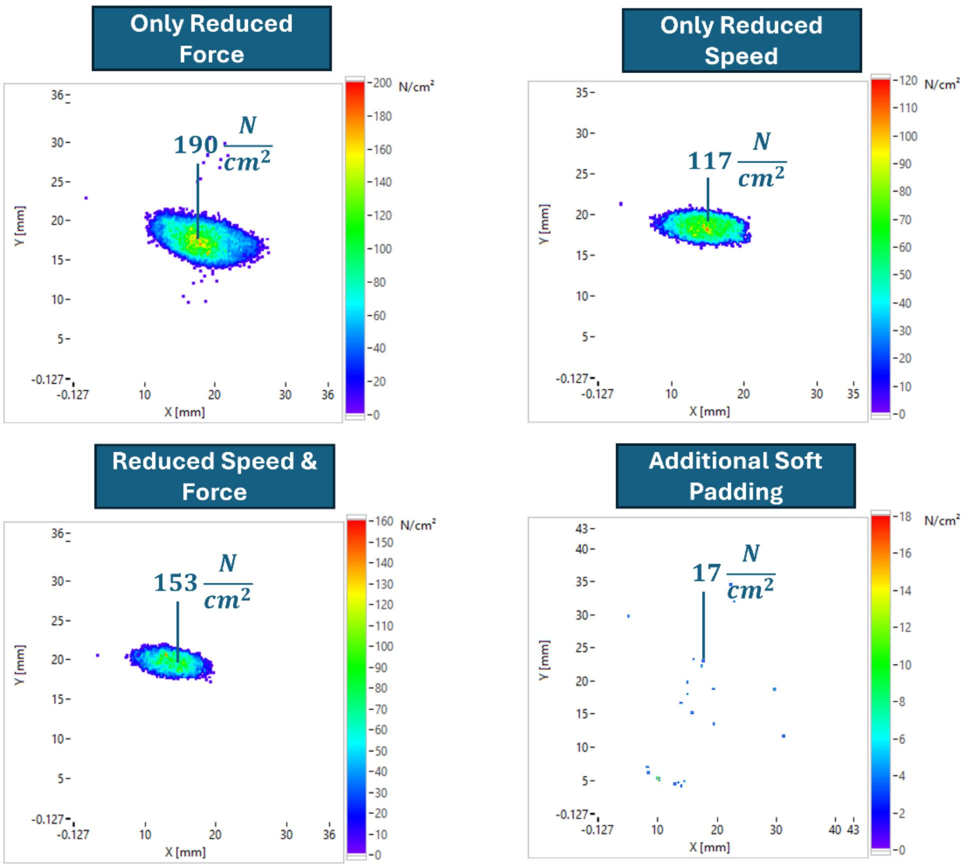

Figure 50 Pressure distribution maps for different upper-body regions during contact with the PFMD. The peak pressure values are shown for the skull, forehead, face, neck, back, shoulders, and chest. These measurements reflect localized contact pressure during transient impact events.